ARTIFICIAL NEURAL NETWORK BASED PROTECTION OF POWER TRANSFORMERS

MARZIA RABBI ZAMAN

ARTIFICIAL NEURAL NETWORK BASED PROTECTION OF POWER TRANSFORMERS

by

©Marzia Rabbi Zaman

A thesis submitted in partial fulfillment
of the requirement for the degree of
Doctor of Philosophy

Faculty of Engineering and Applied Science
Memorial University of Newfoundland

St. John's Newfoundland Canada

August 1996

Abstract

In this work, an artificial neural network based algorithm for a three phase power transformer protection scheme is developed and implemented in real time using the DS-1102 digital signal processor. Distinguishing between the magnetizing inrush and internal fault currents is always a consideration for power transformer protection. Existing methods, mostly based on harmonic restraint, are not very reliable for modern transformer protection. The reason for loss of reliability is that the use of low-loss amorphous material in modern transformer cores causes reduced second harmonic content of the magnetizing inrush current. Other methods based on the transformer equivalent circuit model are susceptible to parameter variations and hence are not suitable under all operating conditions. The work presented here shows the usefulness of the artificial neural network which is able to distinguish between the magnetizing inrush and the internal fault currents without harmonic decomposition or using the transformer equivalent circuit model. The inherent advantages of the generalization and the pattern recognition characteristics make the artificial neural network based method quite suitable for distinguishing between magnetizing inrush and the internal fault currents. In this work, a two-layer artificial neural network with sixteen inputs and one output is designed. The data to train and test the artificial neural network are experimentally obtained. The artificial neural network is trained with an input

data set and subsequently tested with a different data set. The off-line test results show that the artificial neural network is quite capable of distinguishing between the magnetizing inrush and internal fault currents. Finally, the on-line implementation successfully establishes the efficacy of the ANN based algorithm for power transformer protection.

Acknowledgments

I would like to express my deep gratitude and thanks to my supervisor Dr. M.A. Rahman for his guidance, useful discussions, constant encouragements and constructive criticisms of my work throughout the program and also for the financial support he has provided me during the last year of the program through the Canadian International Development Agency (CIDA). I would also like to thank the National Science and Engineering Research Council (NSERC) for the financial support they provided for the two years of my Ph.D study. I would like to express my appreciations to the School of Graduate Studies and the Faculty of Engineering and Applied Science. My thanks to CIDA for sponsoring the Memorial University of Newfoundland and Bangladesh Institute of Technology project which provided me the initial opportunity of pursuing my studies at Memorial.

I would like to thank Dr. J. Sharp, Associate Dean, Graduate Studies, Faculty of Engineering and Applied Science, and also my colleague Mr. Hoque for their useful suggestions, encouragements and moral support throughout my Ph.D program.

I would also like to acknowledge the members of my Ph.D supervisory committee, Dr. M.K. Lewis, Dr. B. Jeyasurya and Dr. S.A. Saoudy, for their useful comments and suggestions.

Special thanks go to my husband for his continuous moral support and help. Finally, I would like to dedicate this thesis to my parents.

Contents

List of Figures

List of Tables

Chapter 1

Introduction

1.1 General

Protective relaying is an important consideration in power systems because, even-though careful design, maintenance and operation can minimize the occurrence of short circuits and any other undesirable events, these abnormalities can not be eliminated completely. The main task of a relay is to take prompt action against any abnormal or undesirable situation by eliminating the faulty element from the system while maintaining in service as much of the remaining unfaulted system as possible. Removing the faulty element is performed by circuit breakers which are operated by the relaying device. A well-designed and efficient protective system requires five main design criteria - reliability, speed, selectivity, economics and simplicity [1]. The first of the criteria, reliability, consists of two elements namely dependability and security. The dependability ensures the correct operation in response to any disturbance due to system fault, while security provides the ability to avoid mal-operation from all extraneous causes of system disturbance. It is worth mentioning that the security is as important as the dependability, because tripping of circuit breakers not associated

with the trouble area can sometimes be as disastrous as a failure to trip. Unfortunately, these two aspects tend to counter one another, hence a compromise between the two is required. The speed of the operation of the protective relaying is another important factor, which ensures minimum equipment damage. A high speed relay is considered to be the one which operates in less than a time of three cycles. Selectivity ensures minimum equipment removal from the service . This is required because of the interrelated structure of the circuit breakers and relaying devices. Economics, as always, is considered an important issue in order to provide maximum protection at minimum cost. Design simplicity makes the implementation and maintenance easy.

The relaying technology used in modern power systems can be categorized as i) electromechanical relay, ii) solid state or static relay and iii) computerized (microprocessor) relay. The electromechanical relay was introduced in the 1900s and is still widely used by utilities for protection of power system apparatus. The main four types of widely used electromechanical relays are : magnetic attraction, magnetic induction, D'Arsonval and thermal. The development of solid state semiconductor devices made possible the introduction of static relays in late 1950s. There are inherent advantages of static relays over the conventional electromechanical relays, such as lower maintenance, less burden to current transformer, improvement in sensitivity, speed and reliability, compactness in size, etc.. Because of these advantages many electromechanical relays are replaced by the static relays. Microprocessor based computer relays were introduced during the 1980s. The rapid development of digital technology has made it possible to have modern digital relays. Digital relays process the data by performing arithmetic operations. The basic operation of a digital relay involves sampling the analog waveform, digitizing the sampled data and storing it for future manipulation depending on the particular algorithm. Some of the advantages

of this type of relay over the conventional relays are the following.

- Flexibility - This is considered to be the most attractive feature of digital technology. Since the relay is designed using programmable digital processors, it is possible to make necessary changes through software which can meet any desired operating characteristics. Very often these are not practically realizable through hardware.

- Reliability - The enhanced self-checking ability improves its reliability to a great extent.

- Improved relay performance - By changing the relay operating characteristics, it is possible to improve the relay performance in terms of speed, sensitivity and selectivity. It is much easier to make changes in digital relays than in conventional relays in order to meet in-situ complex applications.

- Size - Due to the introduction and advancement of integrated circuits, it is possible to make compact relaying devices. Moreover, several relaying functions can be integrated in a single unit.

- Less burden to the current transformers.

The three phase transformer is one of the most essential elements in a power system, hence the protection of a three phase transformer is of critical importance. The protection of a three phase transformer is a challenging problem, because a designer has to consider various factors which include magnetizing inrush, over excitation, tap changing, current transformer saturation, internal, ground and external faults. Distinguishing between the magnetizing inrush current and the internal fault current is one of the most difficult tasks in this protection scheme, because sometimes high

magnetizing inrush current might lead to mal-operation of the relay [1]. In general, the differential protection method is quite popular and is widely used for detecting internal faults of a three phase transformer. The differential relay involves converting the primary and secondary currents to a common base and comparing them. When there is an internal fault in the transformer the current rises up to about 10 times the current under normal operating conditions [2]. This current can be used to operate the relay which will protect the transformer from damage due to any internal fault.

There are many existing protective relaying techniques for power transformer protection. Research in this area is on going with the objective of achieving faster, more accurate, more reliable and less expensive relays. Magnetizing inrush is always taken into consideration in designing a transformer protective relay. The following section provides a brief overview of the existing differential relaying techniques for transformer protection.

1.2 Literature Survey on Differential Relaying Techniques for Transformer Protection

As mentioned earlier, one of the most important considerations in relay design for transformer protection is to take into account the effect of magnetizing inrush. Therefore, designing a relay for transformer protection requires a good insight of the characteristics of the magnetizing inrush. For the study of digital protection of transformers, the simulation of the magnetizing inrush is an essential requirement. Since the 1940s much research has been carried out in order to derive a mathematical expression for magnetizing inrush current. Specht [3] developed formulae and curves for calculating approximately the magnetizing inrush for the single phase transformer. Blume, *et al.*

[4] studied the inrush phenomenon and its effects on system operation. The mechanism by which the inrush is produced, the significance of the inrush current from standpoint of system operation and the methods for reducing inrush or mitigating its effects have been covered in the literature. The theory of magnetizing inrush is also studied by Finzi and Mutschler [5] with a view to developing a comparatively simple formula that expresses the first and subsequent peaks of inrush current in terms of line voltage and other system parameters. However, the magnetizing inrush is even more complex for a three phase transformer because of the mutual interaction of the fluxes between the phases. Sonnemann, *et al.* [6] provided a detailed analysis of inrush phenomenon in a three phase transformer bank. Nevertheless, it should be mentioned here that they did not consider the effect of mutual coupling. In the 1980s when the digital technology became very popular due to its inherent advantageous features, the digital relaying began to replace the conventional relaying techniques. The pre-requisite for designing a good digital protection scheme for the transformer is an accurate simulation model for the magnetizing inrush. Realizing the importance of a good model for simulating various inrush conditions, Rahman and Gangopadhyay [2] were the first to carry out work on digital simulation of the magnetizing inrush of polyphase transformers. A generalized but detailed analysis incorporating both sequence impedance and mutual coupling has been performed [2]. Two methods for simulating the magnetizing inrush in a three phase transformer using numeric techniques have been developed. The simulation waveforms were compared with experimentally obtained inrush waveforms which showed a close match between simulated and experimental waveforms.

There are many factors which need to be considered in order to design a good model of a three phase transformer. These include nonlinearity between the flux and

the current, hysteresis and eddy currents, skin and proximity effects, transient effects at high frequencies, accuracy in calculating or measuring the leakage and mutual inductances, and capacitances between turns and from turn to ground. Much work [7]-[9] has been carried out in this direction but none of it considers all of these factors together. This is why the research in this area is still ongoing. Among the recent works [10]-[13], the model developed by Leon and Semlyen [13] is worth mentioning. They have paid special attention to the transient effects for a wide range of frequencies in the transformer model which is although important, is not usually considered. Also, considered in the model are the capacitances between the turns and from turns to ground, eddy current losses in the laminations, and the nonlinearity between the flux and current. Simulations have been performed using the model over a wide range of frequencies and the simulation results are compared with test results. A somewhat close agreement between the simulation and test results has been obtained. However, as has been pointed out in reference [13], the model does not include the hysteresis. The absence of hysteresis in the modeling makes the simulation less accurate. By performing harmonic analysis on various inrush waveshapes it has been seen that there is sufficient second harmonic component to restrain the relay operation during inrush. The internal fault current, on the other hand, contains a much higher fundamental component than the second harmonic. Normally, the ratio of the second harmonic component to fundamental determines whether the current is an inrush or internal fault. However, sometimes the inrush becomes so severe that the second harmonic to fundamental ratio falls below the typical threshold value of about 15% and causes mal-operation of the relay during inrush. Despite these limitations, harmonic restraint is still the most commonly used method for the differential protection of a power transformer.

There exist many techniques for differential protection of power transformers. Due to many advantageous features of digital techniques, most of the conventional electromechanical and static relays are being replaced by digital relays. However, the principle of most of the existing digital relays are based on the conventional harmonic restraint differential relays. The conventional methods of differential transformer protection are based on mainly two techniques : i) implementation of delay in the relaying device and ii) restraining or blocking the relay depending upon the harmonic components of the differential currents [1]. The first method is not attractive because of possible danger due to time delay and hence has become obsolete. However, the second method is widely used for transformer protection.

1.2.1 Electromechanical and Static Relays

The simplest form of differential relay for the transformer protection is known as the unbiased differential relay [1]. In this type of relay, the differential current is assumed to be zero under normal operating condition and no restraining coil is used in the relay. Under fault condition, the differential current becomes high and operates the relay. This differential protection scheme is unreliable because there is no way to prevent the relay operation if there is any unbalanced current caused by the difference in the current transformer (CT) characteristics and/or CT saturation. In order to eliminate this problem a modified differential protection scheme is employed which is commonly referred to as percentage differential relay. The basic principle is same as that of the unbiased relay, except in this scheme, two restraining coils are used in addition to the operating coil. In conventional percentage differential relay the through-currents produce the restraint proportional to the amount of current flowing, and the internal fault currents produce differential currents which flow through

the operating coil of the relay. However, these relays are susceptible to false tripping. Numerous methods have been developed to avoid false tripping during magnetizing inrush. As mentioned earlier, there are several relays which use delays in the relaying circuit to avoid false tripping. The delays are produced by means of slow-speed induction-disk type relays with high current and long time settings. Another method uses temporary desensitizing for a fixed time interval where the desensitizing is being controlled by voltage relays operated by the transformer voltages. Before the introduction of coordinated high speed relays, induction-disk relays with time setting long enough to outlast the inrush was sufficient. Contemporary methodology has made it mandatory to use high speed differential relay for transformer protection in order to maintain system stability. Due to the large amount of exciting current flowing through the transformer during the switching, a normal percentage bias relay is not sufficient enough to ensure correct operation of the relay under all possible circumstances. The conventional way of dealing with this problem is to use harmonic restraint relay [1]. In general, the magnetizing inrush current contains considerably higher second and fifth harmonic components than those present in the internal fault current. In 1938, harmonic restraint relay was introduced [1]. This method exploits the harmonic characteristics of the magnetizing inrush current. In its simplest form, the harmonic restraint relay has two filters – one to extract the fundamental component of the current which passes through the operating coil of the relay and the other to extract the second harmonic component of the current which is used for the restraining coil. The analog implementation of this relay is carried out using the L-C tuned circuit given in the Westinghouse reference book [1].

Kennedy and Hayword [14] studied the spectral characteristics of the internal fault and magnetizing inrush currents in order to develop a harmonic restraint relay for

transformer protection. According to them it is better to use all harmonic components as restraint rather than using the second harmonic only. The relay designed using the second harmonic restraint only is suitable for typical magnetizing inrush, but it may not be suitable for the currents coming from the saturated power transformers and current transformers (CTs). On the other hand, the relay designed using the third harmonic may be able to avoid tripping due to the CT saturation current, but may not be able to distinguish between inrush and true internal fault currents. A practical relay with harmonic restraint is intended primarily for bus differential service [14]. Based on the same principle, Hayward [15] designed a new type of relay which was able to distinguish between the internal fault current and the magnetizing inrush current by their difference in waveform, operating with high speed on internal fault and restraining from operation by magnetizing inrush current. The Westinghouse type HDD relay with harmonic restraint [1] has been widely accepted as a high speed sensitive transformer differential relay which operates entirely from current transformer and requires no auxiliary desensitizing means and potential transformers. In the Westinghouse HDD type percentage differential relay with harmonic restraint, the restraint is achieved by two tuned circuits. During heavy internal fault due to current transformer saturation, harmonics are generated and the restraint signal might be sufficient enough to block the operation of the relay. To ensure tripping under such conditions an instantaneous over-current relay unit without any restraint is provided whose pick-up time is set at a value above the maximum inrush current.

The CT saturation is still a major limitation of the Westinghouse HDD type relay in certain applications. An improved version of the Westinghouse HDD type relay known as BDD relay was designed [16] which was smaller in size and less burdensome to the current transformer.

In 1958, Sharp and Glassburn [17] presented a high-speed harmonic restraint differential relay for two winding and three winding transformers which successfully discriminates between true internal fault currents and false differential currents arising from external faults and/or an inrush. The relay consisted of a differential unit and a harmonic-restraint unit. Ratio-matching taps were provided on each unit to compensate for the main current-transformer ratio mismatch. The design used the second harmonic only for restraint, as it is assumed that this component will be always present during inrush, and is much less predominant for internal faults. According to Sharp and Glassburn [17], the tuned circuit designed for the restraint unit not only provides proper response of the unit to fault and inrush, but also provides a very good response during under-frequency conditions.

In 1975, Einvall and Linders [18] developed a three phase differential relay with harmonic restraint for multiple winding transformers. The design of this relay included simplification of the frequency selective circuits and a new algorithm for quick determination of the harmonic components of the applied current. This relay was found to be quite sensitive, the response time to any internal fault was less than two cycles and in the case of severe fault, it was less than one cycle.

1.2.2 Digital Relays

Rockfeller [19] is the first researcher who introduced a detailed scheme of fault protection using a digital computer. The problems associated with the use of a digital computer in a sub-station have been addressed in the literature [19]. In 1971, Mann and Morrison [20, 21] published their work on transmission line protection using computer techniques. Based on their work, the first digital computer relay for transmission line protection was designed as a joint project of pacific Gas and Electric Co.

and the Westinghouse Electric Co.. A feasibility study for both the primary and the backup protection using a digital computer was discussed by Cheetham [22, 23].

Due to the rapid advancement of digital technology and the enormous inherent advantages of digital methods, analog relays are being replaced by the digital relays and the digital protection of power system apparatus has become an active area of research. Over the last 25 years, a number of digital relaying algorithms have been proposed [24]. The output of an algorithm is determined by the application in which it is used. For example, if a digital algorithm is used in a distance relay for transmission line protection, the algorithm determines the impedance of the line from the location of the relay. In the case of differential relay for transformer protection, the same principle of digital algorithms can be used to distinguish between the inrush and internal fault currents. The digital algorithms for transformer protection are the focus of this research. These are briefly discussed below.

Most of the existing digital relays for transformer protection are based on harmonic restraint principle. The harmonic analysis is done by digital processing of the current samples. The main design objective is to find a fast and accurate algorithm to calculate mainly the fundamental, second harmonic and sometimes fifth harmonic components from the current samples.

Sykes and Morrison [25] attempted to extract fundamental and second harmonic components of the current by using two recursive filters. The difference between the magnetizing inrush and internal fault is based on the fundamental and second harmonic component derived from the differential current through the filters. For any current greater than the restraining current, the trip signal was sent indicating an internal fault had occurred. The scheme is implemented off-line on simulated inrush and fault data. The computer used was an IBM 360/50 and the program used was

FORTRAN IV. The algorithm is very simple, but the response time is quite slow, because the algorithm was developed for a single phase transformer which may not work properly for a three phase transformer. Simplicity is the main feature of this scheme with the drawback of slow response time.

The cross-correlation algorithm proposed by Malik, *et al.* [26] is very similar to the concept of Discrete Fourier Transform (DFT). The algorithm involves the calculation of odd and even functions of any harmonic component from the current samples. In order to speed up the arithmetic computation the sine and cosine functions can be replaced by odd and even square waves, but it will not be quite so accurate. The ratio of second harmonic to fundamental component is compared to a specified threshold value. If the ratio is greater than the threshold value, an inrush is declared, otherwise an internal fault is declared. The cross-correlation algorithm was tested using off-line simulation on a CDC 6400 computer. The response time was found to be within 1/2 to 3/4 cycle of a 60 Hz waveform using sine and cosine functions and about 3/4 to 15/16 cycle for odd and even functions. The algorithm was not tested in real time.

The finite impulse response (FIR) algorithm proposed by Schweitzer [27] does not require any multiplication and division. Finite impulse response filters are used with coefficients either +1 or -1 at any instant during one cycle time period. The algorithm involves determination of four Fourier sine and cosine coefficients for the fundamental and the second harmonic components using the sampled current data. Then the fundamental and second harmonic components are calculated. The algorithm was tested off-line using FORTRAN-IV program on simulated inrush and fault data. It is worth mentioning that although it has been tested for 8 samples per cycle, this algorithm can be extended for higher than 8 samples. However, the algorithm works better for a small sampling rate. The response time is about one cycle of 60 Hz. The

over-excitation case can not be detected using this algorithm.

The FIR algorithm was implemented by Larson, *et al.* [28] on a Motorola MC 6800 microprocessor for protection of a 500 VA transformer. The fault detection time is found to be between 1.25 cycles to 1.5 cycles based on a 60 Hz signal.

Ramamoorty [29] was the first who introduced the Fourier transform approach to extract different harmonic components of current or voltage from one cycle of fault transient samples. Subsequently Thorp and Phadke [30] presented discrete Fourier transform (DFT) algorithm for digital protection of power transformer. Their algorithm [30] was tested on data obtained from a model transformer using a sampling rate of 12 samples per cycle. The response time in the case of an internal fault is about one cycle.

Using the rectangular transform technique, a fast and accurate algorithm has been developed by Rahman and Dash [31]. The algorithm involves computation of Fourier sine and cosine coefficients for any signal. The response of this algorithm is reasonably fast because the calculation of these coefficients involves only addition and subtraction. The algorithm was tested on a PDP-11/60 computer using simulated transformer data. The protection scheme was also implemented on-line using an Intel 8085 micro-processor and tested using data obtained from a 3-phase, 400V, 60Hz laboratory transformer using a sampling rate of 12 samples per cycle.

Walsh function was used by Horton [32] and Jeyasurya and Rahman [33] for calculating fundamental and second harmonic component from the sampled current. The Walsh function can be considered as a squared up version of sine and cosine functions [34]. They can take only +1 and -1. The sign changes at the instant n, if n is a power of 1/2. Therefore it is much easier and less time consuming to calculate the Walsh coefficients than to calculate Fourier coefficients directly. Since

the relationship between the Fourier and Walsh function coefficients is known [34], the Fourier coefficients can be calculated, once the Walsh coefficients are obtained. This algorithm was tested with digitally simulated inrush and short-circuit fault current data. An Intel 8088 microprocessor was used for the digital data processing with a sampling frequency of 960 Hz i.e. 16 samples per cycle [33]. The response time found is about 9-14ms which is less than one full cycle.

The Harr function was used by Fakruddin, *et al.* [35] for extracting frequency component from power system relaying signal. The sine and cosine components of any harmonic component can be determined from Haar-Fourier relations. By using the combined second and fifth harmonic magnitudes of the differential current and comparing it with the fundamental, a trip signal is provided. However, this algorithm is quite complicated in terms of computation. Hence, the time required is usually longer compared to other algorithms.

A digital relaying algorithm based on a five-state Kalman filter has been developed by Murty and Smolinski [36]. The inrush and fault conditions are distinguished by the fundamental and second harmonic components of the differential current. The relay was implemented on a TMS320 digital signal processor and tested on-line for a three phase transformer [36]. The relay operating time for an internal fault with the first current sample is about one half cycle, whereas the operating time for a fault at the 12th or 13th current sample is about one cycle. One limitation of this algorithm is that it has no provision for higher order harmonics. Consequently, it might cause an error in the estimation due to the omission of higher harmonics. Later, Murty and Smolinski [37] extended their previous work by increasing the Kalman filter from five to eleven states to accommodate the fifth harmonic component. In their work [37], they used the percentage differential characteristic and over-excitation restraint

of the relay. The relay operation time is about one cycle if the fault occurs at the first current sample and much longer for a fault occurring at the 13th or 14th current sample. Moreover, they used a threshold of 25% which is quite high for modern transformers with amorphous core material. A lower threshold will definitely increase the operating time. Also, the Kalman filter coefficients are calculated based on a model transformer and thus the coefficients are subject to variation due to the operating conditions of the different transformers. Therefore, for a different transformer the algorithm may not work properly unless the coefficients are recalculated. Considering all the above features this particular algorithm was found to be unsuitable for on-line implementation [37].

In 1981, Degens [38] used the least squares curve-fitting technique to find the ratio of the second harmonic component to the fundamental of the differential current for restraining an inrush. It is assumed that the time constant of the dc component is unknown and the inrush current does not contain more than five harmonic components. The algorithm was used with a threshold of 12.5% i.e. if the ratio of second harmonic component to fundamental is smaller than the threshold, a trip signal is issued. The response time found for an internal fault is about two cycles. Later on, Degens [39] extended his work and implemented a digital filter using a microprocessor with a faster tripping option in the protection scheme. For a severe fault, the time taken was about 5 to 10 ms, whereas for other faults such as winding faults, the tripping time was around 33 ms.

Rahman *et al.* also developed a weighted least-square technique for differential protection of the transformer which is quite similar to Degens [38, 39] except that they used the root mean square error (RMSE) criterion technique to select the proper harmonic orders, data window, weighing matrix and sampling rate. The power trans-

former fault or inrush model is dependent on the type of transformer and the operating conditions. The lowest RMSE gives the correct model of the fitted data. The weighting matrix of this algorithm requires the fault and inrush data for a number of case studies in order to obtain the best weight factor. The computation burden is very heavy and hence is unsuitable for on-line implementation.

Sachdev and Nagpal [41] also developed a least square technique for differential protection of power transformers. The hardware and software aspects of this relay have been well described in their paper [41]. The relay was tested in a laboratory using a 15 kVA, 2540/480 V, delta-wye transformer. The trip command was issued in approximately one and half cycles for most internal faults. However it took longer when the transformer was switched on with a low level internal fault.

Dash and Rahman [42] used the spectral observer technique for digital protection of a 3-phase power transformer. The recursive discrete time filter interpolates signal samples and generates Fourier coefficients either by using spectral observation or functional expansion. The algorithm provides high speed operation during internal fault as well as sufficient restraint for inrush conditions. On-line tests for a 3-phase, 50 Hz, 415 V, 4 kVA laboratory transformer using LSI-11/23 microcomputer was performed. The results are quite satisfactory and the fault detection time was within 3/4 of a cycle.

Among the recent works, the algorithm developed by Lihua, *et al.* [43] for digital protection of transformers is worth-mentioning. The main goal of this work was to lessen the computational burden and thus obtain high speed operation. The algorithm involves designing three all-zero filters for extracting the fundamental, second and fifth harmonic components of the differential current. They also introduced two performance evaluation indices in order to compare quantitatively different algorithms

in terms of the number of computation needed and the log ratio of the undesired frequency component to the desired frequency component, respectively. Based on the fact that the voltage magnitude only drops when an internal fault occurs, the voltage restraint can be used to replace the harmonic restraint to prevent the relay from false tripping. The authors also developed [43] a voltage restraint algorithm which uses two measured voltages and the rated voltage of the transformer to decide whether an instantaneous tripping or a restraint is required. This algorithm is very simple and quite fast. However, the simplicity is obtained at the cost of using another group of A/D converters for the phase voltages. As suggested [43], the combination of the above two types of restraint can be used to obtain the highly reliable differential protection required for large power transformers. It should be mentioned here that these algorithms are only tested off-line using simulated data. This needs to be tested on-line with an actual transformer to prove the efficacy of the algorithms in real-time.

Hermanto, *et al.* [44] presented a detailed design of a stand-alone prototype digital relay using the discrete Fourier transform algorithm for the three phase power transformer protection. The major contribution of their work is the detailed description of both the hardware and the software aspects of the prototype relay.

A comparative study on various algorithms for differential protection of three phase transformers is made by Habib and Martin [45]. The comparative analysis made in this reference [45] is based on the problem of differential protection and detection of the exciting-current. Two performance indices based on time and frequency were chosen. According to their study [45] the discrete Fourier transform (DFT) algorithm is found to be the best method for implementing the digital relay for the differential protection of transformers. Rahman and Jeyasurya [46] presented a comparative study of six different algorithms namely, Fourier Analysis, Rectangu-

Algorithm	Sampling Interval μs	Number of Arithmetic Operation			Time for Arithmetic Computations	Percentage of Sampling Interval
		$+,-$	$\times,\div$	$\sqrt{x}$	$(1\cdot\phi)$ (μs)	
Fourier	1024	51	14	2	380	36%
Rectangular	1042	106	8	2	410	39%
Walsh	1042	116	14	2	526	50%
Harr	1042	96	16	2	512	49%
Finite	1042	84	4	2	298	29%
Curve	1389	46	19	2	447	32%

Table 1.1: Computational requirements for transformer protection algorithms [46]

lar Transform, Walsh Function, Harr Function, Finite Impulse Response and least square curve fitting for the digital protection of power transformers. All algorithms were tested off-line using VAX-11/785 mainframe computer. The sampling frequency was 960 Hz and the results are given in Table 1.1. The work was extended by So and Rahman [47]-[49] who also found that the discrete Fourier transform is the most efficient algorithm in terms of speed and accuracy for the differential protection of power transformers. They designed a stand-alone protection system to test all these algorithms on-line using a TMS 320C30 digital signal processor.

1.2.3 Recent Trends

Conventional harmonic restraint relays are based on the second, third or higher harmonic components of the difference current as restraint. This avoids tripping during the magnetizing inrush condition. However, due to increase in the operating voltage,

CT saturation, parallel capacitance for adjusting phase angle or distributed capacitance of long extra high voltage (EHV) transmission lines, etc., the difference current during internal faults also contains considerable amount of harmonic components [50]. Thus, the security of differential relay becomes questionable. Also, the current comparison is not very sensitive to inter-turn faults and CT saturation, etc. [51]. Moreover, it has been reported that due to the use of high quality low-loss amorphous material, the percentage of all harmonics may be as low as 7.5% of the fundamental in modern transformers [52, 53]. These factors adversely affect the operation of the existing harmonic restraint relaying techniques. Therefore, recent research trends have deviated from the harmonic restraint concept. Some algorithms have been recently developed which do not use the harmonic restraint concept, rather they use the phase currents, voltages and/or the electromagnetic model of the transformer to detect the transformer internal fault while preventing mal-operation of the relay during energization [52]-[57].

Liu, *et al.* [50] investigated the possibility of non-operation or operation with longer tripping time of the relay due to lower harmonic restraint setting for modern transformer protection. Three well-known algorithms namely – i) least square curve fitting, ii) Fourier analysis and iii) rectangular transform were analyzed for a large number of faults and energization of a transformer. The sample data used were based on the on-line test of a laboratory transformer. It is observed that during the internal fault, the second harmonic component can be as high as 68% of the fundamental and in such cases, using these algorithms the tripping time might be as high as 5 cycles for a heavy fault [50]. The authors [50] modified the existing algorithms and developed three schemes to solve this problem. In these schemes no attention has been paid to the percentage value of the harmonics during energization of the

modern transformers. The instantaneous tripping differential current is added in the first scheme. This avoids non-operation in heavy faults but provides operation with a longer timer delay for light faults. The second scheme uses phase voltage restraint in the differential current protection of the transformer. It can quickly operate for heavy faults and might operate with a delay for some light faults. However, in the case of the worst possible fault, i.e. the winding fault, this scheme is not able to operate reliably. In the third scheme, the second harmonic restraint differential current relay is controlled by the phase voltage. The relay will cancel the second harmonic restrain if one of the phase voltages is less than 70% of the rated voltage, otherwise it is allowed to restrain the relay. Although this scheme is better than the previous two, this also suffers from some limitations. For example, in the case of inrush, the phase voltage in a long line may become lower than 70% of the rated voltage until one cycle after the energization inception; and during this time if the percentage differential characteristics are satisfied, the protection will mal-operate [51].

It has been observed that the change in the primary voltage of the transformer is also a good indication of an internal fault. Thorp and Phadke [57] presented a voltage restraint algorithm for the transformer protection. The voltage is estimated from the primary voltage samples. If the calculated voltage is lower than a predefined threshold value, then a fault is declared. Since most of the transformers in industry use CTs to measure current signal, thus voltage restraint algorithm is not very useful in practical applications.

The voltage restraint method needs less computation but the availability of the voltage magnitude window restricts its use. Phadke and Thorp [55] continued to work in this direction and developed a new algorithm which uses the flux-current relationship in order to obtain the restraint function for the transformer protection.

The mutual flux linkage of a transformer can be calculated from the measured voltage and current samples. Tests were performed in the American Electric Power Service Corporation (AEP) power system simulator laboratory on a model transformer [57]. The data were taken and then an off-line performance study was made based on the data. The response time was found to be about one cycle. The method needs both the current and voltage samples and hence is not found to be an attractive method.

Much work has been reported on equivalent circuit modeling of the power transformer [51, 54, 56, 58, 59]. Inagaki, *et al.* [54] developed such an algorithm which involves the calculation of inverse inductances of the transformer windings using the phase voltages and currents. The algorithm was tested with computer simulated data of a large power transformer. It has also been tested on an actual 21 kV single phase transformer. The algorithm needed phase current which is a major limitation because for the delta connected winding it might not be possible in some transformers to access the phase current.

Sachdev, *et al.* [58] proposed an algorithm which involves the calculation of primary phase voltage using the measured values of the quantized phase voltage and current samples. The algorithm also requires some transformer parameters such as primary and secondary winding leakage inductances and mutual flux linkage of the primary and secondary windings. The estimated voltage was compared with the measured voltage and the difference (error) was calculated. If the error point lies in the fault region of the relay characteristic curve, the value is one, otherwise it is zero. Once the counter is assigned a new value, a trip command is updated by adding the new value of the counter and subtracting the value of the counter index taken sixteen samples earlier. A trip signal is sent if the trip index exceeds a specified value. A slight modification of the previous work is presented in reference [59] in

which the sampling instants of the voltages and currents were offset by a time equal to one half of the inter-sampling time interval. Both algorithms were tested off-line with some simulation data electromagnetic transient program (EMTP). The algorithms are computationally intense. Also it depends on the winding currents which are required to be estimated from line currents. The algorithm proposed by Sidhu and Sachdev [56] does not require any information about the winding current. They developed a transformer model and used the modal transformation for decoupling. The algorithm, however, needs the positive and negative sequence impedances of the transformer in order to use it in the model. The proposed algorithm was implemented on a Texas Instrument TMS320C25 digital signal processor and the capability of the developed system was tested on a 15 kVA, three-phase transformer.

In general, the use of transformer equivalent circuit models has inherent limitations. This is because, the parameters are subject to variation during the different working conditions even without internal faults. The variation is caused by many factors such as core saturation, temperature fluctuation, change in on-load tap-changer, etc. The algorithms developed using name-plate data cannot work properly under different working conditions. There is still a need for a good model for the three phase transformer which will take into account all the factors such as nonlinearity between the flux and current, hysteresis and eddy current loss, leakage and mutual inductances, transient effects in high frequencies. Realizing the importance as well as difficulties of developing a good model of a three phase transformer, much work has been done so far [11]-[13]. However, none of the models is able to consider all of the above mentioned factors. Since a model based method has limitations for power transformer protection, it seems at this point an alternate method to solve the protection problem should be attempted. One promising method is the application of

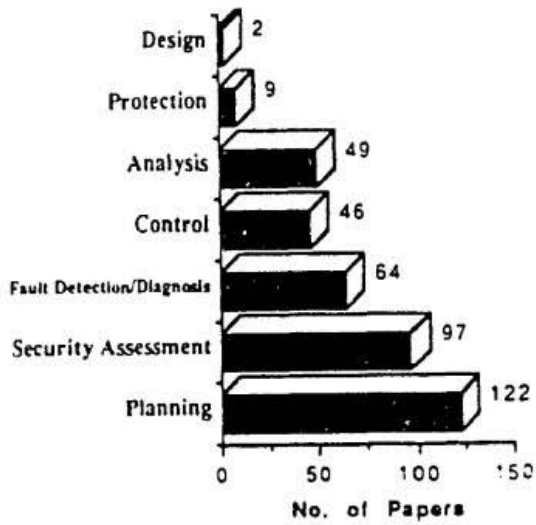

Figure 1.1: Classification of papers on applications of ANNs to power systems[60].

the artificial neural network in the protection of power transformers.

In recent years, artificial neural network (ANN) has become a very useful tool in many applications especially those which involve pattern recognition. In power systems, some typical ANN application areas include : planning, security assessment, fault detection/diagnosis, control, analysis, protection, design etc. [60]. The most popular applications of ANNs in power systems are load forecasting [61]-[64], security assessment [65, 66] and fault detection/diagnosis [67]-[69]. However, the application of ANN in the power system protection is still quite new. An extensive survey is done based on the reported papers in ANN applications in different areas in power systems [60]. According to the survey as shown in Fig. 1.1, less than 3% of the ANN applications are done in protection area [60]. There is still a wide scope of research in this area.

Few works are reported on the application of neural network to the power transformer protection [70]-[73]. Perez, *et al.* [70] used the ANN as a tool for distinguishing

between the magnetizing inrush and internal fault. The method is independent of harmonic contents of the current. Moreover, it does not require equivalent circuit model parameters, thus it is insensitive to parameter variations. The basic requirement for this method is to gather as much inrush and internal fault current information as possible in order to train the ANN. Perez, *et al.* [70] carried out their work on a single phase transformer having limited experimental inrush data and simulated internal fault current data. The initial results indicate the power of the ANN in distinguishing between the magnetizing inrush and internal fault currents. Bastard, *et al.* [72] also investigated the scope of using the ANN in transformer protection. They emphasized performance of the ANN based algorithm over the conventional algorithms under the saturated CT condition. This work is also based on a single phase power transformer. No on-line test was performed in this work. It is clear that there is ample scope for innovation in the area of developing an ANN based differential relay for a three phase power transformer protection and implementation in real time.

1.3 Problem Identification and Purpose of the Work

As mentioned earlier, there are many existing digital techniques which are based on the second and fifth harmonic restraint concept. Although the second and fifth harmonic components have been so far considered as the indication of whether the measured differential current is an internal fault or magnetizing inrush, recent works [58, 59] show that in certain cases, the internal fault might also contain considerable amount of second and fifth harmonic components. Moreover, it has been reported [59] that high quality, low-loss amorphous core materials in modern transformers have

resulted in lower harmonic contents in the magnetizing inrush current. Hence, the recent trend of transformer protection is deviating from the conventional harmonic restraint concept. The proposed work of this thesis is an attempt to solve this problem by using the artificial neural network (ANN) which has attracted many researchers because of its tremendous power of solving many nonlinear problems, particularly in the field of pattern recognition [74]. The artificial neural network has great power. Some of its inherent advantages over the conventional methods include parallel distributed architecture of information processing, ability to generalization, insensitivity to parameter variation and equivalent circuit model independency. The problem of distinguishing between the magnetizing inrush current and internal fault current can be considered as a current signature verification problem. Hence, the choice of the ANN seems to be appropriate in solving this problem.

In order to make the ANN algorithm more reliable and useful it is important to train the ANN using large number of experimental data for various inrush and internal fault conditions for a three phase transformer. Significant progress has been made during the course of this investigation on developing an ANN based algorithm for a three phase laboratory power transformer protection [71, 73]. A dedicated feed-forward ANN structure has been designed for this purpose and the network has been trained with experimentally obtained inrush and internal fault current data. The back-propagation algorithm is used for training the ANN. The trained network has been tested both off-line and on-line and the tests give quite satisfactory results. The algorithm is implemented in C programming language using the DS-1102 digital signal processor in a three phase stand-alone digital relay. The accuracy and speed under various operating conditions which include inrushes, over-excitation,and internal faults are observed and found to be satisfactory.

In the next chapter, the various features that need to be considered while designing a relay for the power transformer protection are discussed. Also discussed in the second chapter, the basic principle of the harmonic restraint differential relay with an example of typical analog relay and an efficient digital relaying algorithm for the transformer protection using the discrete Fourier transform (DFT). The DFT algorithm for transformer protection is also implemented in real time and the results are given at the end of Chapter 2. In Chapter 3, the artificial neural network is introduced and the proposed ANN structure for the transformer protection is discussed. Chapter 4 includes the description of the experimental setup for data acquisition for different inrush, fault and over-excitation conditions. The data processing, ANN training and off-line test results are also presented in Chapter 4. A comparison study between the DFT and ANN for the transformer protection is included. Chapter 5 gives details of the on-line implementation of the ANN based algorithms for a test transformer. The experimental setup, test procedures and the on-line results are presented. Finally the thesis is concluded in Chapter 6 by pointing out the major contributions and future scopes of study.

Chapter 2

Basic Principle of Power Transformer Protection

In a power system, the power transformer is one of the essential pieces of equipment. Although its rugged construction makes it quite reliable, heavy internal fault current might cause severe damage if immediate action against the fault is not taken. In general, differential relay with harmonic restraint is used for three phase power transformer protection. Before describing the basic principle of this relay, it is important to understand the various features of a transformer such as magnetizing inrush, over-excitation, CT saturation etc., which make the power transformer protection so complex and difficult. In the following sections, these features are described in detail. Followed by that are the differential relaying principle and a brief description of a typical analog relay for transformer protection. Finally, an efficient digital relaying algorithm is discussed with some simulated results.

2.1 Magnetizing Inrush and Other Considerations

While designing a protection scheme for power transformer, a designer has to consider many issues such as magnetizing inrush, over-excitation, current transformer (CT) saturation, etc. Magnetizing inrush is quite difficult to handle. Therefore, in this section the magnetizing inrush phenomenon is described more elaborately than the other considerations. The problem involved in magnetizing inrush is difficult to handle, because it may not be possible to predict the nature and magnitude of the inrush current beforehand. There is still a lack of an established model of magnetizing inrush current due to its complex and unpredictable characteristics. The complexity becomes even more for a three phase transformer than for a single phase transformer. At first, the magnetizing inrush is studied in detail for a single phase transformer and using the basic concept, the same phenomenon is discussed for a three phase transformer.

2.1.1 Magnetizing inrush in a single phase transformer

When a single phase transformer is energized, under steady state and secondary side open-circuited condition, the transformer draws an exciting current which produces a flux sufficient enough to produce a back emf exactly opposite to the applied voltage. In general, the level of this flux is about 1.6 Tesla (T) and is produced by less than 1% of rated load current [76]. The flux at some point in time reaches a level of about 2 Tesla for a modern transformer, where the iron core gets saturated and a high exciting current is demanded to produce that flux. The flux may remain in the core after the transformer is de-energized. This flux is known as residual flux. Thus, each time the transformer is energized it results in a high inrush current as a result

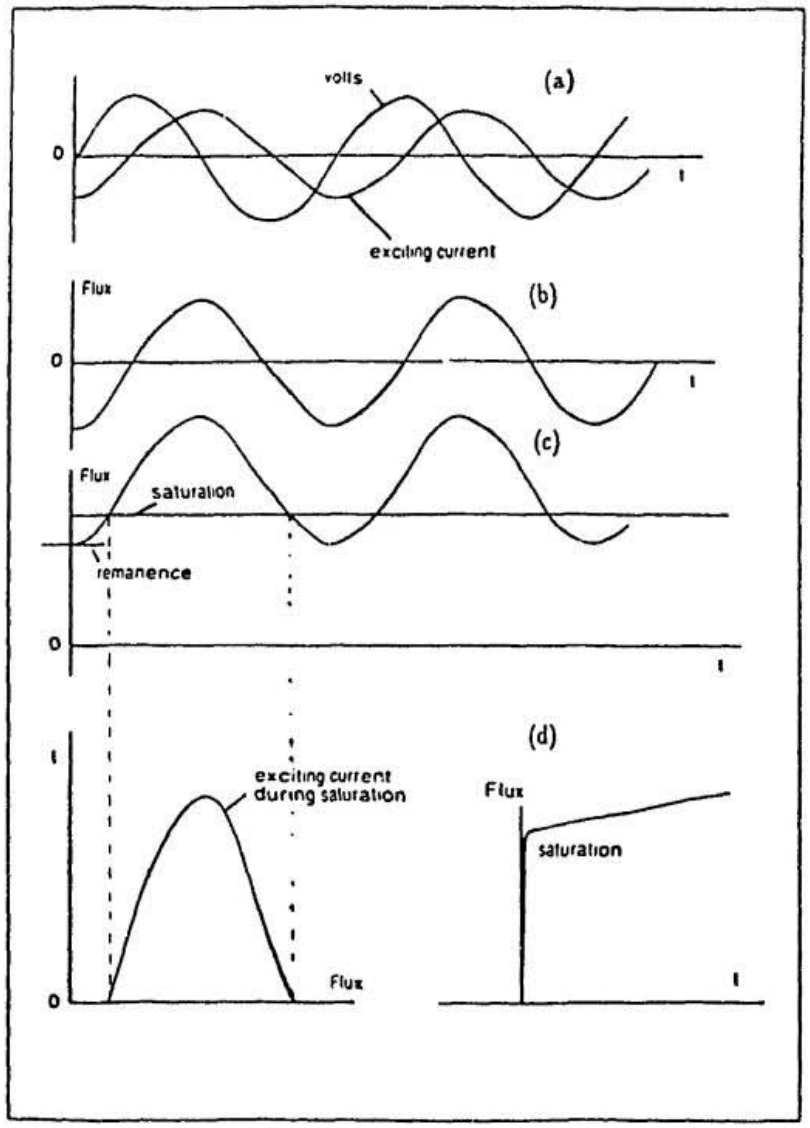

Figure 2.1: Voltage, exciting current and flux waveshapes; (a) supply voltage and exciting current; flux waveshapes (b) no residual magnetism, (c) with residual magnetism, (d) nonlinear relationship between exciting current and flux [76]

of transient saturation of the core and the residual magnetism. This exciting current also known as the magnetizing inrush lags the applied voltage usually by about 90° and the magnitude of the current depends on the point on the voltage waveform i.e. the point at which the transformer is energized i.e. it depends on the magnitude, the polarity and the rate of change of the applied voltage. Fig. 2.1(a) shows the relationship between the applied voltage and the exciting current as a function of time. The flux will increase as long as the voltage is positive and start decreasing as the voltage goes to negative. In this particular case, the switching is done at the positive going zero position of the voltage which results in a peak flux density of at $\omega t = 90°$ as shown in Fig. 2.1(b). The flux density peak is maximum at this point assuming there is no residual flux. It is worth noting that worse condition occurs when the sinusoidal voltage supply is switched on when the voltage is zero with positive slope, and when the residual flux linkage is at its maximum possible value [2, 77]. If B_r is the residual flux density and B_m is the peak value of the flux density waveform, the maximum value of the flux density will be $(B_r + B_m)$ and this will occur at $\omega t = 90°$ as illustrated in Fig. 2.1(c). The exciting current that is needed to produce this amount of flux can be found using the magnetizing curve as shown in Fig. 2.1(d). Similarly, it can be shown that the minimum flux will be obtained if there is no residual flux and the transformer is switched on at 90° of either half of the voltage waveform. In mathematical form the instantaneous flux can be expressed as

$$B(t) = -B_m \cos(\omega t) + B_m + B_r \tag{2.1}$$

If the core will go into the saturation when $B(t) = B_s$, the position can be calculated from equation (2.1) as

$$\theta = \cos^{-1}\left[\frac{B_m + B_r - B_s}{B_m}\right] \tag{2.2}$$

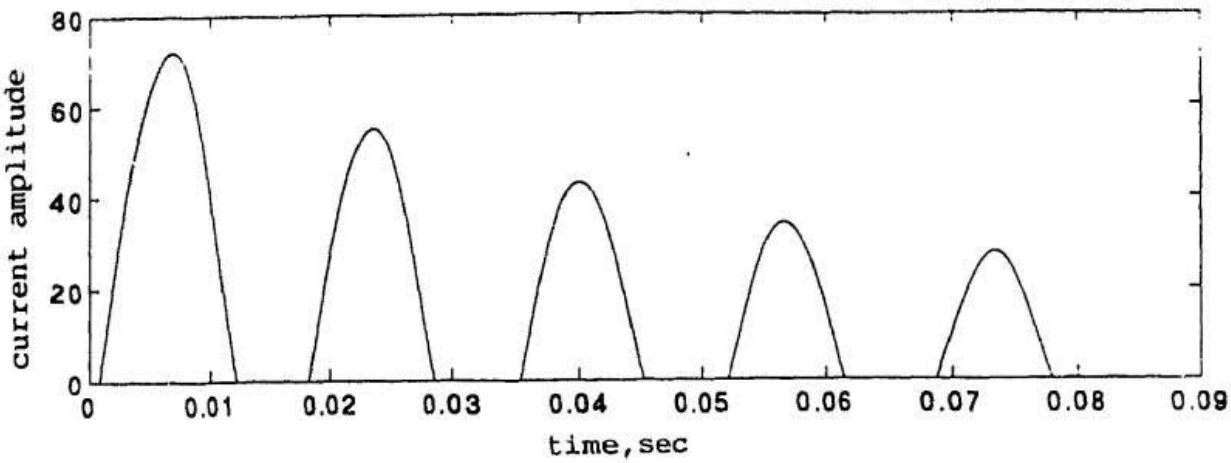

Figure 2.2: A computer simulated magnetizing inrush waveform

where, θ is the saturation angle. The maximum duration of inrush current in each cycle can be calculated as [76]

$$\gamma = 2(180^o - \theta) \tag{2.3}$$

This angle will decrease as the magnitude of inrush current decreases with time [76]. A computer simulation of the magnetizing inrush is shown in Fig. 2.2 [2].

2.1.2 Inrush in three phase transformer

In practice, the inrush waveforms are more complicated in a three phase transformer than that in a single phase transformer, because there are mutual interactions between the phases. The flux in the core of a three phase transformer is a combinational effect of all three phases. The characteristics of the magnetizing inrush vary depending on the various types of connection of the three phase transformer. For example, for an wye-delta transformer, the current circulating through the delta contributes to the current in all three phases and also to the magnetic flux in the core. Figure 2.3 shows a three limb transformer with remnant flux present in phases

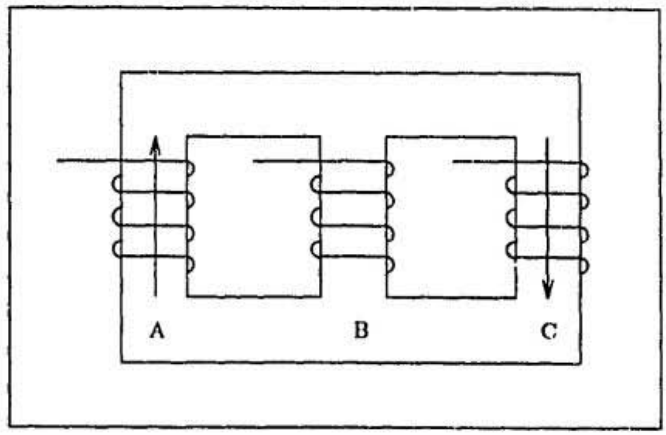

Figure 2.3: Three limb transformer

A and C, and Fig. 2.4 illustrates the mutual interaction betwe n the phases in a wye-delta transformer. As can be seen from Fig. 2.4, when the limbs of phases A and C are not saturated, the exciting current in phase B is small, because the magnetic flux will be easily produced in the highly permeable material. However, when one of the limbs approaches the saturation because of the combination of the remnant flux and the exciting current in that phase, the reluctance seen by the centre limb will increase and the exciting current will start rising. Finally when both the outer limbs have reached their saturation, the centre limb sees maximum reluctance and thus maximum current will flow in phase B. The situation is quite different for a delta-wye transformer; because there is no circulating current and thus no interaction between phases. In this case, the three phase transformer can be considered as three independent single phase transformers [2]. However, in both cases the current magnitude is quite high, at least in two phases. That makes the protection scheme difficult as it has to distinguish between the fault current and the inrush current, considering the fact that the magnitude of inrush current may become as high as that of the fault

current.

2.1.3 Over-excitation

Sometimes the transformer's peak magnetic flux density exceeds its normal operating range which is about 1.6 to 1.8 T in steady state for a typical transformer. The transformer in this situation is referred to as over-excited. There are many reasons for over-excitation such as, i) increase of three phase supply voltage, ii) a decrease of supply frequency, iii) mal-operation of the tap-changing service, iv) short circuit close to the terminal of the wye side of the transformer. It is not generally considered a fault unless it is so severe that it might cause core and winding damage. During over-excitation considerable amount of differential current might flow and cause mal-operation of the relay. It is thus important to recognize the current under over-excitation and distinguish this current from the typical load or fault current. There are significant third and fifth harmonic components present in the current under over-excitation which can be used as an identifier for current under over-excitation. Usually the third harmonic component is not used as a restraint because a delta connection of the transformer might inherently stop this component. As a rule of thumb, a maximum 40% fifth harmonic restraint is used to prevent the relay operation under normal over-excited condition. A higher value is not recommended as it might cause permanent damage to the transformer [1].

2.1.4 Current transformer saturation

The current transformer (CT) is one of the essential elements in a differential protection scheme because it provides suitable data acquisition means for protection purpose. The saturation of the current transformer occurs during heavy internal

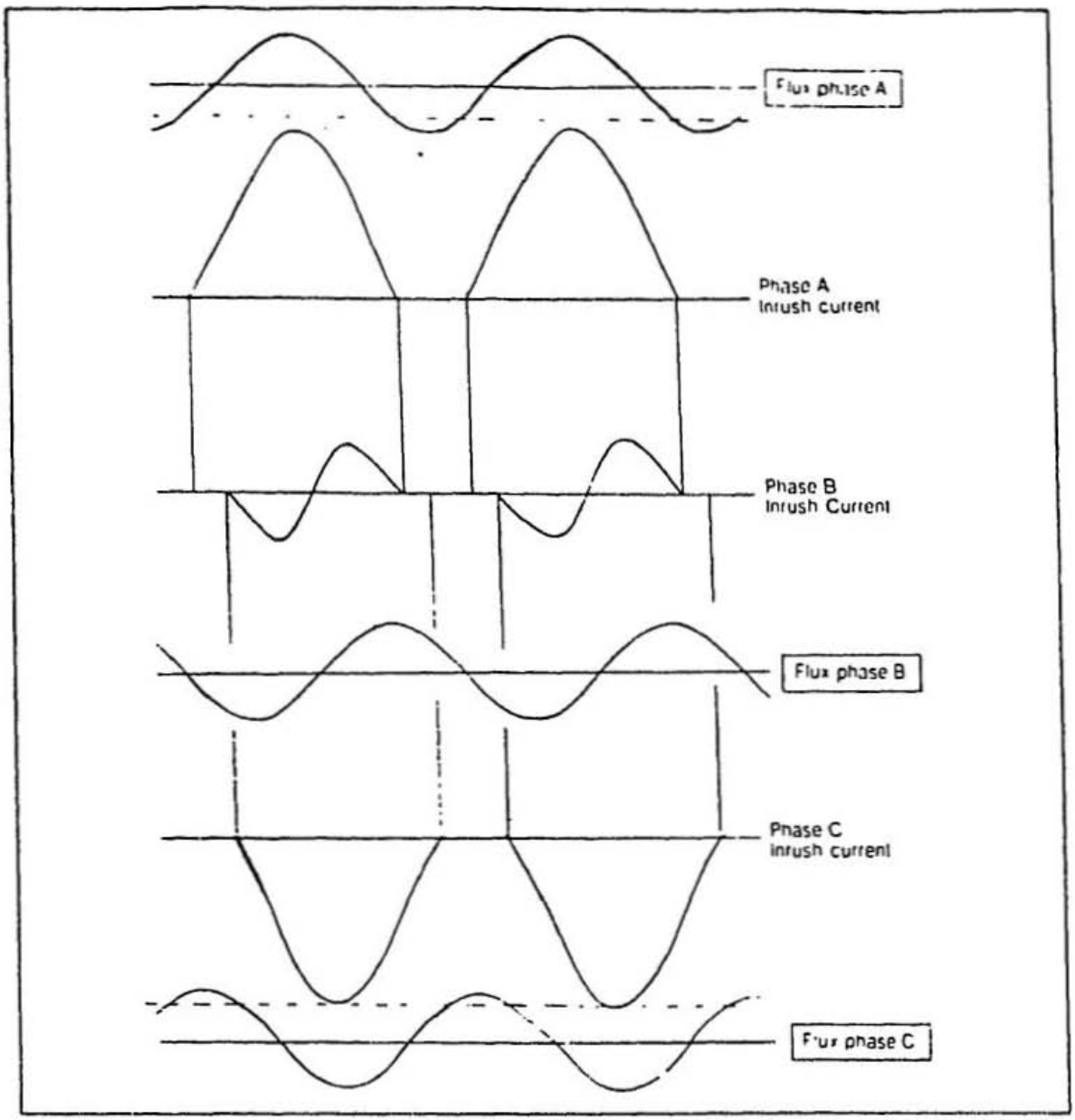

Figure 2.4: Mutual interaction between phases in a wye-delta transformer[76].

fault with slow decaying large dc component. Current transformer saturation affects the performance of the relay. Due to many possible reasons, such as differences in the voltage level, fault level, turns ratios, unavoidable mismatch of CTs, etc. one side of the CT becomes saturated which causes a spill current to flow through the operating coil of the differential relay during an external fault and thus might cause mal-operation. In general, percentage differential relays are used to minimize the possibility of mal-operation. However, instantaneous tripping is provided to avoid relay mal-operation during heavy internal fault.

2.2 Basic Protection Scheme

This section provides a brief description of the basic principle of transformer differential relay. Basic transformer differential protection involves converting primary and secondary currents per phase into a common base and comparing them. The difference between the primary current and secondary current is known as differential current. The primary and secondary currents can not be taken directly from the primary and secondary sides of the transformer. They need to be reduced down first and that is done by the current transformers (CTs). For a three phase transformer, six CTs are required, two for each phase of the primary and secondary sides. The polarities of the CTs should be determined and the connections are made accordingly. Otherwise it might cause mal-operation of the relay. Under normal operating condition, if the connections are made properly, the differential current should be very small, e.g., about 5 % of the full load current of the transformer. However, during internal fault of the transformer this current rises up to $10 - 20$ times the current under normal operating condition. The connection of the CTs also depends on the

connection of the main transformer bank. For a delta-wye or wye-delta bank, the CTs should be connected in opposite order i.e. the CT on the wye side should be connected in delta and the CTs on the delta side should be connected in wye. The reasons for making such connection are : i) to block the zero sequence current in the line and ii) to compensate for the 30° phase shift introduced by the delta-wye or wye-delta connection of the transformer bank. This is better illustrated in Fig. 2.5. As shown in Fig. 2.5(a) for a delta-wye transformer, if the CTs on both sides are connected in wye, there is a zero-sequence current flowing through the operating coil which might result in mal-operation of the relay. On the other hand, a proper connection as shown in Fig. 2.5(b) prevents any zero sequence current from flowing through the differential circuit and thus eliminates the possibility of mal-operation due to the zero sequence current. The primary ratings of the current transformers are also important considerations, and they should match with the rated primary and secondary currents of the main transformer. Moreover, in order to protect a transformer with on-line tap-changer, special attention must be paid so as to incorporate bias feature if a low-fault setting and high operating speed are required.

As mentioned earlier, the unbiased differential relay is the simplest relay for differential protection of a transformer. It is assumed that the current transformers on both sides are perfectly identical. Hence under normal operating condition, there is no current flowing through the operating coil. On the other hand, during internal fault, the difference in the current is no longer zero and this current will operate the relay indicating there is an internal fault. This simplest differential protection scheme is not reliable because there is no way to prevent the relay operation if there is any unbalanced current caused by the difference in CT characteristics and/or CT saturation. In practice, it is difficult to build two identical CTs and thus to eliminate

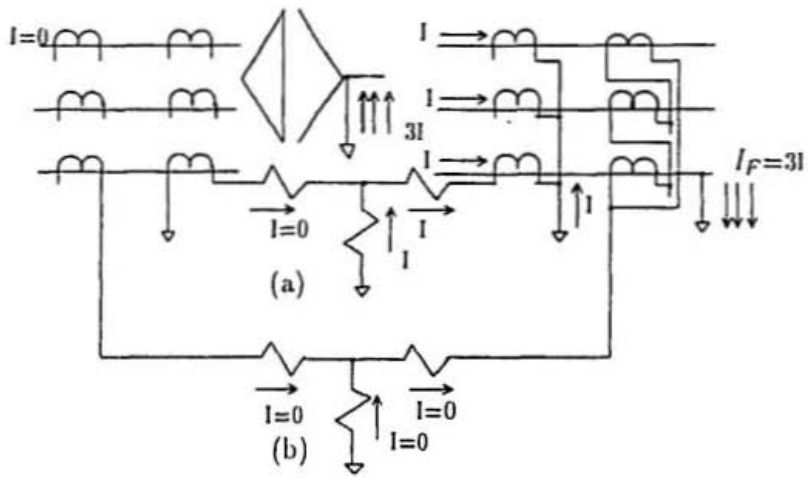

Figure 2.5: CT connections for a delta-wye transformer bank [1]; (a) Y-Y – causing a differential current of I, (b) Y-Δ – no differential current.

the possibility of CT mismatch. To eliminate this problem a modified differential protection scheme is proposed which is referred to as percentage differential relay. The basic principle is same as before except in this scheme two restraining coils are used in addition to the operating coil as shown in Fig. 2.6. This allows a certain percentage of current to flow through the operating coil without operating the relay and thus eliminates the possibility of mal-operation due to unbalanced current flowing through the operating coil caused by CT mismatch and/or CT saturation during heavy external fault. A small percentage of bias is effective in order to avoid incorrect relay operation against current transformer errors, protective circuit asymmetry and normal exciting current of the protected transformer. Higher percentages are required to prevent it against the mal-operation caused by significant imbalance of current resulting from tap-changers. In general, the percentage bias relays are made such that a suitable percentage setting can be made according to the prevailing circumstances

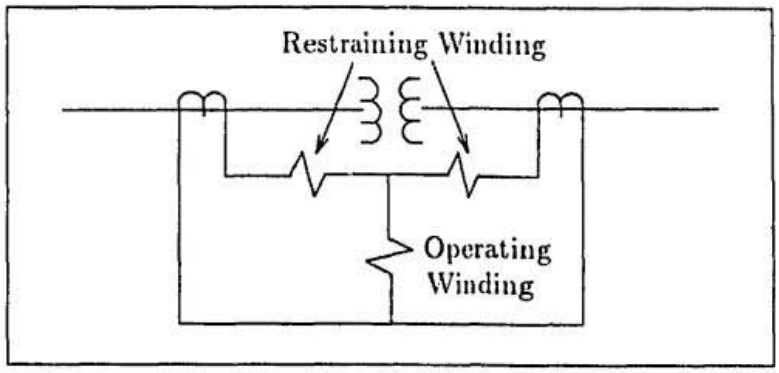

Figure 2.6: A percentage differential relay

[1].

As mentioned earlier due to the magnetizing inrush phenomenon, large exciting current with peak value of as high as 10 times the rated current of a transformer may be present after it is energized. As a result, the normal percentage bias differential relay is not sufficient to ensure correct operation of the relay under all possible circumstances. The conventional method of dealing with this problem is to use harmonic restraint concept because it has been found that the magnetizing inrush current contains considerably higher second and fifth harmonic components than those present in an internal fault current. The simplest percentage differential relay with harmonic bias has two filters – one for extracting the fundamental component at 60 Hz and allowing this current to flow through the operating coil, and the other for extracting and allowing the other current components (in general, the second and the fifth) to flow through restraining coil. The analog implementation of these filters are usually done by using simple L-C tuned circuit. The schematic of a typical harmonic restraint variable percentage differential relay [1] which uses L-C filter is shown in Fig. 2.7. It is evident from Fig. 2.7 that the second harmonic 120 Hz current is fed in the

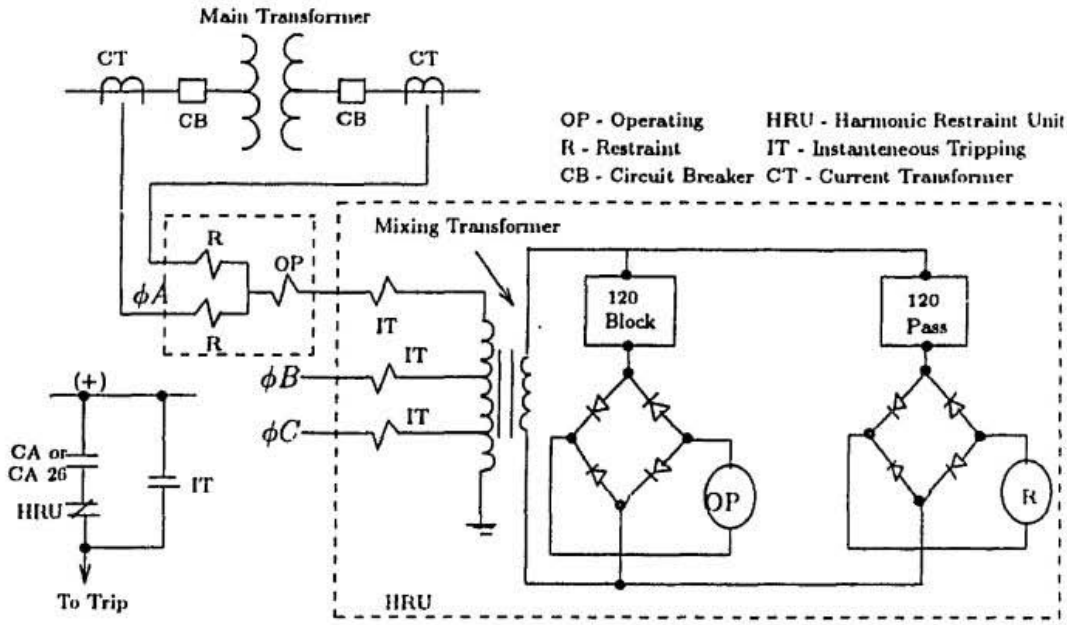

Figure 2.7: A typical harmonic restrained percentage differential relay [1]

restraint circuit (R), whereas the fundamental 60 Hz current is used in the operate circuit (OP) of the power transformer differential relay. It is worth mentioning here that the analog filters are now mostly obsolete with the rapid advancement of digital technology which provides design flexibility, more reliability and faster operation. Analog filters are being replaced by digital filters in most application areas and filters for harmonic restraint in differential relays are no exception.

2.3 Digital Algorithms for Transformer Protection

There exist many digital relaying algorithms for power transformer protection. In chapter one, some of these algorithms have been reviewed. Most of these algorithms

are based on harmonic restraint and they are very similar to each other. The only difference is the method of calculating different harmonic components. Also as mentioned in Chapter one, it has been found that among these algorithms discrete Fourier transform (DFT) is recognized as the best one in terms of accuracy, speed and memory requirement. In this section, a brief description of the DFT algorithm and how this algorithm is used in the transformer protection are discussed.

2.3.1 Discrete Fourier Transform

It was first proposed by Ramamoorthy that the fundamental component of a current or voltage waveform from a fault transient can be obtained by correlating the stored samples of reference sine and cosine waves [29]. The theory is developed from the basic Fourier series which states that any periodic function $f(t)$ having a finite number of discontinuities in the interval of $(0, T)$ can be modeled in this interval as:

$$f(t) = \frac{a_0}{2} + \sum_{k=1}^{\infty}(C_k \cos(k\omega t) + S_k \sin(k\omega t)) \tag{2.4}$$

where

$$\begin{aligned} \frac{a_0}{2} &= \frac{1}{T}\int_0^T f(t)dt \\ S_k &= \frac{2}{T}\int_0^T f(t)\sin(k\omega t)dt \\ C_k &= \frac{2}{T}\int_0^T f(t)\cos(k\omega t)dt \end{aligned} \tag{2.5}$$

a_0 is the average value or dc component and S_k, C_k are the sine and cosine components of the Fourier coefficients, respectively. If the waveform is sampled at equi-spaced interval of time, spaced ΔT apart, so that there are total $N/\Delta T$ samples per cycle, then S_k and C_k can be represented as :

$$S_k = \frac{2}{N}\sum_{n=0}^{N-1} x(n)\sin\left(\frac{2\pi kn}{N}\right) \tag{2.6}$$

$$C_k = \frac{2}{N}\sum_{n=0}^{N-1} x(n)\cos\left(\frac{2\pi kn}{N}\right) \tag{2.7}$$

where $x(n)$ is the sampled waveform at the nth instant.

The above equations can be expressed in matrix form as shown below :

$$\begin{aligned} \mathbf{S} &= \mathbf{C_s}\,\mathbf{X} \\ \mathbf{C} &= \mathbf{C_c}\,\mathbf{X} \end{aligned} \tag{2.8}$$

where $\mathbf{S}, \mathbf{C}$ are the vectors containing the sine and cosine components of the sampled waveform, respectively, $\mathbf{C_s}, \mathbf{C_c}$ are the system matrices containing sine and cosine coefficients, respectively and $\mathbf{X}$ is the vector containing the samples of the waveform to be analyzed. The vectors $\mathbf{C}, \mathbf{S}$ and $\mathbf{X}$ are of length N and the system matrices $\mathbf{C_s}$ and $\mathbf{C_c}$ are of size $N \times N$. For the power transformer protection scheme, a data window of 16 samples per cycle i.e. $N = 16$ is usually chosen. The sine and cosine system matrices are

$$\mathbf{C_s} = \begin{bmatrix} \sin\left(\frac{2\pi.1.1}{16}\right) & \sin\left(\frac{2\pi.2.1}{16}\right) & \cdots & \sin\left(\frac{2\pi.16.1}{16}\right) \\ \sin\left(\frac{2\pi.1.2}{16}\right) & \sin\left(\frac{2\pi.2.2}{16}\right) & \cdots & \sin\left(\frac{2\pi.16.2}{16}\right) \\ \vdots & & & \\ \sin\left(\frac{2\pi.1.16}{16}\right) & \sin\left(\frac{2\pi.2.16}{16}\right) & \cdots & \sin\left(\frac{2\pi.16.16}{16}\right) \end{bmatrix} \tag{2.9}$$

and

$$\mathbf{C_c} = \begin{bmatrix} \cos\left(\frac{2\pi.1.1}{16}\right) & \cos\left(\frac{2\pi.2.1}{16}\right) & \cdots & \cos\left(\frac{2\pi.16.1}{16}\right) \\ \cos\left(\frac{2\pi.1.2}{16}\right) & \cos\left(\frac{2\pi.2.2}{16}\right) & \cdots & \cos\left(\frac{2\pi.16.2}{16}\right) \\ \vdots & & & \\ \cos\left(\frac{2\pi.1.16}{16}\right) & \cos\left(\frac{2\pi.2.16}{16}\right) & \cdots & \cos\left(\frac{2\pi.16.16}{16}\right) \end{bmatrix} \tag{2.10}$$

From the system matrices the amplitude of the k th harmonic can be computed as :

$$F_k = \sqrt{(S_k^2 + C_k^2)} \tag{2.11}$$

where F_k is the kth harmonic Fourier coefficient and $k = 1, 2, ..., N$.

2.3.2 Application of DFT in transformer protection

Basically, discrete Fourier transform (DFT) is a method to extract the different frequency components from a time-domain signal i.e. the DFT coefficients are the coefficients of some frequency-selective filters. In the application of power transformer protection, three such filters are being used for extracting the fundamental, the second harmonic and the fifth harmonic components. From the above equations, F_1, F_2 and F_5, representing the fundamental, the second and the fifth harmonic components, respectively, can be determined. The frequency responses of the fundamental, second and fifth harmonic filters are also shown in Figs. 2.8(a)-(c).

In the case of magnetizing inrush, the ratio of F_2/F_1 is usually higher than 17.7%, whereas during an internal fault this ratio falls well below 17.7%. This is illustrated in Figs. 2.9 and 2.10. Figure 2.9 (a) shows an experimentally obtained inrush current waveshape in a transformer. Although the current magnitude is quite high for the first few cycles, due to the strong second harmonic component, the ratio F_2/F_1 is higher than the threshold of 17.7% as shown in Fig. 2.9(b) and the relay will restrain from operation. On the other hand, in the case of an internal fault as shown in Fig. 2.10 (b), the ratio falls below the threshold of 17.7% after sometime and thus operates the relay. The ratio between the fifth harmonic and the fundamental i.e. $F_5/F1_1$ is also calculated, because in the case of over-excitation the ratio F_2/F_1 might fall beyond 17.7% although there exists no fault in the transformer. In this situation the ratio of F_5/F_1 is however higher than its normal value of about 6.5% which is used as the restraining signal. Figure 2.11(a) shows a typical current waveshape for over-excited condition where the transformer is energized with a supply of almost 1.7 times the rated voltage. As can be seen from Fig. 2.11(b), although the F_2/F_1 ratio falls below 17.7%, the relay will be restrained by the F_5/F_1 ratio since this is higher than its

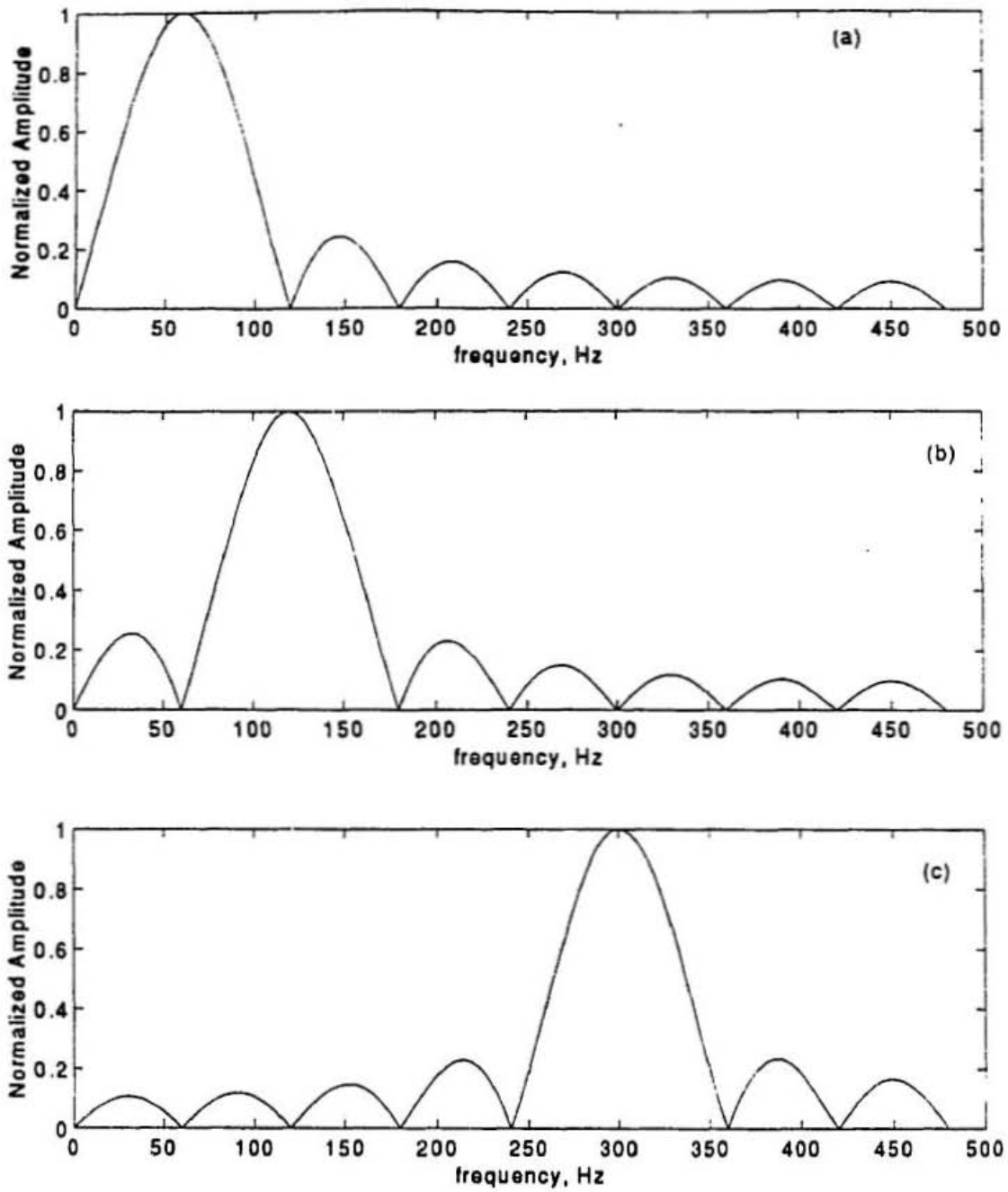

Figure 2.8: Frequency responses of the filters : (a) fundamental, (b) second harmonic, (c) fifth harmonic.

threshold value as shown in Fig. 2.11(c).

2.3.3 On-line implementation of the DFT algorithm

One portion of this thesis is focused on the implementation of the DFT algorithm in real-time using DSP – DS-1102 on a laboratory power transformer. This has been done successfully. Sixteen-point DFT is used in this experiment. This is to ensure the accuracy in the fifth harmonic extraction [44]. The hardware part of the experimental setup is same as used for ANN algorithm which will be discussed in details in Chapters 4 and 5. The algorithm is written in C language for the DS-1102's compiler. The sine and cosine coefficients are loaded in the program for calculating the fundamental, second harmonic and fifth harmonic components from 16 differential current samples. The on-line test results closely agree with the simulation results. The faults are detected within one cycle time period after the fault inception. Many inrush cases and eight different primary side and secondary side fault cases with and without load are observed. Some sample results are presented through Figs. 2.12-2.15. In these figures, the decision of the DFT is shown by means of the voltage which remains high (about 5 V) if there is no fault and goes to low (0 V) if there is a fault. In each of the following figures the DFT response is shown at the top and the differential current in phase A is shown at the bottom. Also note that the currents in all cases are allowed to flow for only about three cycle time period just to avoid any damage that might be caused due to the high fault current. In Figs. 2.12 (a) and (b), the DFT response for two inrush conditions are illustrated. The inrush currents are recognized perfectly. The control voltage remained high throughout the time the current is allowed to flow. In most of the fault conditions, the response of the DFT is within one and half cycle time periods as shown in Figs. 2.13-2.15. It is worth noting

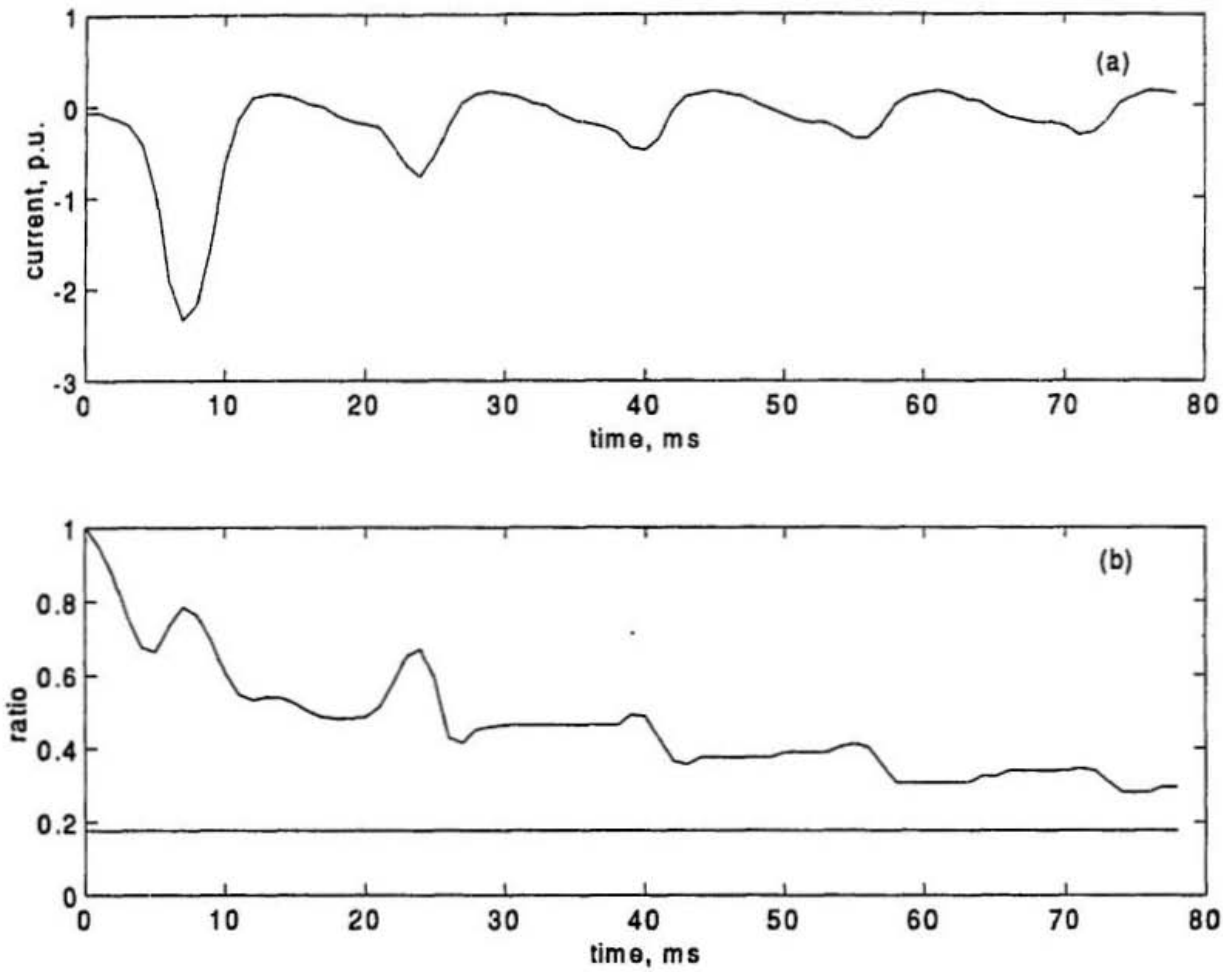

Figure 2.9: Magnetizing inrush : (a) differential current, (b) ratio of second harmonic to fundamental.

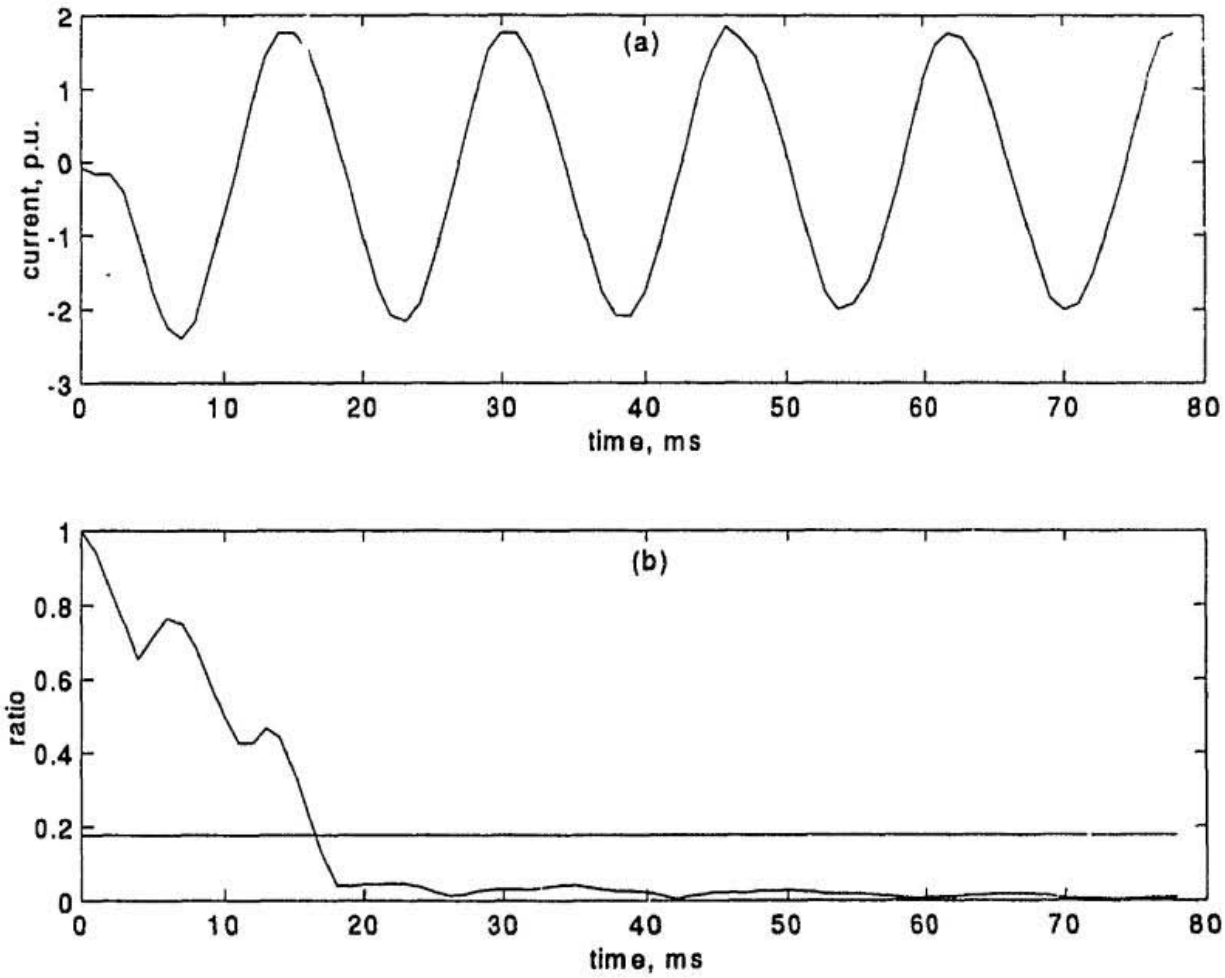

Figure 2.10: Internal fault : (a) differential current, (b) ratio of second harmonic to fundamental.

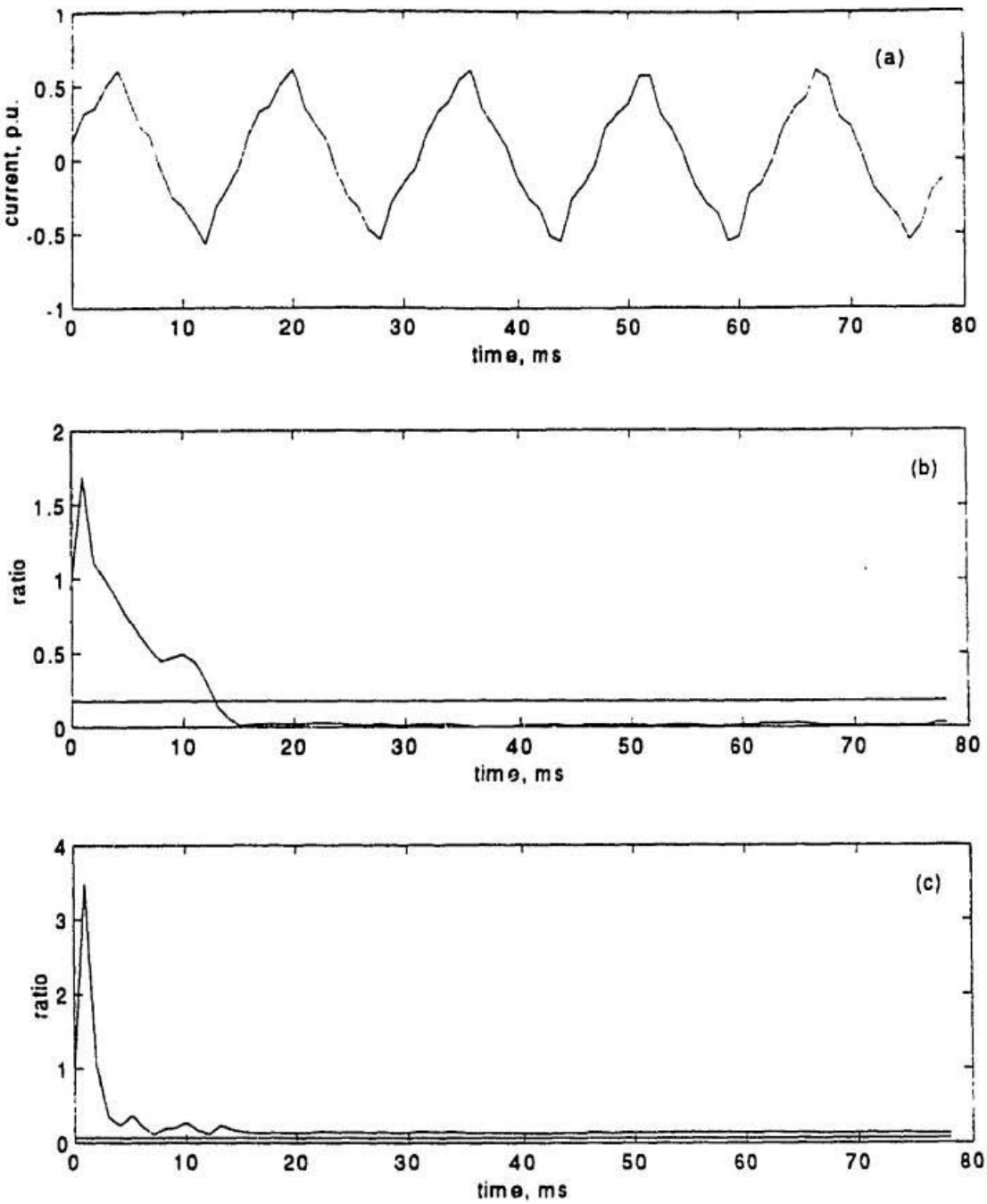

Figure 2.11: Over-excitation : (a) differential current, (b) ratio of second harmonic to fundamental, (c) ratio of fifth harmonic to fundamental.

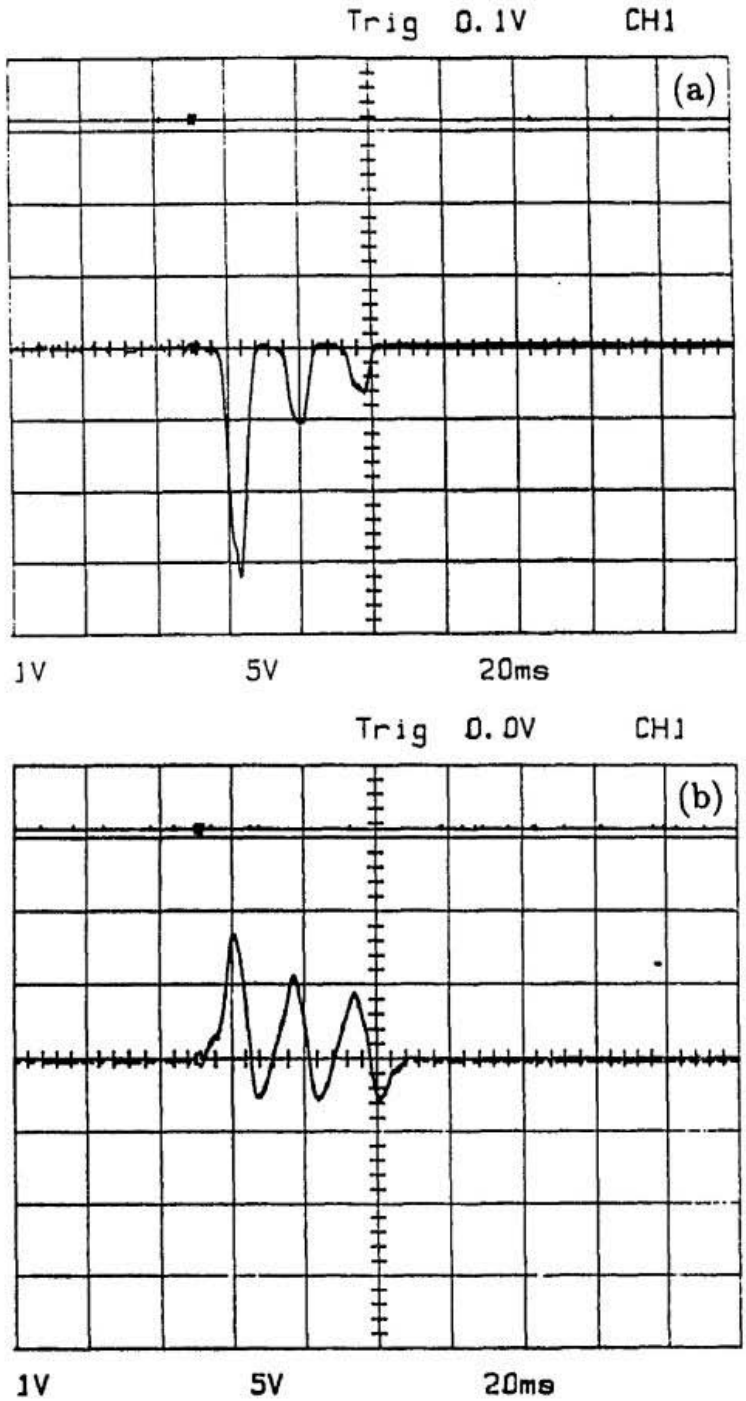

Figure 2.12: Response of DFT to inrushes: (a) without load, (b) with load; (Y-scale:1V = 12.5 A).

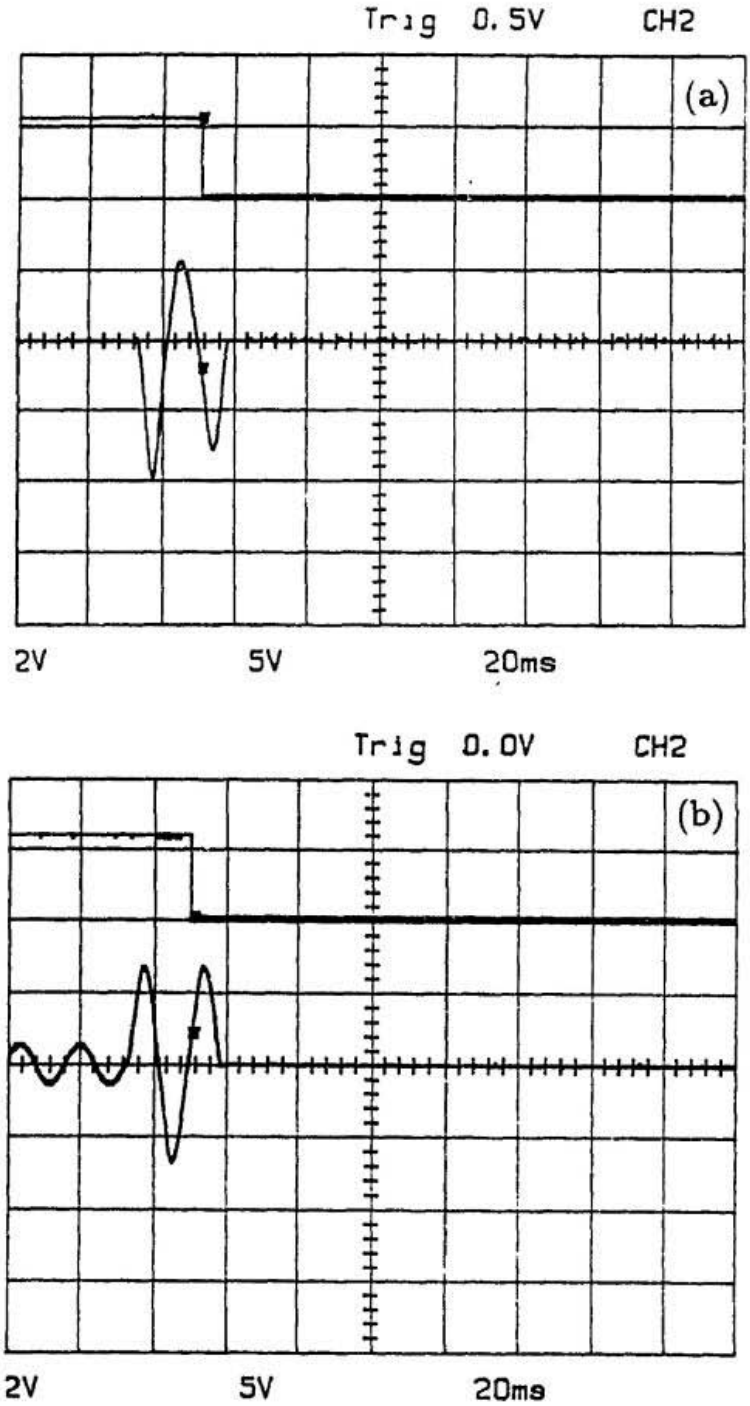

Figure 2.13: Response of DFT to primary side faults: (a) phase to phase fault occurred before inrush without load, (b) phase to phase fault occurred after inrush with load; (Y-scale:1V = 12.5 A).

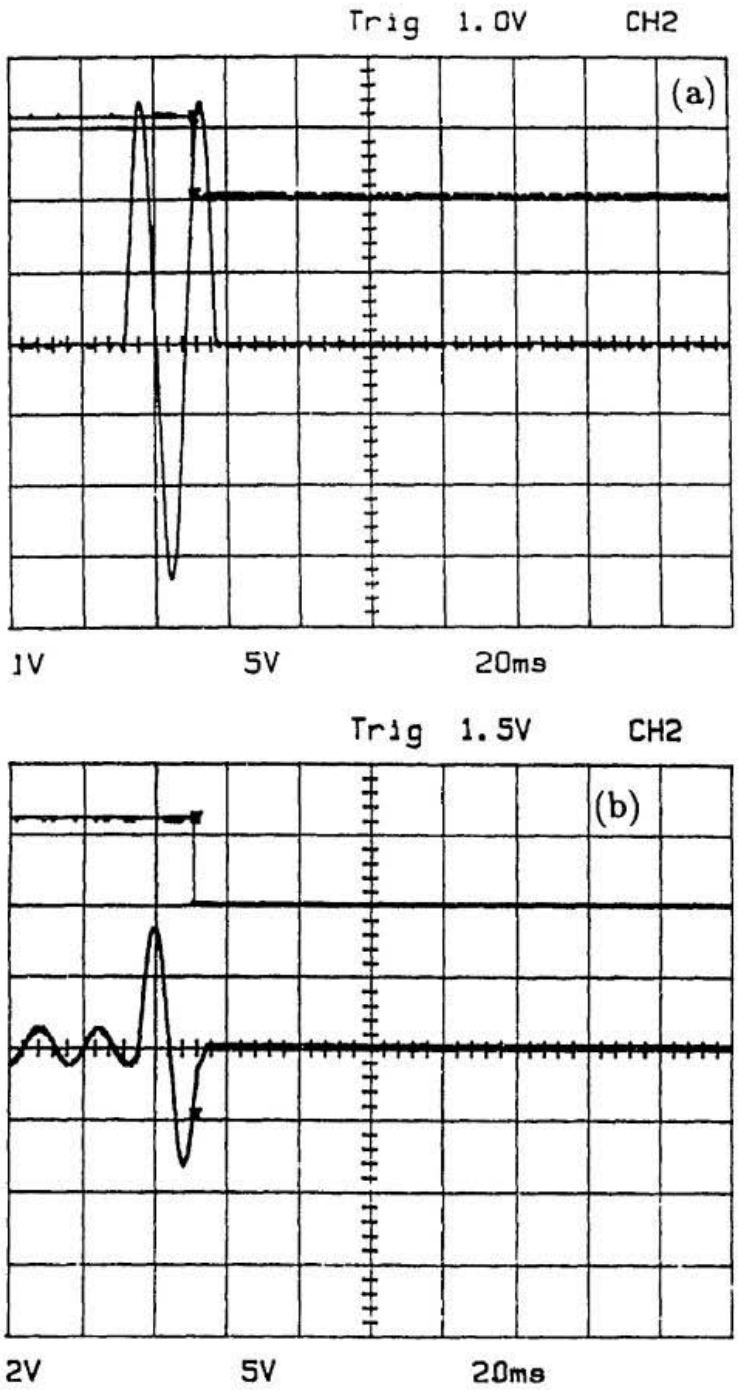

Figure 2.14: Response of DFT to secondary side faults: (a) phase to ground fault occurred before inrush without load, (b) phase to phase fault occurred after inrush with load; (Y-scale:1V = 12.5 A).

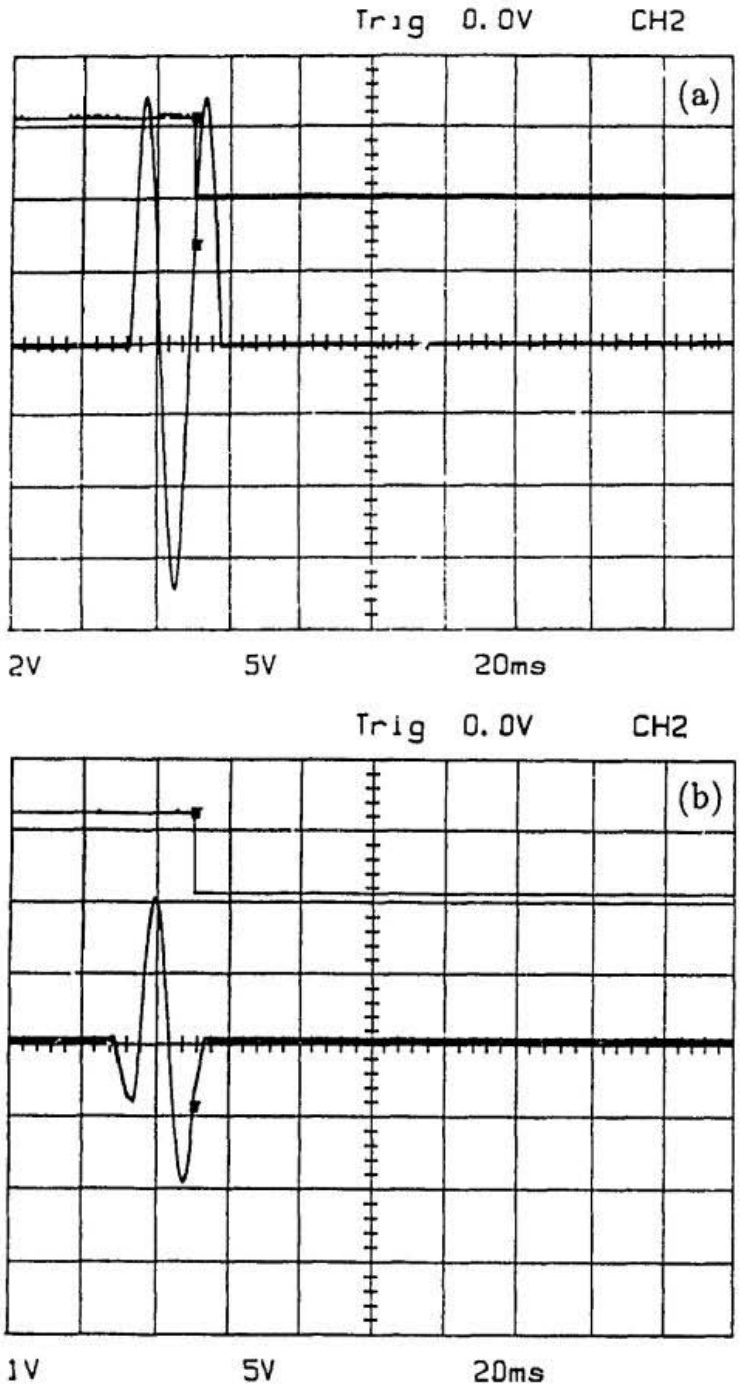

Figure 2.15: Response of DFT to secondary side faults: (a) phase to phase fault occurred before inrush without load, (b) between tap fault occurred before inrush with load; (Y-scale:1V = 12.5 A).

that there is a delay between the trip signal and the interruption of current. This is due to the characteristics of triac switches used in the experiment. It is also observed that the response time is threshold dependent. The results presented in this section are with a threshold of 17.7% for the second harmonic to fundamental ratio, which is same as used in reference [38]. The algorithm is tested with different thresholds and it is found that quicker response during fault is obtained at the expense of the system reliability. Thus, there is always a trade-off between the speed and the accuracy.

For transformer protection, differentiating between the internal fault current and magnetizing inrush current waveforms is still a big problem. The method described in this section works quite satisfactorily in theory. In practical situation, the harmonic contents of the differential current might get affected by many factors such as CT saturation, load tap changing, application of new transformer core material, etc.. Under these conditions, there is no guarantee that the algorithm will work properly since it is very sensitive to the relative distribution of the harmonic components of the signal. The recent development of artificial neural network (ANN) technology opens a new door to many research areas, particularly in pattern recognition applications. This technology might provide a better solution to the problem of distinguishing magnetizing inrush and fault currents. The following chapter provides an insight of the ANN which includes the general feed-forward neural network structure, its features and an efficient learning algorithm for the ANN. Also, a description of the innovative design of the ANN suitable for the successful adaptation in the power transformer protection is given in the next chapter.

Chapter 3

Artificial Neural Network

3.1 Introduction

In recent years, artificial neural networks (ANN) have gained wide attention and used successfully in many application areas. The concept of an ANN is derived from human brain structure which composed of billions of small building blocks known as the *neurons* having trillions of connections known as the *synapses* among them. Human brain is considered as a highly complex, nonlinear and parallel computer (information processing system) having the capabilities of organizing neurons to perform certain computational tasks such as pattern recognition, perception and motor control [74]. In many real-time applications, the same type of tasks are needed to be performed and it has been observed that human brain outperforms modern digital computers in pattern recognition and classification of real-time data in the presence of a noisy and distorting environment. Therefore, the features from the physiology of brain are borrowed as a basis of new processing model which brings into the picture today's artificial neural network technology.

The artificial neural networks is an information processing system that extracts

the information from the input and produces an output corresponding to the extracted information. Like human brain, ANNs also have the capabilities of learning and self organization. Moreover, the capabilities of performing massive parallel processing makes it more powerful than the conventional Von Neumann digital computers in which the instructions are executed sequentially [74]. ANNs can also provide, in principle, significant fault tolerance, since damage to a few links need not significantly impair the overall performance. A neural network not only provides a feasible solution to problems which are difficult to deal with, but also provides an insight of the nature of the problem. Neural network processing is distinguished from signal processing because of its inherent capability of dealing with nonlinearity. Modern signal processing techniques perform linear interpolation if an unfamiliar input signal is presented. That implies, the resulting output lies in a hyperplane between outputs for two known inputs. On the other hand, a neural network is fully capable of mapping the unfamiliar input vector to an arbitrary surface where it belongs to. Thus it can be said that an ANN generalizes instead of performing table-lookup.

As far as power system applications, there are some works where ANN has been successfully used to solve various problems such as load forecasting [61]-[64], detection of high impedance arcing faults and incipient faults [67]-[69], fault diagnosis of transformer [75], prediction of power system voltage harmonics [78], transient stability problem [33, 66], power system security assessment [63], etc.. Few works have been reported so far in area of power transformer protection [70]-[73].

As mentioned earlier, the concept of the ANN is extracted from human brain model which is a very composite structure with billions of neurons connected to each other in various fashions. There are many existing structures for the ANN. Among these structures, the feed forward neural network is quite popular. Also like the human

brain, the ANN needs to be trained as it has also the ability to learn something and recognize it later if properly trained. Therefore, besides designing a good structure of an ANN, it is also important to develop a good training algorithm. There exists many different training algorithms based on different criteria.

Pattern recognition is one of the problems where the ANN seems to be the best choice as a solution. The problem of transformer protection is considered as a pattern or current signature recognition problem. This thesis is a successful attempt in solving the transformer protection problem using the ANN. Since the ANN is a new field, the theoretical background of the ANN needs to be exposed before discussing the design of the ANN in this particular problem of distinguishing between magnetizing inrush and fault currents. In this chapter, a general feed forward neural network structure, its characteristics, working principle and the mathematical background of a training algorithm called back-propagation are discussed. This chapter also describes the proposed ANN based algorithm for power transformer protection.

3.2 General multi-layer feed-forward neural network structure

A general structure of the multi-layer feed-forward neural network (FFNN) is shown in Fig. 3.1. The main features of this structure can be summarized as follows :

- There are one input and one output layers.
- There may be a number of intermediate layers between the inputs and output layer. These layers are termed as hidden layers.

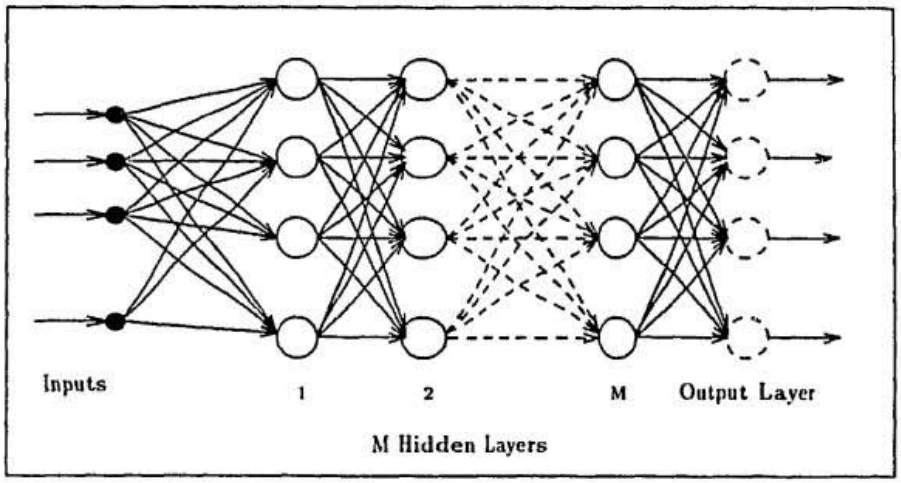

Figure 3.1: A general structure of FFNN

- Each layer consists of several elements known as neurons or processing units as shown in Fig. 3.1 by circles. These are information processing units which are fundamental to the operation of a neural network.

- The number of processing units in the input and output layers depend on the problem of interest. However, the choices of number of hidden layers and number of processing units in each hidden layer are matter of trial and error [74]. It is better to have as small a structure as possible in terms of time requirement. However, too small a structure might run into instability problem and thus might never converge. So it is really important to go through trial and error before the choice has been finally made.

- The source nodes in the input layer of the network supply respective elements of the input vector in the second layer (first hidden layer) of the network. The output of this layer serves as the input to the third layer and so on.

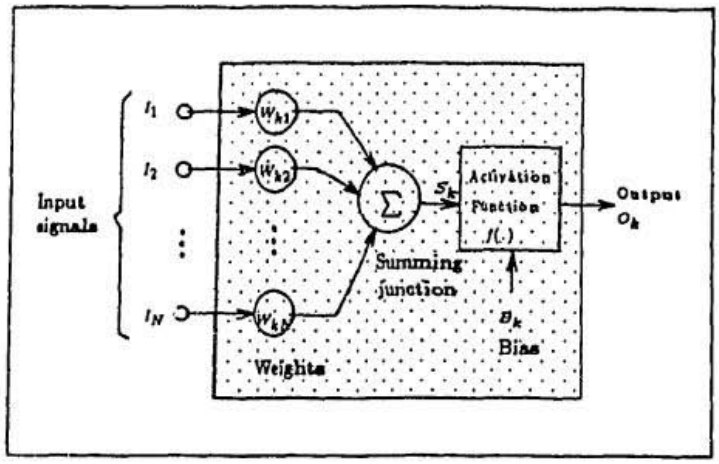

Figure 3.2: A neuron model

- The input of each element in a particular layer originates from all the outputs of all units from the previous layer. Although there are some alternate structures in the literature, those will not be considered in this work.

3.2.1 Neuron model

Figure 3.2 shows the basic structure of a processing unit or neuron. The followings are the three basic elements :

- A set of connecting links associated with a weight or strength of its own. For example in Fig. 3.2, the link between the signal X_j at the j^{th} input node is connected to the k^{th} neuron by a synaptic weight of W_{kj}.
- An adder for summing up all input signals weighted by corresponding synapses of the input.
- An activation function for limiting the amplitude of the output of a neuron.

Each neuron is also associated with a bias factor denoted by B_k for the k^{th} neuron. In general, the mathematical equations which are acting on a neuron k can be described

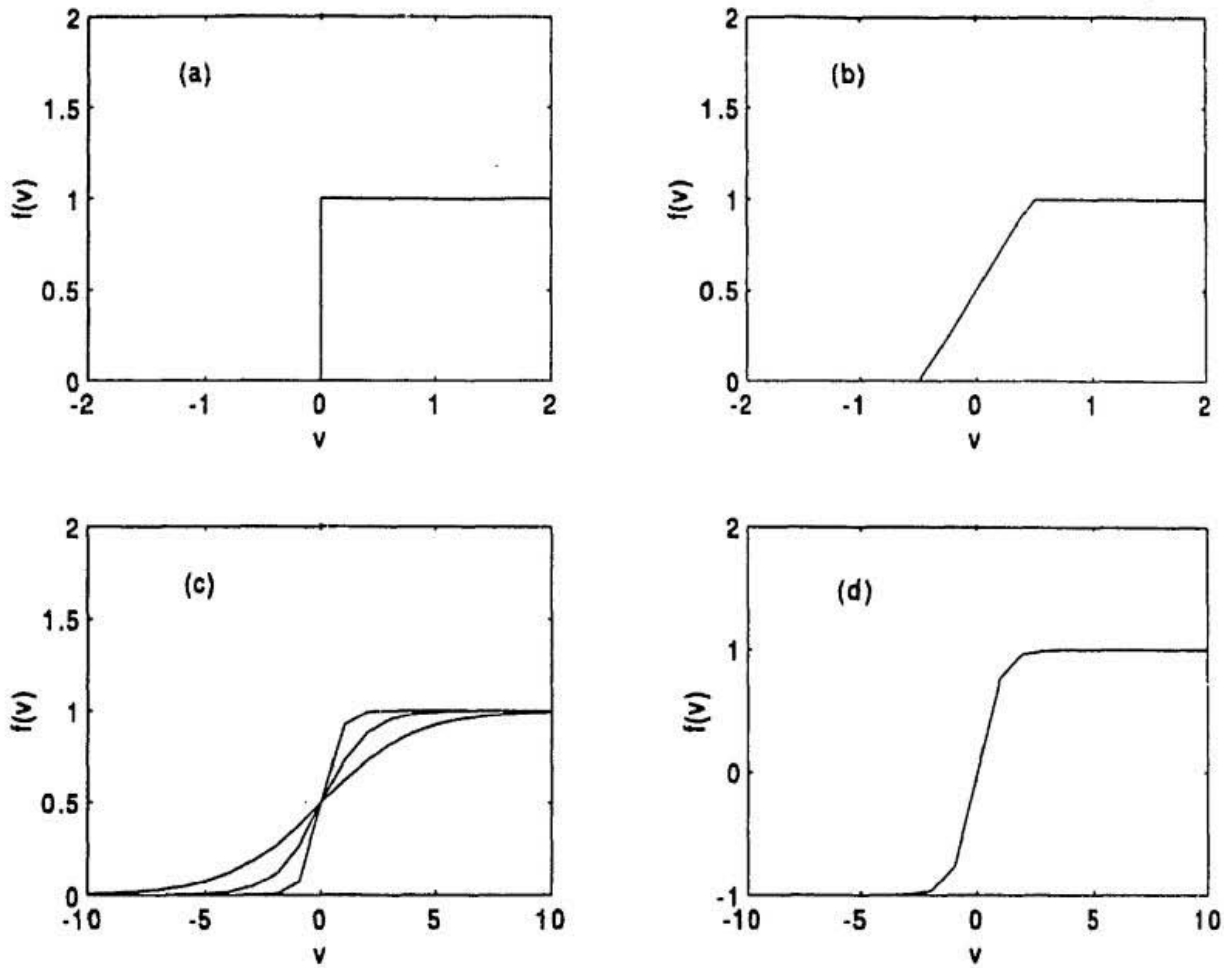

Figure 3.3: Different activation functions; (a) threshold, (b) piecewise linear, (c) log-sigmoid, (d) tan-sigmoid

as follows :

$$sum_k = \sum_{j=1}^{N} W_{kj} X_j \tag{3.1}$$

$$Y_k = f(sum_k + B_k) \tag{3.2}$$

where $X_1, X_2, ..., X_N$ are the input signals ; $W_{k1}, W_{k2}, ..., W_{kN}$ are the synaptic weights of neuron k; sum_k is the linear combiner output; B_k is the bias; $f(.)$ is the activation or transfer function; and Y_k is the output signal of the neuron.

3.2.2 Activation function

The activation or transfer function, denoted by $f(.)$, is acted on the summation of sum_k and the corresponding bias B_k. This defines the output of the neuron in terms of the activity level at its input. The followings are the most commonly used activation functions :

1. **Hard Limiter :** This function shown in Fig. 3.3(a), is mathematically defined as :

$$f(v) = \begin{cases} 1 & \text{if } v \geq 0 \\ 0 & v < 0 \end{cases} \tag{3.3}$$

2. **Piecewise-Linear Function :** The piecewise linear function as depicted in Fig. 3.3(b), can be mathematically expressed as :

$$f(v) = \begin{cases} 1 & \text{if } v \geq \frac{1}{2} \\ (v + \frac{1}{2}) & \frac{1}{2} > v > -\frac{1}{2} \\ 0 & v \leq -\frac{1}{2} \end{cases} \tag{3.4}$$

where the amplification factor inside the linear region of operation is assumed to be unity.

3. **Sigmoidal Function :** This the most common activation function used in ANNs so far. An example of sigmoidal function is log-sigmoid which can be defined as:

$$f(v) = logsig(v) = \frac{1}{1 + e^{-mv}} \tag{3.5}$$

where m is the slope parameter of the sigmoid function. By varying the slope m, different shapes of log-sigmoid can be obtained as shown in Fig. 3.3 (c). Another well-known sigmoid is the tan-sigmoid which can be defined as:

$$f(v) = tansig(v) = \frac{1 - e^{-2v}}{1 + e^{-2v}} \tag{3.6}$$

In all of the above cases, $v = sum_k + B_k$.

3.3 Back-propagation Algorithm

A feed forward neural network (FFNN) is applied successfully for solving problems by training them in a supervised manner with a highly popular algorithm known as the error back-propagation or simply back propagation algorithm [74]. The back-propagation algorithm consists of two passes through the different layers of the network :

- A forward pass: During this pass, input vector is applied to the sensory nodes of the network and its effect propagates through the network layers in the forward direction until it reaches the output layer. Finally, a set of outputs is produced as the actual response of the network. During the forward pass, there is no change in the weight and the bias.

- A backward pass: During this pass, the weights are all adjusted in accordance with the error correction rule. An error is the difference between the target and actual response. The target is known as it is specified before training the ANN and the actual response is obtained through the forward pass. The error signal is propagated back-ward through the network. The weights and biases are adjusted so as to make the actual response of the network closer to the target or desired response.

3.3.1 Network training

For a given vector set of P pairs $(X_1, Y_1), (X_2, Y_2), ..., (X_p, Y_p)$, if there exists a non-linear functional relationship between X and Y

$$Y = \phi(X) \tag{3.7}$$

where $X \in R^N, Y \in R^M$ and R is the set of real numbers, the objective is to train the network so that it learns an approximation [74]

$$Y' = \phi(X)' \tag{3.8}$$

It is worth mentioning that learning of an ANN means finding an appropriate set of weights and biases for which the discrepancy between the Y and Y' would be within a specified tolerable limit. The ANN performs the nonlinear as well as multi-dimensional mapping between inputs and outputs. It is done through extensive training with given input and target vectors. The input vector should contain data such as it covers as much the entire input space as possible. The "steepest-descent gradient" is used in this algorithm. For simplicity the algorithm is described below in detail for an FFNN with one hidden layer. However, this can be easily extended for an FFNN with more than one hidden layer.

3.3.2 Calculation of input/output to hidden and output layer

A vector $X_p = (X_{p1}, X_{p2}, ..., X_{pN})^t$ corresponding to pattern p is applied to the input layer of the network as shown in Fig. 3.1. The net input net, to the j^{th} hidden unit is given by

$$net_j^h = \sum_{i=1}^{N^h} W_{ji}^h X_i + B_j^h \tag{3.9}$$

where the superscript h refers to the quantities at hidden layer, W_{ji}^h is the weight on the connection from the i^{th} input unit to j^{th} neuron at the hidden layer, B_j^h is bias and N^h is the number of neurons in hidden layer.

The output O_j^h, of the jth neuron at the hidden layer can be written as:

$$O_j^h = f_j^h(net_j^h) \tag{3.10}$$

The equations for the k^{th} output node can be calculated in similar fashion as shown below :

$$net_k^o = \sum_{j=1}^{N^o} W_{kj}^o O_j^h + B_k^o \tag{3.11}$$

$$O_k^o = f_k^o(net_k^o) \tag{3.12}$$

where W_{kj}^o is the weight on the connection from the jth neuron of the hidden layer to the k^{th} neuron of the output layer and N^o is the number of neurons in output layer. The superscript 'o' refers to the output layer quantities.

3.3.3 Cost function minimization

As mentioned above, the weights and biases need to be updated until a desired error goal is achieved. The error function of k^{th} output unit for pattern p is given by:

$$E_{pk} = (Y_{pk} - O_{pk}^o) \tag{3.13}$$

where Y_{pk} is the target and O_{pk}^o is the actual output from the kth unit. The total sum squared error also known as the cost function for all the output units for pattern p is given by :

$$\begin{aligned} E_p &= \frac{1}{2}\sum_k E_{pk}^2 \\ &= \frac{1}{2}\sum_k (Y_{pk} - O_{pk}^o)^2 \end{aligned} \tag{3.14}$$

The main objective of the ANN training is to minimize this function for all the patterns. The changes in weights and biases at hidden layer and output layer are determined in the following section. For the sake of simplicity the subscript p is omitted throughout the following derivation. However, it has to be remembered that the cost function needs to be minimized for all output units and for all input patterns.

3.3.4 Output-layer weight and bias updating

According to the steepest descent algorithm, in order to minimize the cost function the change or correction needed in weights at the output layer are proportional to the negative slope of the cost function i.e.

$$\Delta W_{kj}^{o} \propto -\frac{\delta E}{\delta W_{kj}^{o}} \tag{3.15}$$

Now using the chain rule and with few manipulations, it can be written as :

$$\frac{\delta E}{\delta W_{kj}^{o}} = -(Y_k - O_k^{o}) \times \frac{\delta O_k^{o}}{\delta net_k^{o}} \times \frac{\delta net_k^{o}}{\delta W_{kj}^{o}} \tag{3.16}$$

Differentiating both sides of Equations (3.11) and (3.12) with respect to W_{kj}^{o} and net_k^{o}, respectively, the following are obtained

$$\frac{\delta net_k^{o}}{\delta W_{kj}^{o}} = O_j^{h} \tag{3.17}$$

$$\frac{\delta O_k^{o}}{\delta net_k^{o}} = f_k^{o\prime}(net_k^{o}) \tag{3.18}$$

Substituting Equations (3.17) and (3.18) in Equation (3.16), one gets :

$$\frac{\delta E}{\delta W_{kj}^{o}} = -(Y_k - O_k^{o}) f_k^{o\prime}(net_k^{o}) O_j^{h} \tag{3.19}$$

Thus the changes in weights and biases can be derived as shown below :

$$\begin{aligned} \Delta W_{kj}^{o} &\propto -\delta E/\delta W_{kj}^{0} \\ &= -\eta\ \delta E/\delta W_{kj}^{0} \end{aligned} \tag{3.20}$$

where η is the learning rate parameter of the back-propagation algorithm. The use of negative sign in Equation (3.20) accounts for gradient descent in weight space.

From Equations (3.19) and (3.20), the change in weight W_{kj}^{o} is found to be :

$$\Delta W_{kj}^{o} = \eta(Y_k - O_k^o) f_k^{o\prime}(net_k^o) O_j^h \tag{3.21}$$

$$= \eta \delta_k^o O_j^h \tag{3.22}$$

where $\delta_k^o = (Y_k - O_k^o) f_k^{o\prime}(net_k^o)$ is referred to as the local gradient. Following the same procedure for updating the bias factor of the k^{th} output unit, ΔB_k^o, the following is obtained as:

$$\Delta B_k^0 = \eta(Y_k - O_k^o) f_k^{o\prime}(net_k^o) \tag{3.23}$$

$$= \eta \delta_k^o \tag{3.24}$$

$$\tag{3.25}$$

Finally, the weight and bias on the kth neuron at the output layer are updated as :

$$W_{kj}^{o}(n+1) = W_{kj}^{o}(n) + \Delta W_{kj}^{o}(n) \tag{3.26}$$

$$B_k^o(n+1) = B_k^o(n) + \Delta B_k^o(n) \tag{3.27}$$

3.3.5 Hidden layer weight and bias updating

Similarly, the weights and biases are updated for the connections and neurons at the hidden layer. The gradient of mean-squared error for the hidden layer weight on the

j^{th} neuron is given by :

$$\begin{aligned}\frac{\delta E}{\delta W_{ji}^h} &= \frac{1}{2}\sum_k \frac{\delta(Y_k - O_k^o)^2}{\delta W_{ji}^h} \\ &= -\sum_k (Y_k - O_k^o) \times \frac{\delta O_k^o}{\delta net_k^o} \times \frac{\delta net_k^o}{\delta O_j^h} \times \frac{\delta O_j^h}{\delta net_j^h} \times \frac{\delta net_j^h}{\delta W_{ji}^h} \end{aligned} \tag{3.28}$$

Now differentiating Equations (3.9)-(3.12) with respect to W_{ji}^h, net_j^h, O_j^h and net_k^o, respectively or- ts

$$\frac{\delta net_j^h}{\delta W_{ji}^h} = X_i \tag{3.29}$$

$$\frac{\delta O_j^h}{\delta net_j^h} = f_j^{h'}(net_j^h) \tag{3.30}$$

$$\frac{\delta net_k^o}{\delta O_j^h} = W_{kj}^o \tag{3.31}$$

$$\frac{\delta O_k^o}{\delta net_k^o} = f_k^{o\prime}(net_k^o) \tag{3.32}$$

Substituting the above set of equations in Equation (3.28), the following relation can be achieved.

$$\frac{\delta E}{\delta W_{ji}^h} = -\sum_k (Y_k - O_k^o) f_k^{o\prime}(net_k^o) W_{kj}^0 f_j^{h'}(net_j^h) x_i \tag{3.33}$$

Applying the delta rule, the change in weight in the hidden layer on the j^{th} neuron can be written as [74]:

$$\begin{aligned}\Delta W_{ji}^h &= -\eta \frac{\delta E}{\delta W_{ji}^h} \\ &= \eta f_j^{h'}(net_j^h) X_i \sum_k (Y_k - O_k^o) f_k^{o\prime}(net_k^o) W_{kj}^0 \\ &= \eta f_j^{h'}(net_j^h) X_i \sum_k \delta_k^o W_{kj}^0 \\ &= \eta \delta_j^h X_i \end{aligned} \tag{3.34}$$

where

$$\delta_j^h = f_j^{h'}(net_j^h) \sum_k \delta_k^o W_{kj}^o \tag{3.35}$$

Similarly, the change in bias factor of j^{th} neuron on hidden layer, ΔB_j^h is given by :

$$\Delta B_j^h = \eta \delta_j^h \tag{3.36}$$

Therefore, the updated weights and biases at the hidden layer on j^{th} neuron at $(n+1)^{th}$ instant are given as:

$$W_{ji}^h(n+1) = W_{ji}^h(n) + \eta \delta_j^h X_i \tag{3.37}$$

$$B_{ji}^h(n+1) = B_{ji}^h(n) + \eta \delta_j^h \tag{3.38}$$

3.3.6 Summary of the algorithm

After knowing how to calculate the various quantities needed during the training, it seems worthwhile to summarize the complete algorithm. The following are the steps which are involved in this algorithm

1. Applying the input training vector pairs X_p and Y_p.

2. Calculating the net input to the hidden layer units :

$$net_{pj}^h = \sum_{i=1}^{N} W_{ji}^h X_{pi} + B_j^h \tag{3.39}$$

   where N^h is the number of units in the hidden layer.

3. Calculate the output of the hidden layer units which will be the input of the output layer units as shown below :

$$O_{pj}^h = f^h(net_{pj}^h) \tag{3.40}$$

4. Calculating net input to the output layer units :

$$net_{pk}^o = \sum_{j=1}^{N^o} W_{kj}^o net_{pj} + B_k^o \tag{3.41}$$

5. Calculating the ANN outputs :

$$O^o_{pk} = f^o(net^o_{pk}) \tag{3.42}$$

6. Calculating the error terms for the output units :

$$\delta^o_{pk} = (Y_{pk} - O^o_{pk}) f^{o\prime}(net^o_{pk}) \tag{3.43}$$

7. Calculating the error terms for the input units :

$$\delta^h_{pj} = (Y_{jk} - O^h_{pj}) f^{h\prime}(net^h_{pj}) \tag{3.44}$$

8. Updating the weights and biases on the output layer :

$$W^o_{kj}(n+1) = W^o_{kj}(n) + \eta \delta^o_{pk} O^h_{pj} \tag{3.45}$$

$$B^o_{kj}(n+1) = B^o_{kj}(n) + \eta \delta^o_{pk} \tag{3.46}$$

9. Updating the weights and biases on the hidden layer :

$$W^h_{ji}(n+1) = W^h_{ji}(n) + \eta \delta^h_{pj} X_{pi} \tag{3.47}$$

$$B^h_{ji}(n+1) = B^h_{ji}(n) + \eta \delta^h_{pj} \tag{3.48}$$

10. Calculating the error term :

$$E_p = \frac{1}{2} \sum_{k=1}^{N^o} E^2_{pk} \tag{3.49}$$

11. When the error is sr aller than a pre-defined value for all training-vector pairs (X_p, Y_p), the training is stopped.

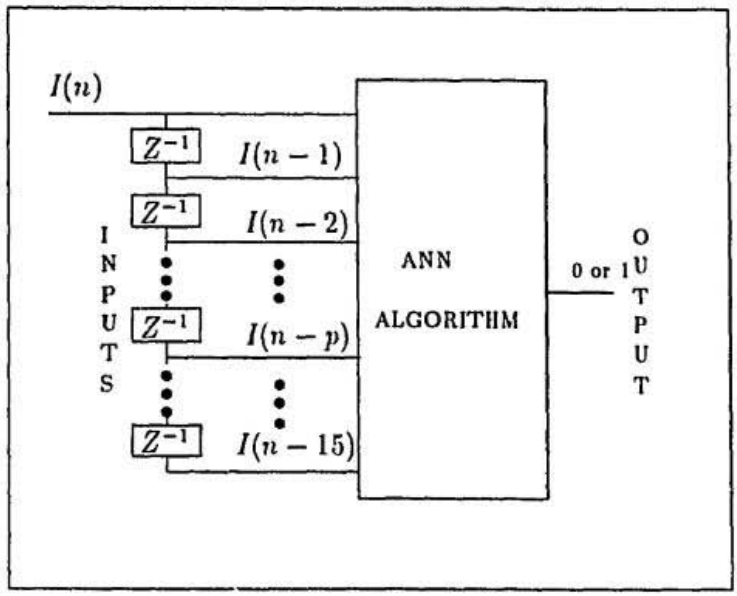

Figure 3.4: The ANN Inputs and Output

3.4 Proposed ANN Design

The most difficult part in applying the ANN technique to any particular problem is to formulate the problem in such a way that ANN can be applied to it. The first step to formulate the problem is to find out the inputs and outputs of the ANN. For the application of power transformer protection, the differential current samples are chosen as the input. The choice is made based on the fact that the differential current contains the information of the transformer conditions i.e. whether the transformer is experiencing a fault or magnetizing inrush. Most of the existing relays also use the differential current samples as the input to the digital relaying algorithm for distinguishing between magnetizing inrush current and fault current [45]-[48]. The next question is how many samples per cycle must be used so that there is enough information in the data, at the same time, the sampling interval is long enough for

processing the data. The sampling rate thus plays an important role in the design. The higher the sampling rate, the better the information content. On the other hand, higher sampling rate means less time available for computation. Spectrum analysis of the differential currents under fault, inrush and over-excitation conditions, reveals that the fundamental, second and fifth harmonic components are significant harmonic components in the differential current [2]. To accommodate up-to fifth harmonic in the sampled current data, the sampling frequency should be at least 600 Hz. Considering the speed of the digital signal processor, the computational requirement and the frequency contents of the current data, a sampling rate of 16 samples per cycle, i.e., 960 Hz. is chosen. For a three phase transformer, there will be three differential currents at each instant. However for training purposes, it is not required to sample all of them, rather the current of one of the three phases is adequate. At each instant, a window of 16 consecutive current samples (the present sample and previous 15 samples) is taken as depicted in Fig. 3.4. Thus the input vector of the ANN is of length 16. The 16 inputs of the ANN are represented by 16 nodes in the input layer of the ANN structure. Once the inputs are defined the output of the ANN is determined. There is one binary output in this ANN, which determines whether or not there is a fault in the transformer. In this work, a value of 0 indicates no-fault (including inrush and over-excitation) and 1 indicates an internal fault. The output of the ANN represents one neuron in the output layer.

After the inputs and output are defined, the next task is to incorporate the hidden layer(s) in the network. In the proposed ANN design, one hidden layer is chosen. The number of units in the hidden layer is varied over a range of 12 to 2. Finally the ANN with 3 hidden units are found to be the optimum structure in terms of computational speed and accuracy. The training of the ANN is done using log-sigmoidal transfer

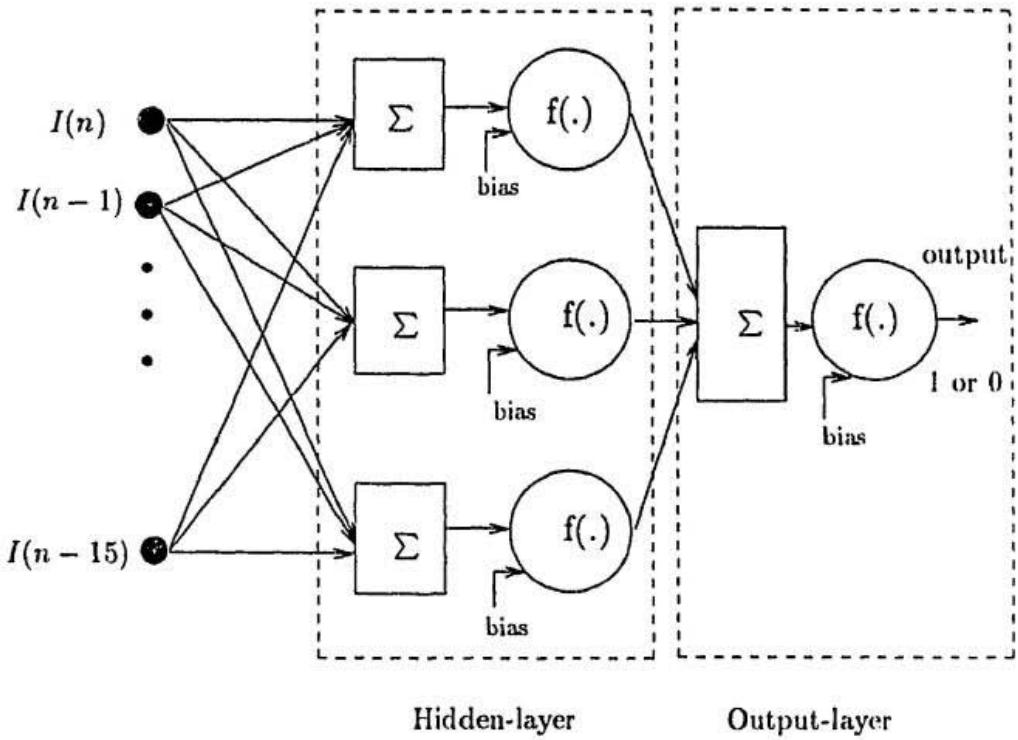

Figure 3.5: The proposed ANN structure for the transformer protection

functions with slope parameter one for all neurons in the hidden layer and output layer. The complete ANN structure for the power transformer protection is shown in Fig. 3.5.

It is worth noting that in the present work, the protection of the transformer using the ANN involves both off-line and on-line implementation. Therefore, it is important to design the network such that the real-time implementation would be easily possible. In real time implementation, one of the major concerns is the number of computations and the time required to do that. For this particular ANN structure, the number of arithmetic computations needed are 47 additions, 51 multiplications and 4 nonlinear

sigmoidal function evaluations. The implementation of the nonlinear function can be difficult and time consuming. One of the alternate options is to replace each nonlinear function with a hard-limiter, provided that the ANN still gives accurate result [70]. Therefore, the ANN has been tested with the software implementation of hard-limiter instead of the nonlinear sigmoidal function evaluation. The software implementation of each hard-limiter requires one comparison (greater than or less than) and decision making (IF statement) statement evaluation. In the proposed ANN structure, there are four hard-limiters.

After the network is designed it needs to be trained with input data. The inputs for this ANN are the sampled current data obtained from experimental data for the magnetizing inrush and different internal fault conditions. The experimental setup, data acquisition and data processing before training the network are described in details in Chapter 4. Also covered in Chapter 4 are: ANN training, off-line test results and a comparison study between the DFT and the ANN algorithms for power transformer protection.

Chapter 4

Training and Off-line Testing of the ANN

This chapter presents an overview of the experimental setup which was used for acquiring current data under different inrush, fault and over-excitation conditions. The data are used to train the ANN so that the ANN is able to recognize the fault and can differentiate between a fault and a no-fault condition. It is possible to train such networks with large amount of simulated data. However, it should be noted that it is still quite difficult to accurately simulate the current particularly for different types of inrush situations in a three phase power transformer. The ANN needs to be trained with a reliable set of inrush and fault current data to cover all possible types that the transformer may experience.

After training the network with one set of data which includes many current samples during various inrush, fault and over-excitation conditions, the network is tested off-line with a different set of data. The off-line test results are presented at the end of this chapter. Also, a comparative study is made between the ANN and DFT algorithms under different normal and adverse operating conditions.

4.1 Experimental Setup for Acquiring Inrush and Fault Data

One of the major tasks of this work is to obtain different inrush and internal fault current data for training and testing purposes. In this work, the experimental data are used for training and off-line testing of the ANN. All experiments are carried on a 5 kVA, 230/550 – 575 – 600V, Δ-Y laboratory prototype power transformer. The circuit diagram of the transformer is given in Fig. 4.1. In Fig. 4.1, three identical CTs were used in the primary side and another three identical CTs were used in the secondary side of the transformer. The ratios of the primary side CTs and the secondary side CTs were chosen such that the differential current would be nearly zero under normal operating condition. The differential current was taken at point 'x' in Fig. 4.1 throughout the experiment. The current data were captured using a Textronics current probe and the TM-503 amplifier unit.

The magnetizing current may take various forms depending on the residual magnetism and the point on the voltage waveform at the time of switching. It is worth mentioning that the magnetizing inrush waveshape at no-load is different than that at load, and both cases have been considered. To acquire the inrush current data, the transformer was energized at random at both no-load and load conditions. Although there are six typical shapes according to reference [70], it was ensured that all possible cases were being taken into account by switching the transformer many times. The current data have been sampled at a frequency of 20kHz and stored in a Tektronix 2212 digital storage oscilloscope; which were next down loaded to the personal computer (PC) though the general purpose interface bus (GPIB). The software package Grab 2212 were used to acquire the data in a format which were latter converted to

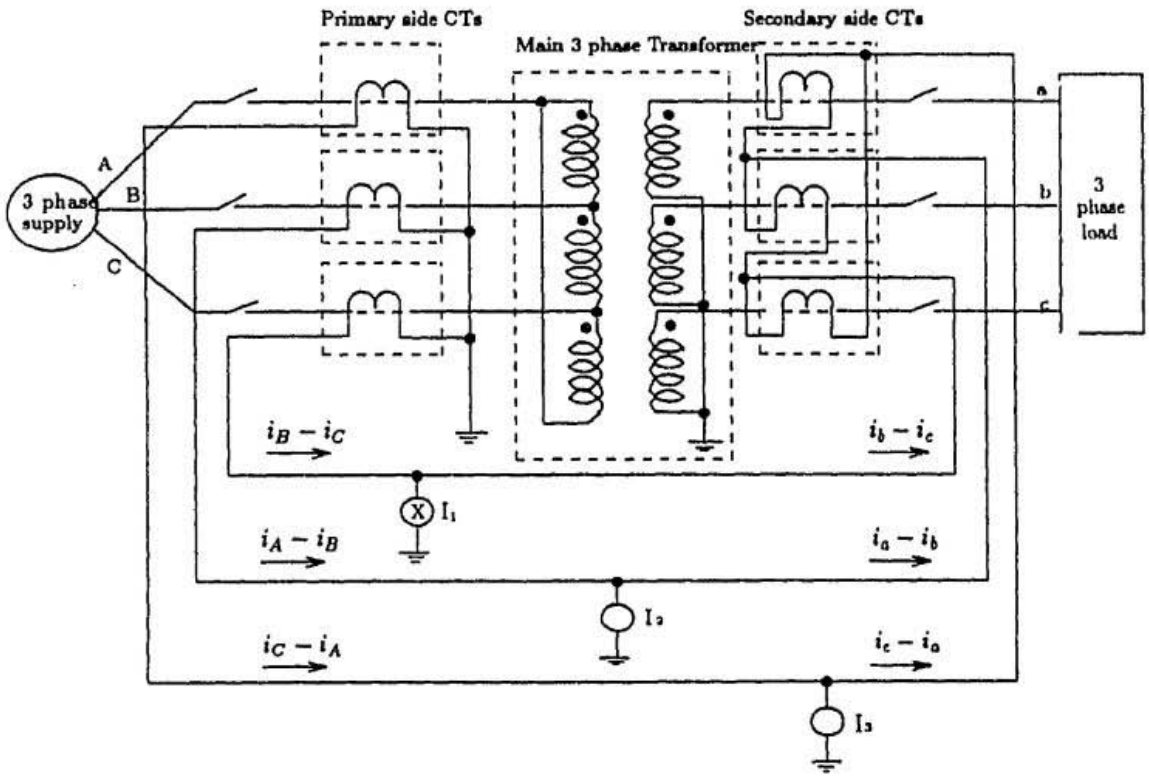

Figure 4.1: Experimental setup for simulating various fault and inrush cases

ASCII for further processing. For each switching, the data obtained were saved in a file. Three identical triac switches and associated control circuits have been used to make the contact between the transformer and the supply for a certain period of time. The details of the triac switch and the electronic circuit are given in the Appendix-A.

A three phase load was connected to the transformer secondary through a 15A breaker which is switched on for taking the readings for different load conditions.

It is worth mentioning that there are large number of different types of internal faults that can occur before or after the transformer is energized and the current waveshapes would be different for these cases even if the fault is same. Many typical faults including line to ground, phase to phase, between taps, external faults, etc. have been investigated. Also, the over-excitation case has been studied. Table 4.1 shows the different inrush and fault cases which have been investigated in this work.

The over-excitation condition has been obtained by increasing the supply voltage by 28% which is about 295 V phase to phase. The data for all cases where the fault has occurred before the energization were taken several times in order to consider the inrush effect on the top of the fault. For each fault data collection, a resistance is used in series with faulty circuit. The resistance does not change the overall waveshape, rather reduces the magnitude of the fault current. Three identical triac switches are used in three phases and those are controlled by three identical controlling circuits with one common push-button switch. For taking the data for other fault cases i.e. which occurred after energization, one triac switch is used in series with the faulty branch. The control circuit of the triac switch is designed in such a way that the fault current never flows through the circuit for more than 5 cycle time period. The data were stored in separate file for each fault type and also for different inrush conditions for the same fault which occurred before inrush.

Table 4.1

List of fault and energization studies

case no.		
	Internal fault on primary	
1	phase to phase fault	no load, after energization
2	phase to phase	loaded, after energization
3	phase to phase	no load, before energization
4	phase to phase	loaded, before energization
	Internal fault on secondary	
5	phase to phase	no load, after energization
6	phase to phase	loaded, after energization
7	phase to phase	no load, before energization
8	phase to phase	loaded, before energization
9	line to ground	no load, after energization
10	line to ground	loaded, after energization
11	line to ground	no load, before energization
12	line to ground	loaded, before energization
13	between tap	no load, after energization
14	between tap	loaded, after energization
15	between tap	no load, before energization
16	between tap	loaded, before energization
	Other cases	
17	over excitation	no load
18	over excitation	loaded
	Energization	
19	inrush with no load	
20	inrush with load	

It should be mentioned here that the next chapter discusses the experimental setup for the on-line tests of the ANN based algorithm for transformer protection. The setup is very similar to what has been shown in Fig. 4.1, except it includes another set of switches which is controlled by the decision of the ANN. The test procedures for Table 4.1 are explained more elaborately in the following chapter.

4.2 Data Processing and the ANN Training

The experimental data files as described in the previous section need to be processed before it can be used for the ANN training. The data obtained after converting them to ASCII format are a series of current samples for about five cycles taken at 20 kHz. At first, these data are down sampled by a factor which gives the resulting data a sampling frequency of 960 Hz. The input pattern consists of 16 consecutive current samples. A window of 16 samples per cycle is slided over the five-cycle data, and for each file 64 input patterns are thus extracted. At first, the absolute value of each sample is taken and then this value is compared to the predefined threshold which gives a binary value of either 0 or 1 depending on whether the value is smaller or greater than the threshold, respectively. The threshold is taken as ten times the value of rated differential current under normal condition which is about 5% of the rated primary current of the transformer. Thus each pattern becomes a 16 bit binary number. It is worth mentioning that in order to incrase the information content of the data, two levels of thresholds are also used in processing the data. However, in that case, it was difficult to obtain the desired convergence of the ANN training. Fig. 4.2 shows the block diagram of the complete data processing scheme. Among the possible $2^{16} = 65536$ different combinations of 0 and 1, it is expected that the inrush

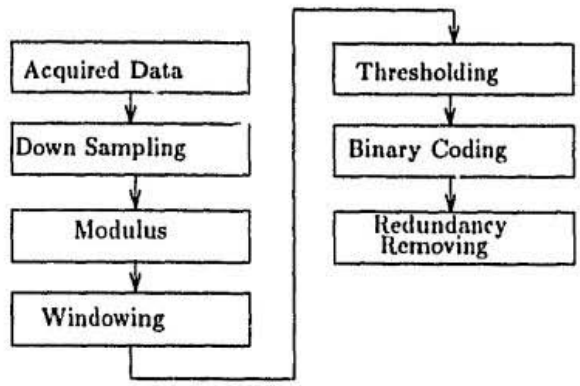

Figure 4.2: Block diagram for processing data prior to ANN Training

and the fault would not have same combinations. However, there would be multiple patterns (combinations of 0 and 1) which are identical in each file and also between same type (either inrush or fault) of the data files. The redundant and duplicate data have been removed after windowing. A set of inrush patterns and another set of fault patterns are found. There are 152 inrush and over-excitation patterns and 44 fault patterns which form an input matrix for the ANN of size 196×16. The target output is given as a vector of length 196 which consists of 152 zeros followed by 44 ones corresponding to the inrush and fault cases, respectively.

Once the input matrix and target vector are ready, the ANN is trained using the MATLAB Neural Network Tool-box [79]. The function *trainbpx*, which is the improved back-propagation algorithm has been used for the training purpose. The improved back-propagation algorithm uses adaptive learning rate and attempts to avoid local minima using a momentum factor [79]. After training, two sets of weight and bias, $[W_1, B_1]$ and $[W_2, B_2]$, have been obtained for the hidden layer and output layer, respectively. These are given in Appendix-B. The training has been done using

log-sigmoidal transfer functions for all units in the hidden layer and the output layer. First, the off-line tests were performed by using log-sigmoidal function. In order to speed up the computation, the log-sigmoidal functions were replaced by software-implemented hard-limiters and the same tests were carried out. It has been observed that the ANN performs accurately with the hard-limiters. The off-line test results in the following section are obtained by using the software-implemented hard-limiter functions for the both the hidden-layer and the output-layer units.

4.3 Off-line Test Results

Once the ANN is trained, it was tested using an appropriate set of weights and biases on a different set of input data. It can be seen from Figs. 4.3-4.7 that for different inrush and fault waveforms, the ANN based algorithm responded accurately according to the input pattern. The decisions in all fault cases were made within one cycle. Figures 4.3(a)-(d) illustrate some samples of primary side phase to phase faults. In Figs. 4.3(a) and (b), the phase to phase faults occurred long after energizing the transformer, without load and with load, respectively. The inrush does not have any effects in these faults. The ANN correctly identified the faults within three quarter of a cycle time period. The same fault without load and with load, but occurred before energizing the transformer are shown in Figs. 4.3(c) and (d), respectively. Although there are some effects of inrush on the waveforms as shown in Figs. 4.3(c) and (d), the ANN had no problem recognizing them as faults and thereby sending the appropriate trip signal. Figures 4.4(a)-(d) demonstrate the secondary side phase to phase faults. In Figs. 4.4(a) and (b), the fault has occurred while the transformer was in operation without and with load, respectively. The ANN responded accurately and promptly

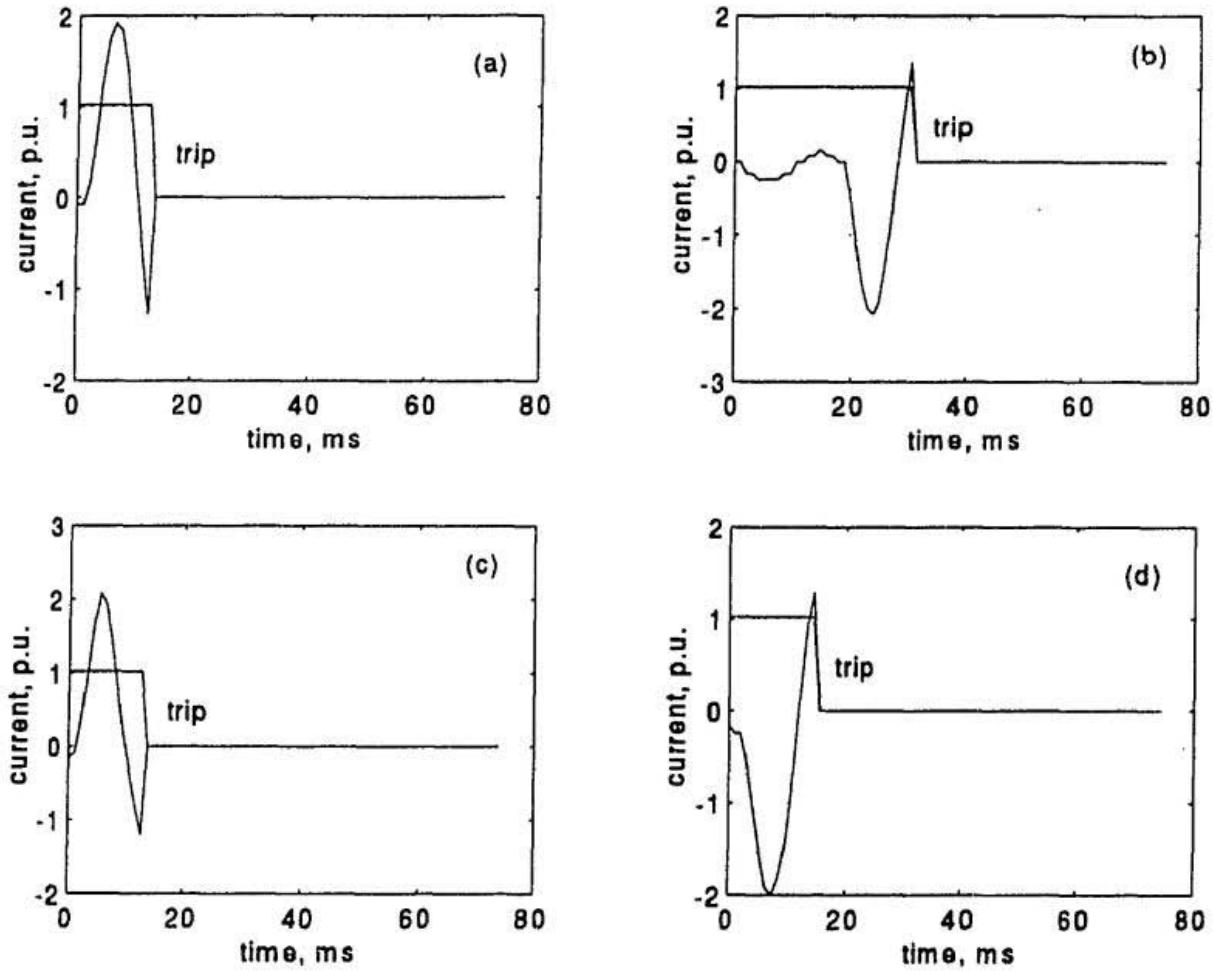

Figure 4.3: ANN responses to primary side phase to phase faults faults: (a) after inrush without load, (b) after inrush with load, (c) before inrush without load; (d) before inrush with load; (Y-scale: 1 p.u. = 12.5 A).

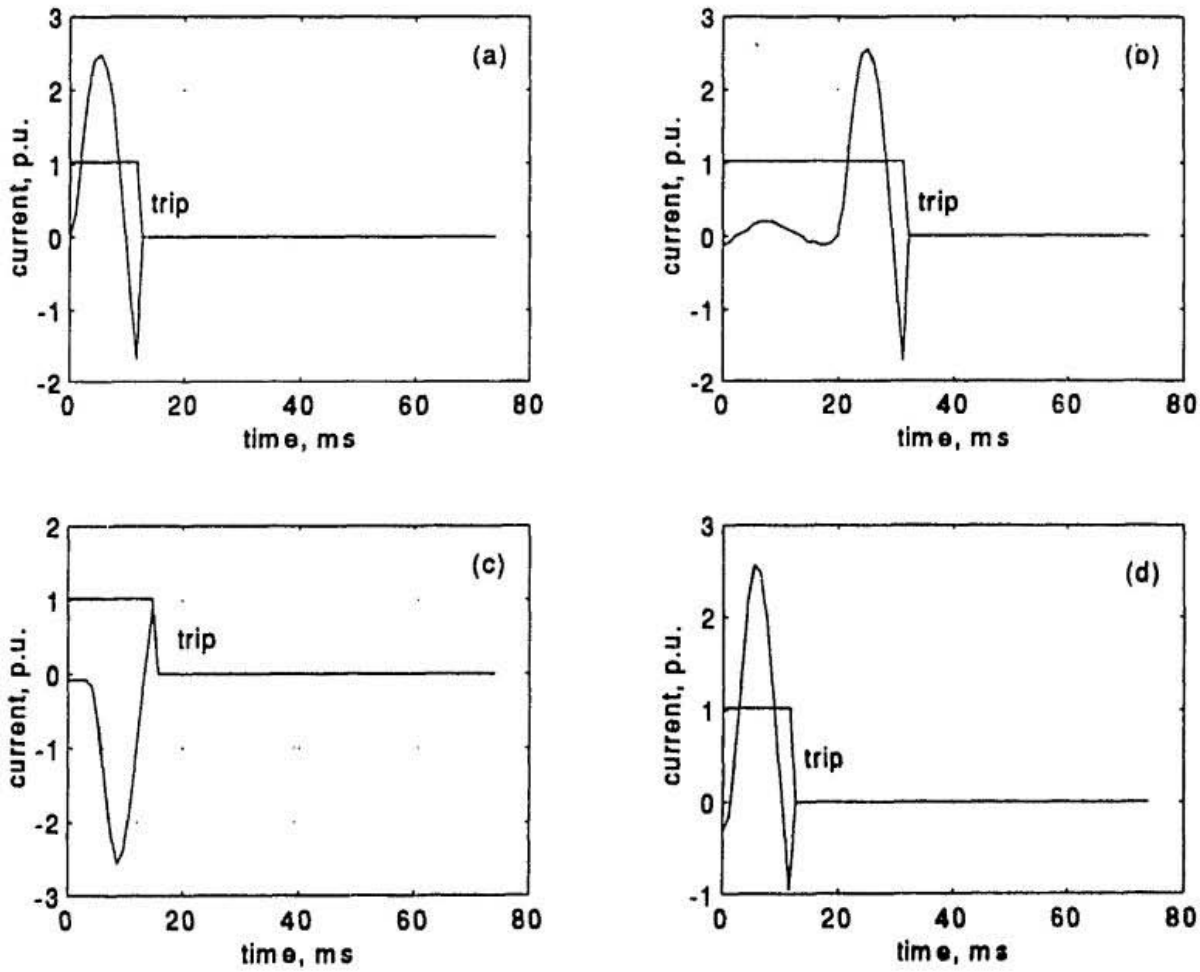

Figure 4.4: ANN responses to secondary side phase to phase faults : (a) after inrush without load, (b) after inrush with load, (c) before inrush without load; (d) before inrush with load; (Y-scale: 1 p.u. = 12.5 A).

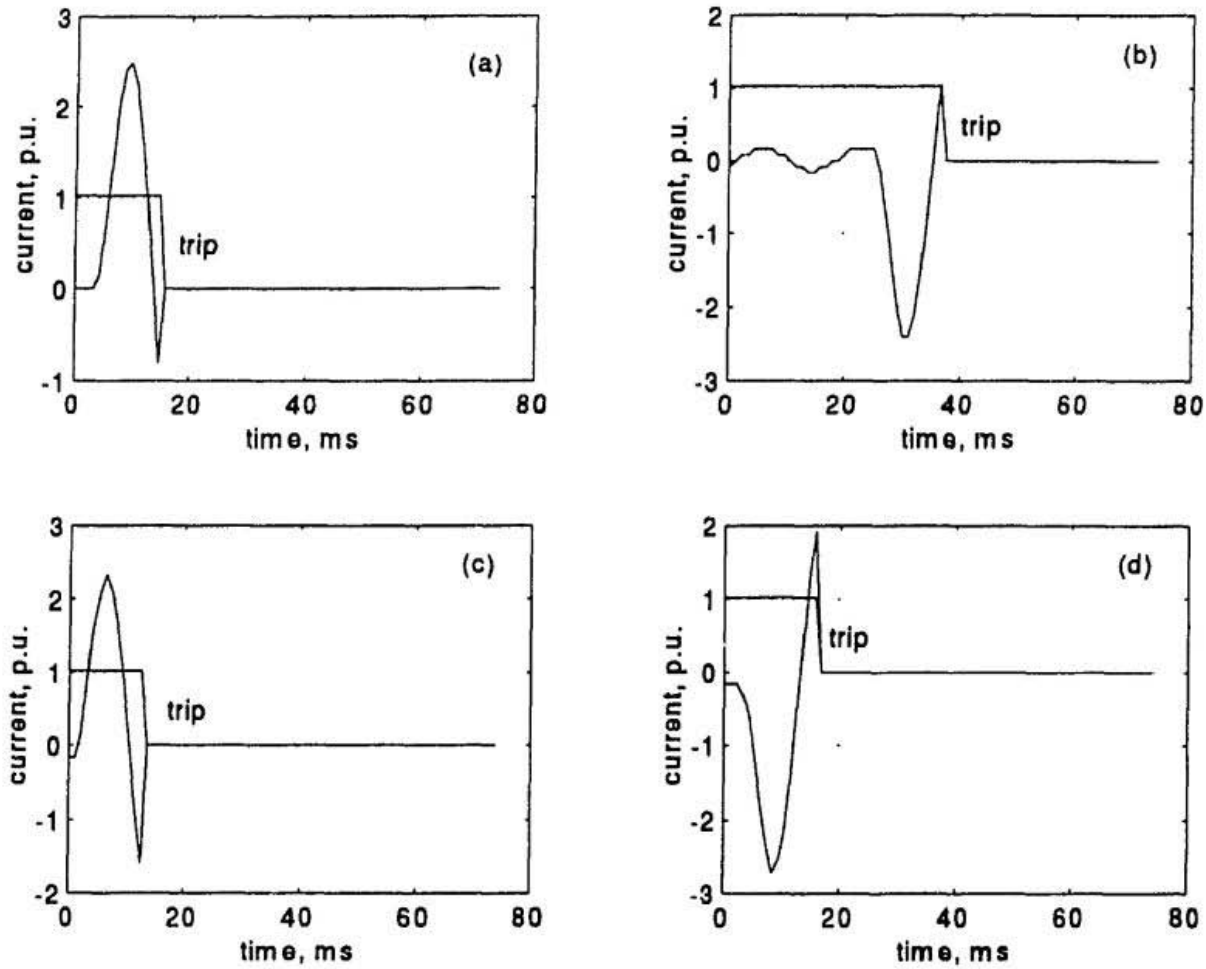

Figure 4.5: ANN responses to secondary side line to ground faults ; (a) after inrush without load, (b) after inrush with load, (c) before inrush without load; (d) before inrush with load; (Y-scale: 1 p.u. = 12.5 A).

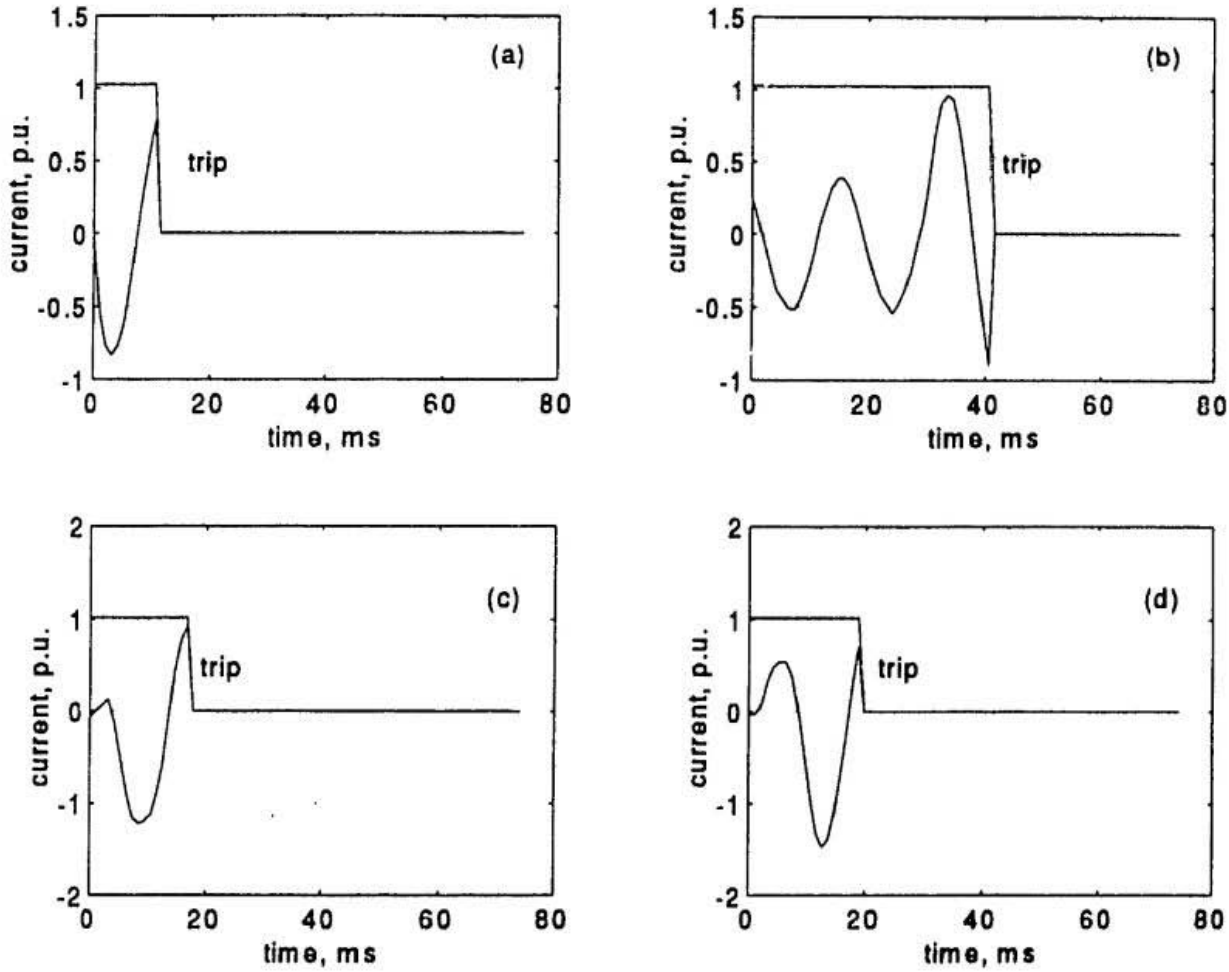

Figure 4.6: ANN responses to secondary side between tap faults : (a) after inrush without load, (b) after inrush with load, (c) before inrush without load; (d) before inrush with load; (Y-scale: 1 p.u. = 12.5 A).

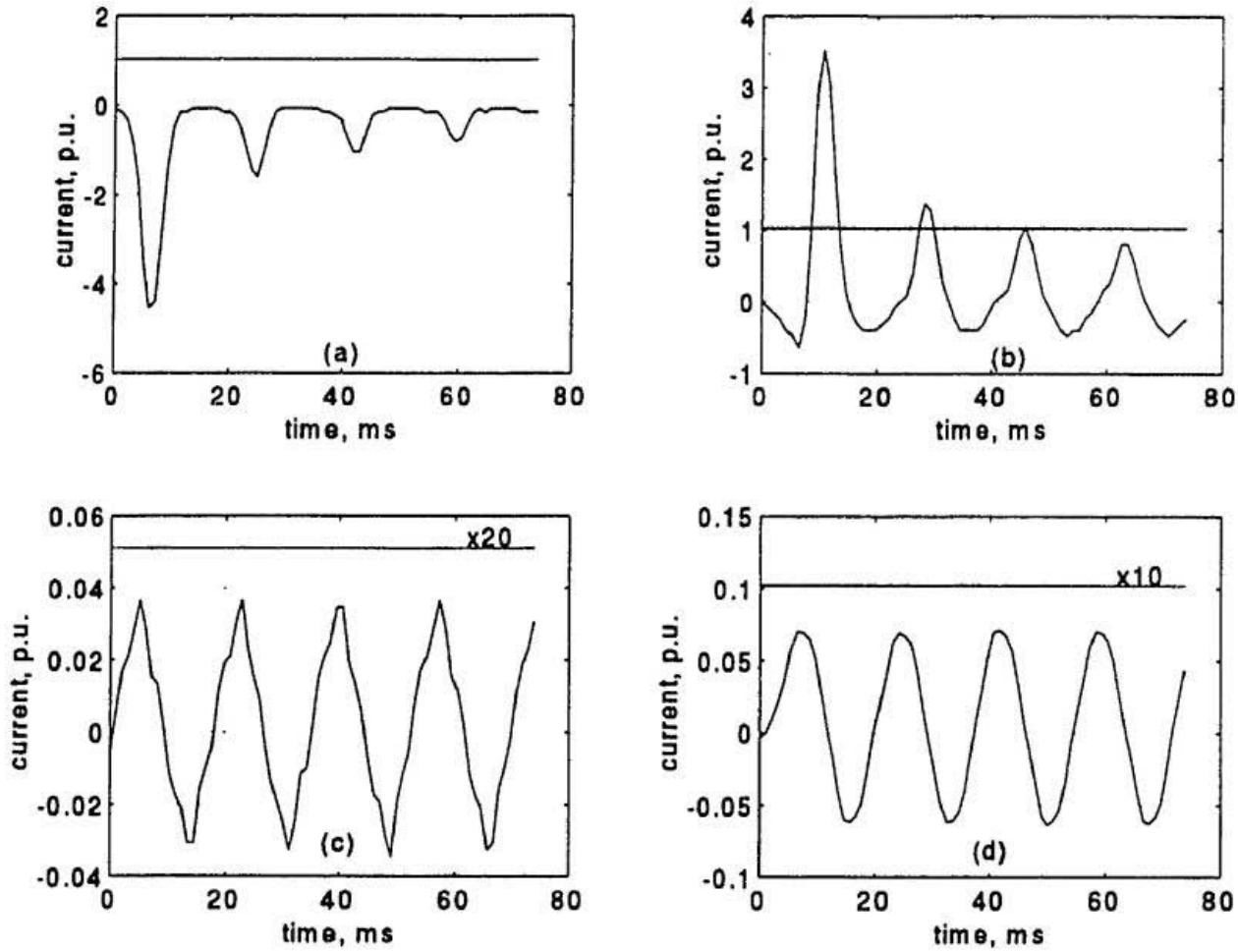

Figure 4.7: ANN responses to different inrush and over-excitation conditions : (a) inrush without load, (b) inrush with load, (c) over-excitation without load, (d) over-excitation with load; (Y-scale: 1 p.u. = 12.5 A).

by sending the trip signal in almost half cycle time period. The same fault is tested without load and with load by switching the transformers with the fault as shown in Figs. 4.4(c) and (d), respectively. In this case, the inrush was followed by the fault. The ANN again sent the correct signal, the control signal became zero and the circuit was interrupted. Figs. 4.5(a) and (b) show the secondary side line to ground fault without and with load, respectively. The fault has occurred in both cases after switching the transformer. The ANN recognized them as faults and proper actions were taken as shown in Figs. 4.5(a) and (b). The same types of fault occurred without and with load before the transformer was switched on, are shown in Figs. 4.5(c) and (d). The ANN sent the trip signal within three quarter of a cycle. Among the various types of secondary side faults investigated, the fault between taps seems to be the most difficult one to detect, due to the lower fault magnitude than the other types. The margin between the pre-fault and the post-fault currents are low as can be seen from Figs. 4.6(a)-(d). Like the other fault cases, the fault between taps is also tested by switching the transformer initially with no fault as shown in Figs. 4.6(a) and (b) for no load and load conditions, respectively. The ANN recognized the faults and sent corresponding trip signals. The ANN responses for the same types of fault that already existed while the transformer was switched on, were also observed as shown in Figs. 4.6(c) and (d) for no load and loading conditions, respectively. The ANN again sent the trip signal by recognizing the fault. The responses are prompt, and are within one cycle in most cases. For the particular case of fault before inrush without load as shown in Fig. 4.6(c), the ANN responded after a cycle time period. The extra time is required because of the sustaining inrush effect on the fault current. Although many inrush cases were tested, two sample inrush test results are presented in Figs. 4.7 (a) and (b). The ANN responses for both the negative and positive inrushes are

observed in Figs. 4.7(a) and (b), respectively. The ANN recognized the waveforms as inrushes and thus did not send any trip signal output. The inrush shown in Fig. 4.7(b) is an inrush with load and as can be seen, it is quite different from the inrush without load as shown in Fig. 4.7(a). Unlike the no load inrush case, this inrush with load has non-zero current for both positive and negative cycles. However, the ANN recognized it as an inrush. The ANN took the correct decision for the steady state over-excitation cases as shown in Figs. 4.7(c) and (d) for no load and load conditions, respectively. As expected, the ANN never interrupted the control signal; because the over-excitation within a range of about 40% is treated as no fault condition. Since the ANN algorithm does not rely directly on the harmonic contents of the current for restraining the relay, the harmonic distortion of the current under such over-excitation does not affect its performance. The harmonic restraint algorithms, however, depend directly on the fifth harmonic content of the over-excitation current to prevent the operation of the relay which may be sometimes misleading.

4.4 A Comparison Between DFT and ANN

The power of the ANN lies in its pattern recognition and generalization capabilities. The proposed ANN algorithm is based on the current signatures verification. The knowledge the ANN gathered during the training is exploited later on. It should be mentioned that although there is a large number of data which the ANN has been trained with, the ANN will always experience new patterns. There may be possible deviations of the patterns from what it has been trained with. There are distortions of the current data due to many reasons such as current transformer saturation, load tap changing, introduction of dc offsets from the measuring equipment, etc. Basically,

these distortions affect the harmonic contents of the current. In this work, some simple but realistic tests are performed by changing different harmonic contents in the original experimental data. The performances of the ANN are then compared with the performances of the discrete Fourier transform (DFT) algorithm which is one of the recognized efficient digital relaying algorithms [2] for transformer protection. The ANN responses are equally good and even better in some cases as the algorithm does not rely directly on the harmonic contents. Also due to its generalization capability, the ANN is able to recognize the current patterns if the deviation is within a certain range. The followings are some of the test results obtained from the ANN and DFT algorithms. The tests are performed through simulation.

4.4.1 Distortion in the inrush current

The second harmonic content of the inrush current is varied by a multiplication factor of 0.5-1.5. The ANN has no problem identifying it within this range. An example is shown in Fig. 4.8(a) where the original inrush current is distorted by reducing the second harmonic content of the current by 1.35 times. The ANN never gave a trip signal output. On the other hand, since the DFT algorithm for the transformer protection depends directly on the second harmonic content, the relay trips at about 27th sample as shown in Fig. 4.8(b). Both the second harmonic to fundamental ratio and fifth harmonic to fundamental ratio fall below their threshold values of 17.7% and 6.5%, respectively as shown in Fig. 4.8(c). Although in practical situations, the relay may be delayed to trip to ensure that it is not a false alarm, the ambiguity remains in this type of algorithm. This example shows that the ANN algorithm is less sensitive to the variations in the harmonic contents of the current. In the next test, a dc offset is introduced in the original inrush current data. In the example

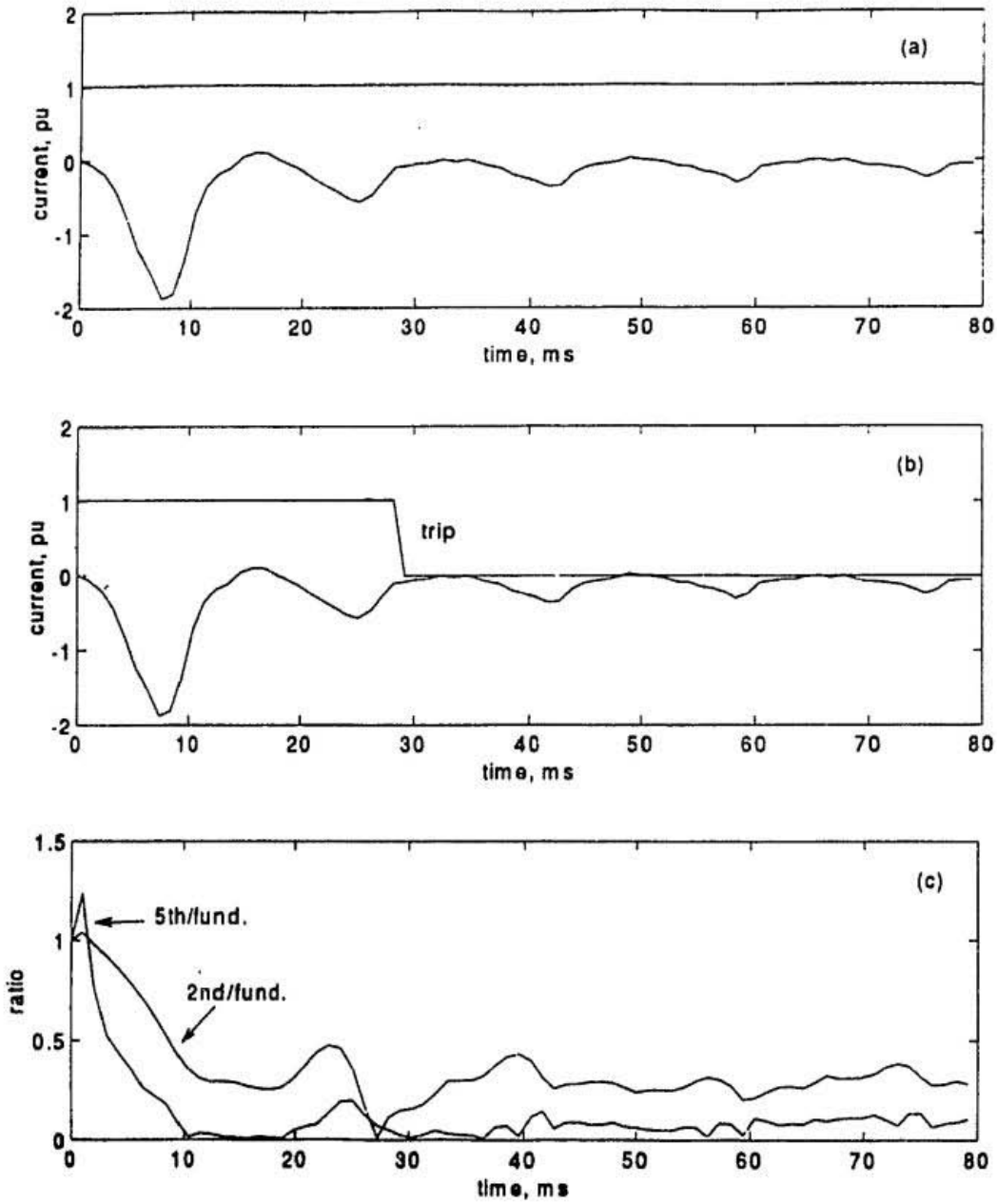

Figure 4.8: Second harmonic content reduced by 35% in the original inrush current (a) Response of ANN, (b) Response of DFT, (c) Ratio of second harmonic to fundamental and ratio of fifth harmonic to fundamental.

shown in Fig. 4.9(a), a negative offset of -0.4 p.u. is chosen. The ANN responds perfectly as it recognizes the current as inrush, whereas the DFT algorithm gives a trip signal output at the end of the fifth cycle. At this point, the second harmonic to fundamental ratio falls below the second harmonic threshold due to the small dc offset. The results are illustrated in Figures 4.9(a)-(c).

Tests were carried out with inrush data in which the fifth harmonic content have been changed over a range of 65% – 135%. Both the DFT and ANN algorithms work properly. In case of the DFT algorithm, the relay is restrained by the second harmonic content. The ANN is also able to recognize the inrush even after the variation in the fifth harmonic content in the original inrush current data.

4.4.2 Distortion in fault current waveform

The second harmonic content in the fault current was increased up to 5 times the original value. Both the ANN and DFT algorithms work satisfactorily, i.e. they are able to recognize the fault under severe distortions of the waveforms. However, the time requirement for detecting the fault increases for the DFT algorithm. As shown in Fig. 4.10(a), the ANN recognizes the fault within three quarters of a cycle time period when the current is distorted by adding more second harmonic content to its original value, whereas the DFT took longer time of about one and quarter cycle as shown in Fig. 4.10(b). The second harmonic to fundamental ratio and the fifth harmonic to fundamental ratio are shown in Fig. 4.10(c).

4.4.3 Distortion in over-excitation current

When the fifth harmonic content of the fault current is increased, the response of the DFT algorithm is long, whereas, the ANN takes more or less the same time for

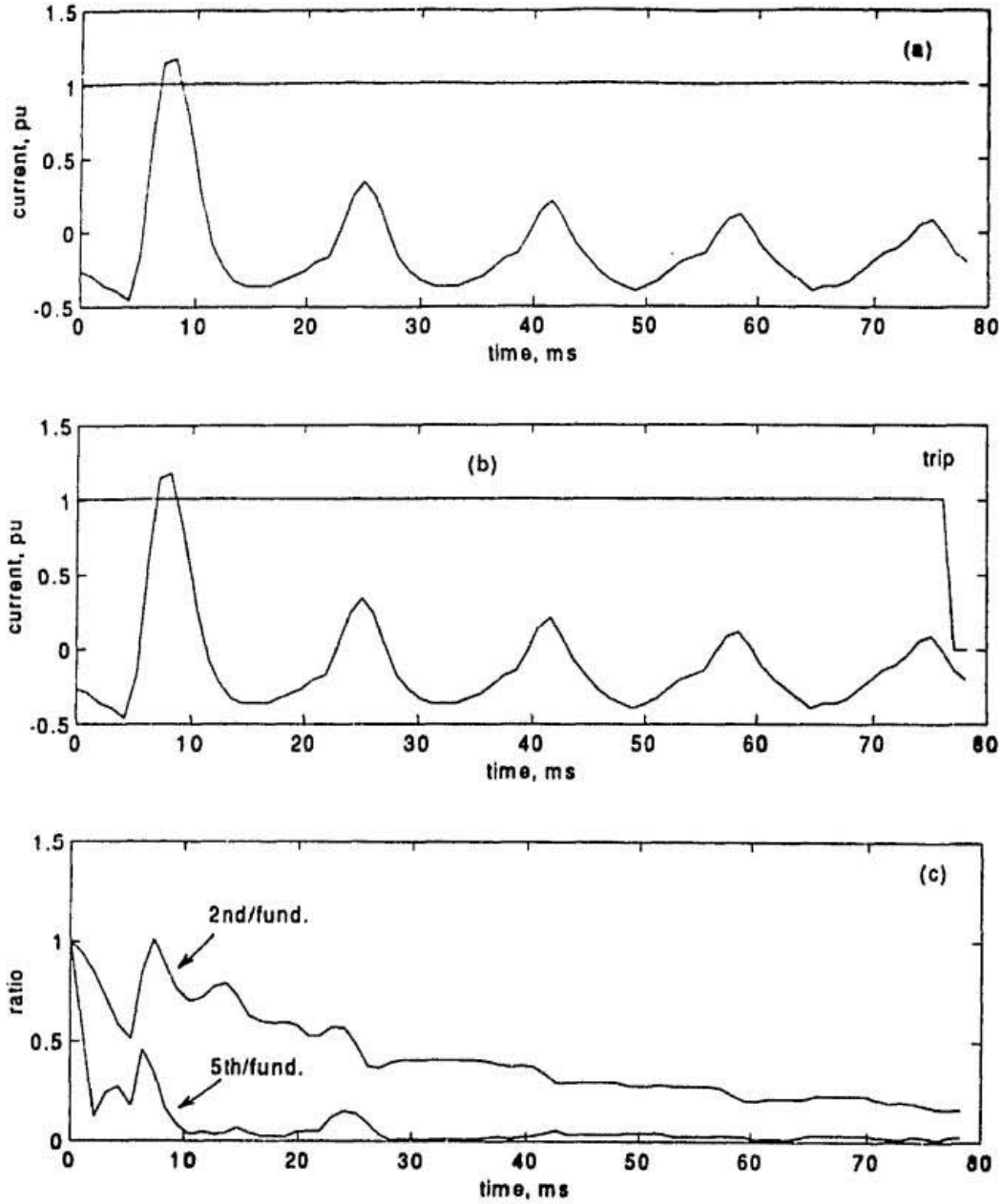

Figure 4.9: DC offset by -0.4 p.u. in original inrush current, (a) Response of ANN, (b) Response of DFT, (c) Ratio of second harmonic to fundamental and ratio of fifth harmonic to fundamental.

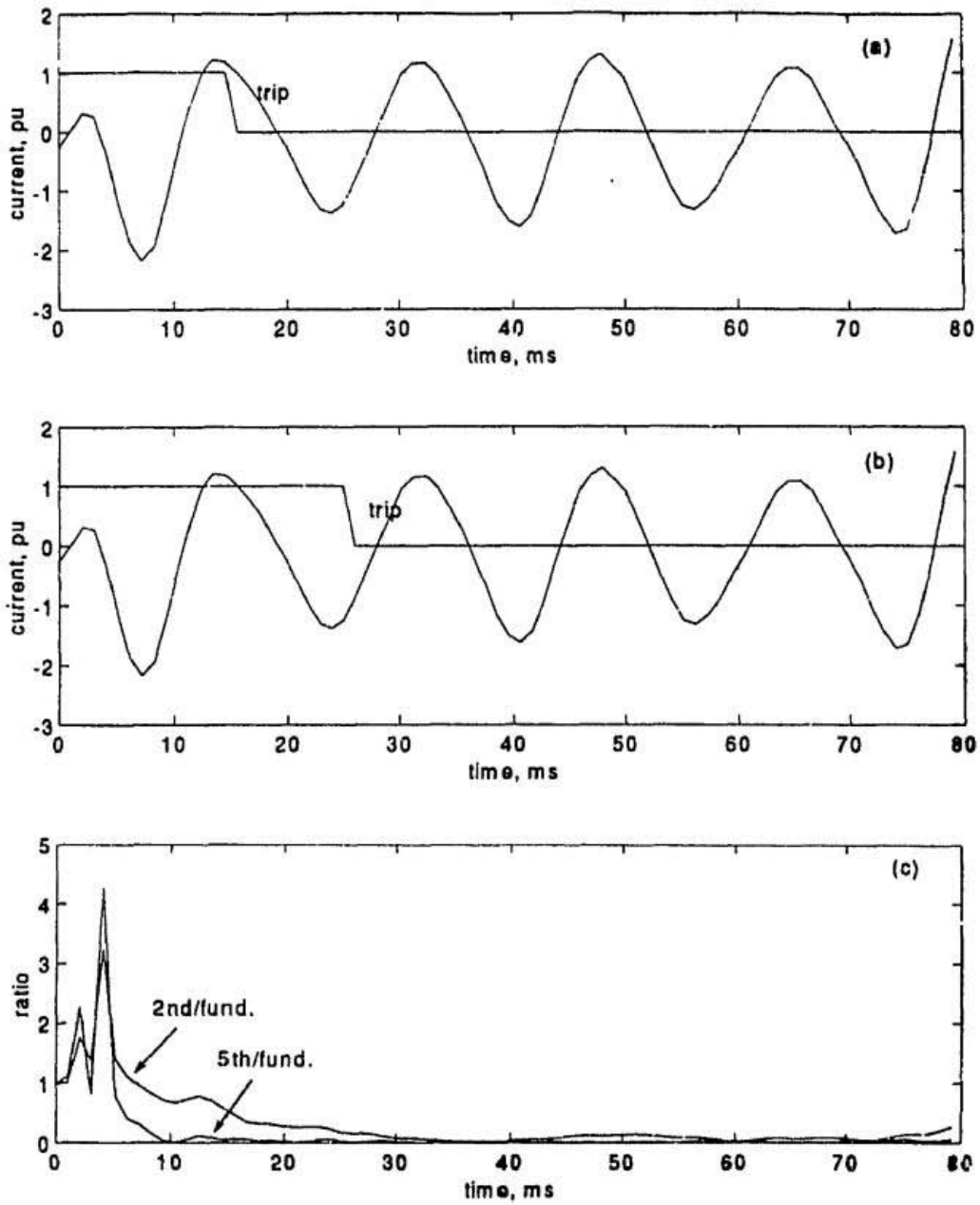

Figure 4.10: Second harmonic increased to double in fault current (a) Response of ANN, (b) Response of DFT, (c) Ratio of second harmonic to fundamental and ratio of fifth harmonic to fundamental.

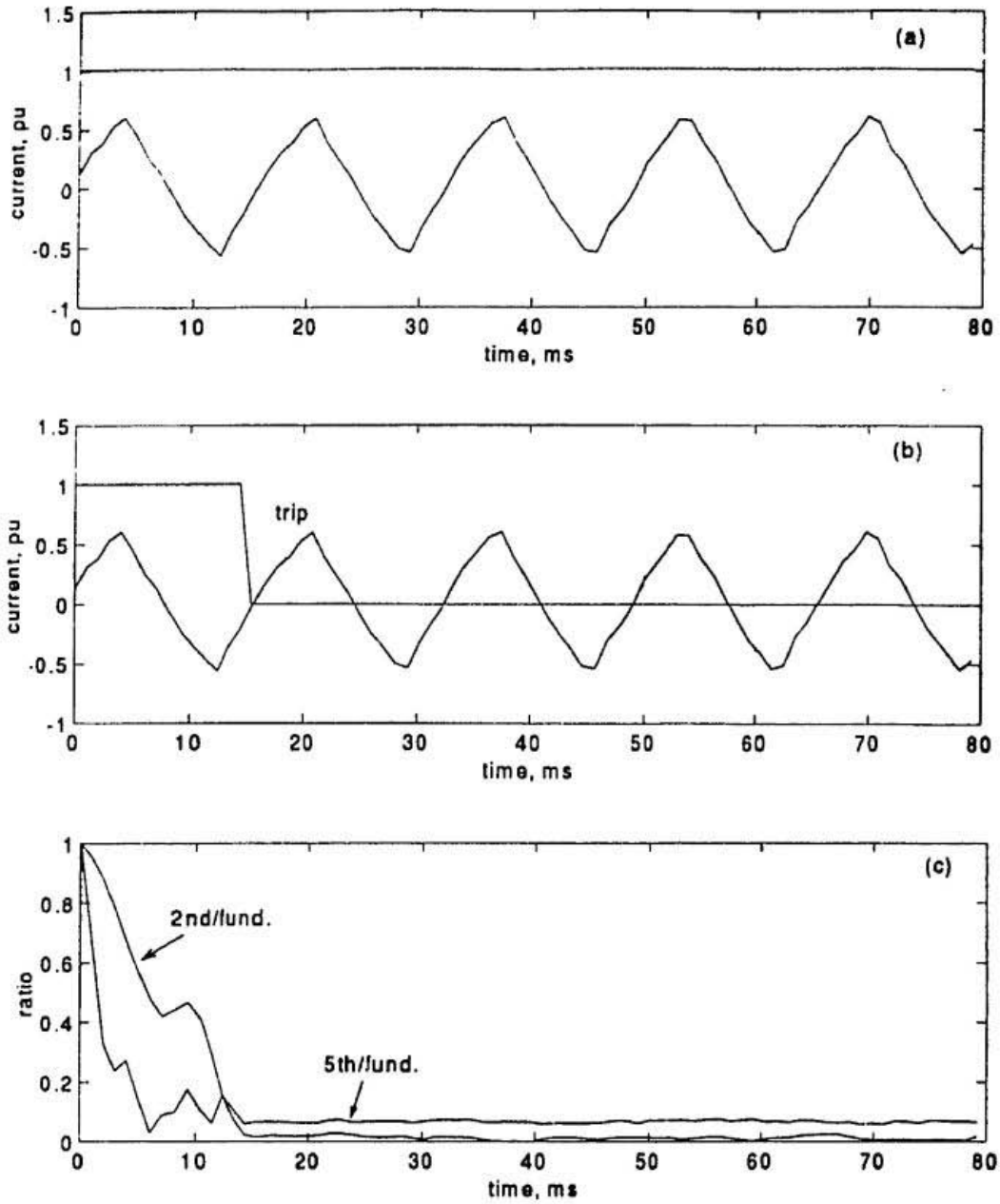

Figure 4.11: Fifth harmonic reduced by half in original over-excitation current (a) Response of ANN, (b) Response of DFT, (c) Second harmonic to fundamental ratio and fifth harmonic to fundamental ratio.

making the trip decision. Thus, the ANN shows its insensitivity to the fifth harmonic distortion.

The effects of the variation of second harmonic content in the over-excitation current are not significant. In the case of the DFT algorithm, the relay is usually restrained from operation by the fifth harmonic content, not by the second harmonic content. Therefore, a change in the second harmonic content in the over-excitation current has insignificant effect on its performance. The second harmonic content of the over-excitation current is changed over a range of about 50% to 150% of its original value. Like the DFT, the ANN also works perfectly in each case.

The next test is performed by varying the fifth harmonic content to over a range of about 40% to 135% of its original value. The ANN did not give a trip signal for the variations for the above range. One example is shown in Fig. 4.11(a) where the fifth harmonic content is changed to 50% of its original value. The DFT algorithm gives a trip signal output as shown in Fig. 4.11(b). It is too sensitive to the variation of fifth harmonic current. Because, the DFT algorithm relies directly on the fifth harmonic to fundamental ratio for the over-excitation condition. The fifth harmonic to fundamental ratio and second harmonic to fundamental ratio are presented in Fig. 4.11(c).

It can be concluded that the off-line test results of the ANN are quite encouraging. However, the algorithm needs to be verified in real-time. This has been done successfully in Chapter 5. The following chapter describes the experimental setup and the on-line test results of the ANN based algorithm for the transformer protection.

Chapter 5

Experimental Results

5.1 Introduction

As an integral part of this work, the simulation of the ANN based algorithm is verified experimentally. To do this, the first requirement is to develop an experimental setup. The on-line implementation of this work involves both hardware and software. In addition to the setup used for data acquisition as discussed in Chapter 4, this setup requires the software implementation of the ANN based algorithm which has been done using a digital signal processor DS-1102. The interfacing between the software and the hardware is also necessary. Before discussing the experimental setup used in this work, a typical digital relaying scheme is illustrated in the following section. Next, the experimental setup for this work is described in details. Finally, the on-line test results for different magnetizing inrush, over-excitation and different fault cases are presented.

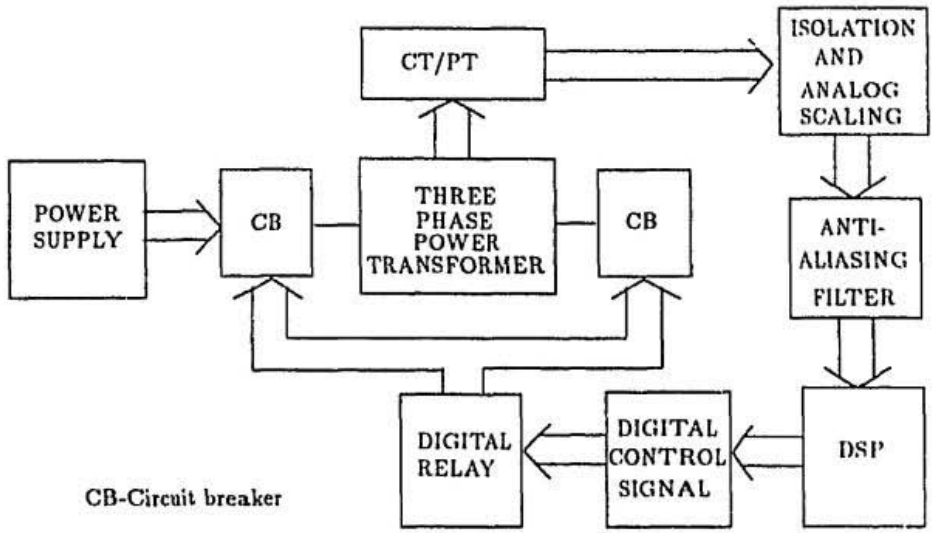

Figure 5.1: Functional block diagram of the relaying scheme

5.2 A Typical Digital Relaying Block Diagram

A stand alone DSP based digital relay has two main components :- the hardware and the software. The functional block diagram of a typical digital relay is shown in Fig. 5.1. The hardware usually consists of the following features.

- The hardware should provide a data acquisition system. The data are usually current signal and/or voltage signal depending on the relaying algorithm. Therefore current transformers (CT) and potential transformers (PT) are provided with proper scaling.

- Analog inputs are required to be passed through a low-pass filter before sampling in order to avoid aliasing. The cutoff frequency of such filter depends on the application of the relay. The cutoff frequency for harmonic restraint differential relay for transformer protection must be at least 300 Hz in order to preserve

the fifth harmonic component which is used for restraining in some cases.

- The sampling is done in the digital signal processing (DSP) board. The sampling frequency must satisfy the Nyquist rate which is twice the cut-off frequency. The hardware should be capable of sampling at least at this rate. Also, depending upon the algorithm to be used for the relaying, the sampling rate may vary. A typical range is about 4 - 20 samples per cycle [81]. The software may be designed to down sample the data as desired.

5.3 Real-time Implementation

The ANN based algorithm was tested on-line on the 5 kVA, 230/550-575-600 core type three phase laboratory power transformer. The complete relaying scheme consists of both the hardware and the software. The processing is performed in software using the DS-1102 digital signal processor. A program is written in C language for this purpose. The software loads the values of the weights and biases of the ANN, which have been obtained through the training. These values are used for the processing and then generating the tripping decision. Figure 5.2 is the block diagram of the on-line implementation of the ANN based relay for transformer protection. The experimental setup is also shown in Fig. 5.3. When the DSP is started, it continuously takes the differential current sample through the DSP's analog channel and converts it to the digital data using its built-in D/A converter. The sampling time used for the data acquisition is 960 Hz i.e. 16 samples per cycle. The digital data are sent to the DSP's memory through the host PC. The most recent data are stored in a circular buffer of size 16 such that the 17th previous sample data are automatically dropped off from the buffer. These 16 current samples are the inputs of the ANN. The processing is

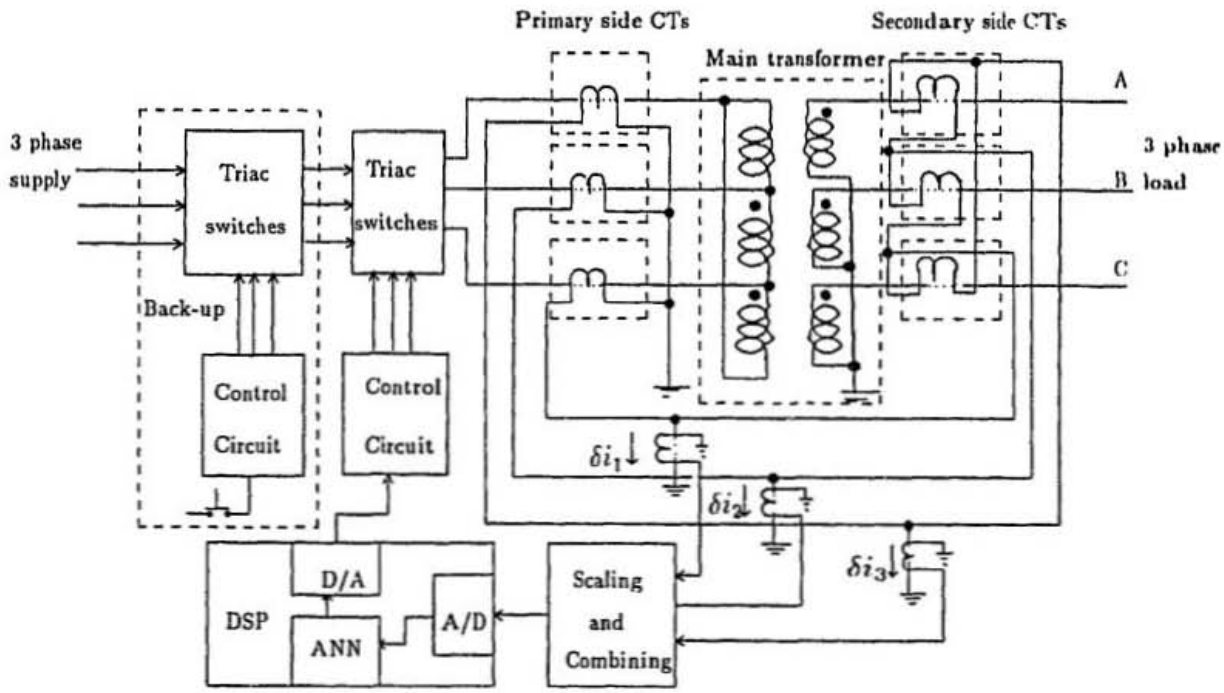

Figure 5.2: Block diagram for the on-line implementation

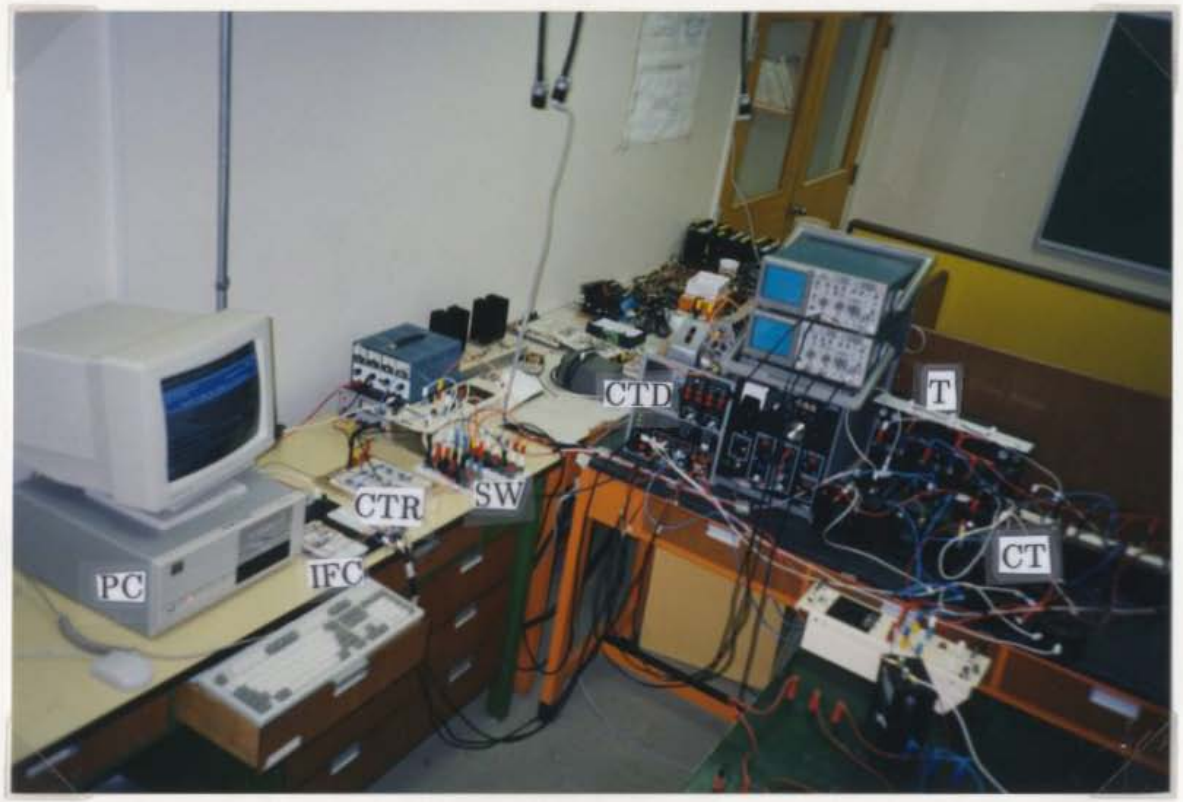

T - Main transformer SW - Triac switches

CT - Current transformers CTD - Current transducers

CTR - Control circuit IFC - Interfacing circuit

PC - Personal computer with DS-1102 installed

Figure 5.3: Experimental setup

done in two steps :- propagation of the input to hidden layer and then the hidden layer to the output. In both the hidden layer and the output layer, hard-limiters are used as the transfer functions of the neurons. Finally the output of the ANN is sent to the control circuit through the DSP's built-in D/A converter. The flow chart of the software for implementing the real-time ANN based power transformer protection scheme is illustrated in Fig. 5.4.

For the experimental testing of the ANN algorithm under different inrush and fault conditions, a number of switches are used. The experimental set-up with the switches is shown in Fig. 5.5(a) and (b). There are mechanical as well as electronically controlled power electronic switches. The purpose of these switches are to simulate different inrush and fault conditions; also to interrupt the circuit against fault in real time. A brief description of these switches are given as follows.

The main switch SW1 is a mechanical switch to turn on the power supply unit as shown in Fig. 5.5(a). A set of three triac switches are used in series with the supply as indicated by SW2 in Fig. 5.5(a). This is controlled through a momentarily contact switch using a control circuit and the control circuit is designed in such a way as to allow the contact for three cycle time period. The detail of the control circuit is given in Appendix-A. This is provided for two reasons - (i) in order to perform the on-line test under various inrush conditions and those fault conditions where the faults had occurred before inrush and (ii) in order to avoid any possible damage to equipment in case of any failure in the ANN controlled switches during the faults in the transformer. Therefore, during the experiment, it is ensured that under no circumstances, the transformer would experience a fault for more than three cycles. Another three phase mechanical switch SW3 is used in parallel with switch SW2 as illustrated in Fig. 5.5(a). This is normally opened, and is closed manually

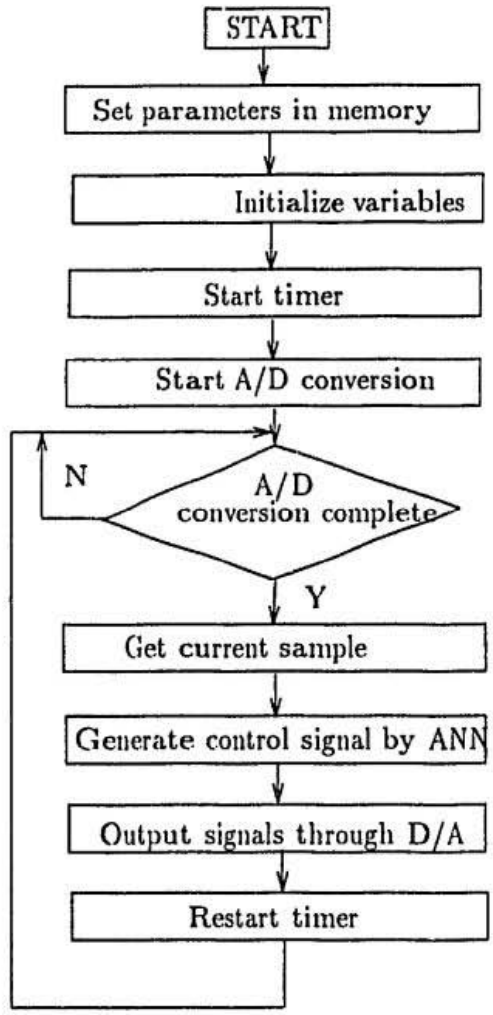

Figure 5.4: Flow chart of the software using the DSP for the ANN based transformer protection

for testing the fault conditions which occurred after an inrush. In such cases, the switch SW2 is bypassed by closing the switch SW3. A set of three triac switches, SW4 are kept always in series with the supply. This is electronically controlled by the digital signal generated from the ANN. These switches are closed under normal operating conditions and only opened if there is a trip signal output from the ANN through the DSP corresponding to a fault. The details of the control circuit is given in Appendix-A. In this scheme, the control signal is the complement of the trip signal, i.e. when the trip signal is *high*, the control signal is *low* and vice versa. Thus for all conditions except the fault, the trip signal of 0 represents 5V of control signal which closes the contacts of the triac switch. On the other hand a trip signal of 1 during fault results in a 0V control signal which opens the triac switches and thus protects the transformer against the fault. Also, a three phase switch SW5 is used for connecting the secondary side of the transformer to the three phase load.

For each fault condition, a branch consisting of a resistor and two switches – SW6 and SW7, connected in parallel, is used as shown in Fig. 5.5(b). This branch is connected between any two points in the circuit depending on the type of the fault to be simulated. For example, in the case of primary side phase A to phase B fault this branch will be connected between the points A and B of Fig. 5.2. Both the switches SW6 and SW7 are normally opened and can be manually closed. SW6 is a triac switch which is controlled by a control circuit with momentary contact switch and it allows a connection for three cycle time period. The momentary contact is made while the mechanical switch SW7 remains opened for testing the fault conditions which occurred after the energization of the transformer. For testing all other cases, this switch is bypassed by closing the switch SW7.

Table-5.1 summarizes the order of switching and the states of the switches for

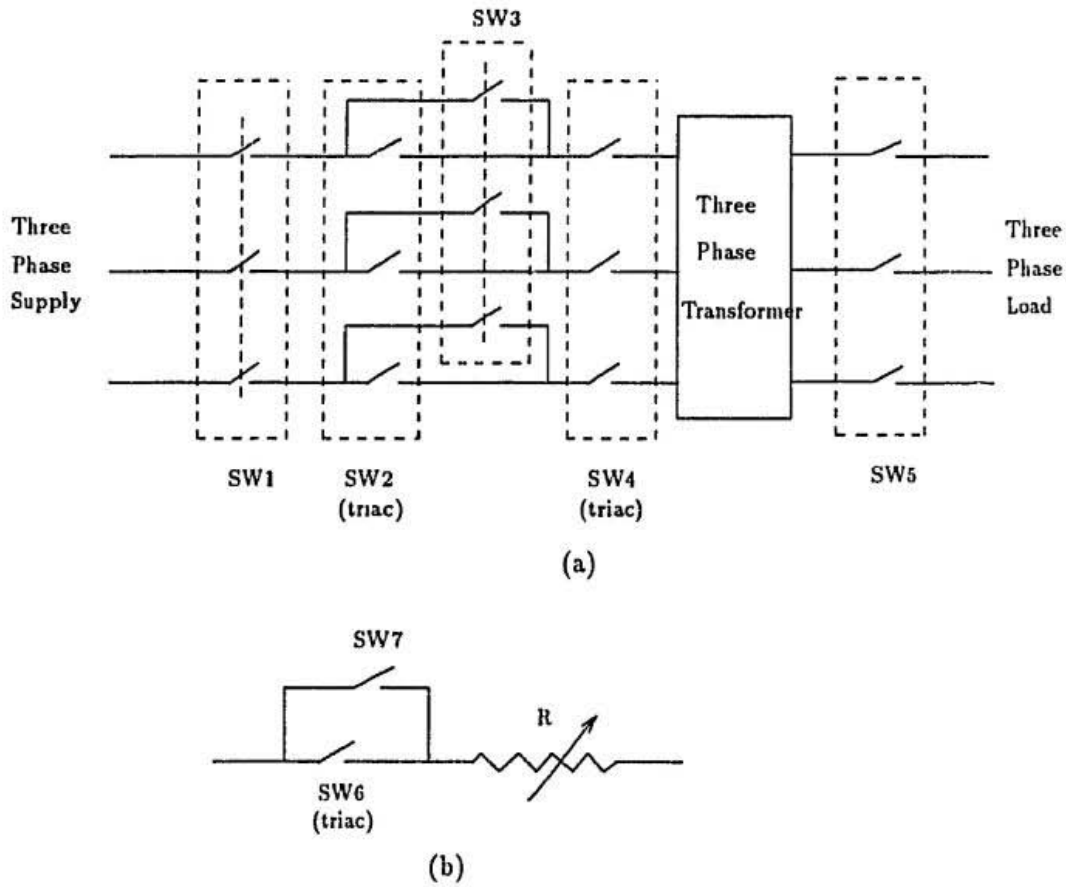

Figure 5.5: Experimental setup with switches

different conditions.

5.4 On-line Test Results for One Phase

The experimental setup was used to test the performance of the ANN algorithm under various inrush, fault and over-excitation conditions. It should be noted that the ANN is trained with single phase data assuming that similar result will be obtained corresponding to the other two phases. Therefore, it is important to ensure in real-time whether this assumption is true. At first, the algorithm is implemented for the single phase case i.e. the ANN takes only one phase data at each instant and then depending on that, it generates the decision. Some of the sample results are shown in Figs. 5.6 and 5.7. As can be seen from Figs. 5.6 and 5.7 that the ANN accurately distinguishes the fault current and inrush current and thus produces appropriate trip signals. However, if the same fault occurs in different phases and everything else remains the same, the ANN may not be able to identify the fault as the current in all three phases will not be affected significantly. One such example is shown in Fig. 5.8, where a phase to phase fault occurred in the primary side which involved phase B and phase C. As can be seen from the Fig. 5.8, although there was a fault, the differential current measured at phase A was not significant enough to be recognized as fault. Therefore, the relay did not respond appropriately. However, it is to be noted that the other two phase currents in Fig. 5.8(b) are quite significant. Therefore, if the same fault occurs, but the current of either phase B or phase C is measured and used by the ANN, it will be able to detect the fault. This has been successfully verified.

Case	Condition	SW1	SW2	SW3	SW5	SW6	SW7
Inrush	no load	closed[2]	closed[3]	open[1]	open[1]	-	-
Inrush	with load	closed[2]	closed[3]	open[1]	closed[1]	-	-
Fault	no load, before inrush	closed[3]	-	closed[2]	open [1]	closed[4]	open[1]
Fault	with load, before inrush	closed[3]	-	closed[2]	closed [1]	closed[4]	open[1]
Fault	no load, after inrush	closed[3]	closed[4]	closed[2]	open [1]	-	closed[1]
Fault	with load, after inrush	closed[3]	closed[4]	closed[2]	closed [1]	-	closed[1]
The numbers in the superscripts show the order of switching. Also note that the the switching of SW4 is not shown above; because it is always controlled by the decision of the ANN.							

Table 5.1: Switching for different inrush and fault conditions

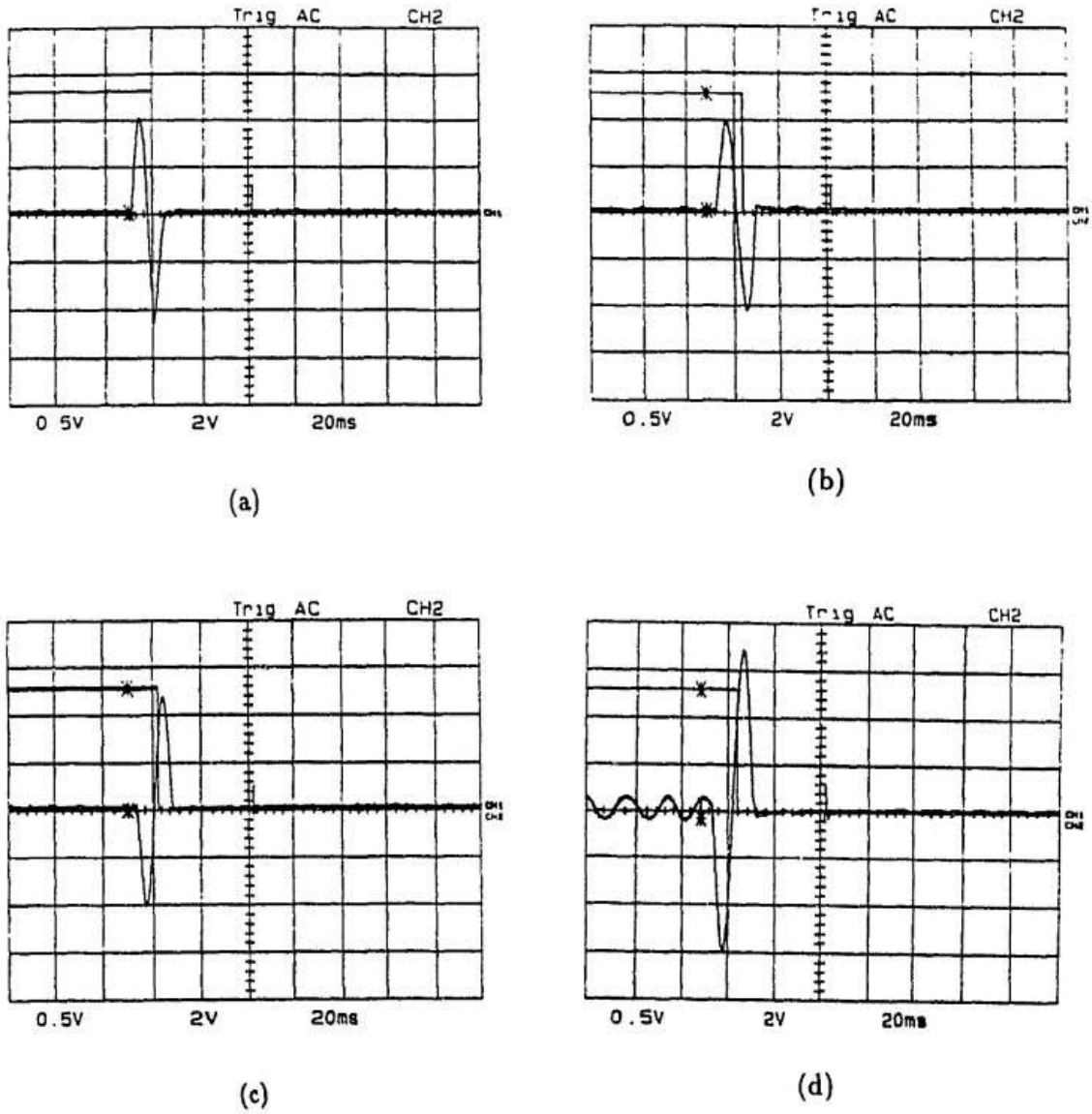

Figure 5.6: ANN responses to different faults: primary side - (a) phase to phase fault with load before inrush, (b) phase to phase fault without load after inrush; secondary side – (c) phase to ground fault without load before inrush, (d) phase to phase fault with load after inrush; (Y-scale 1V = 12.5 A).

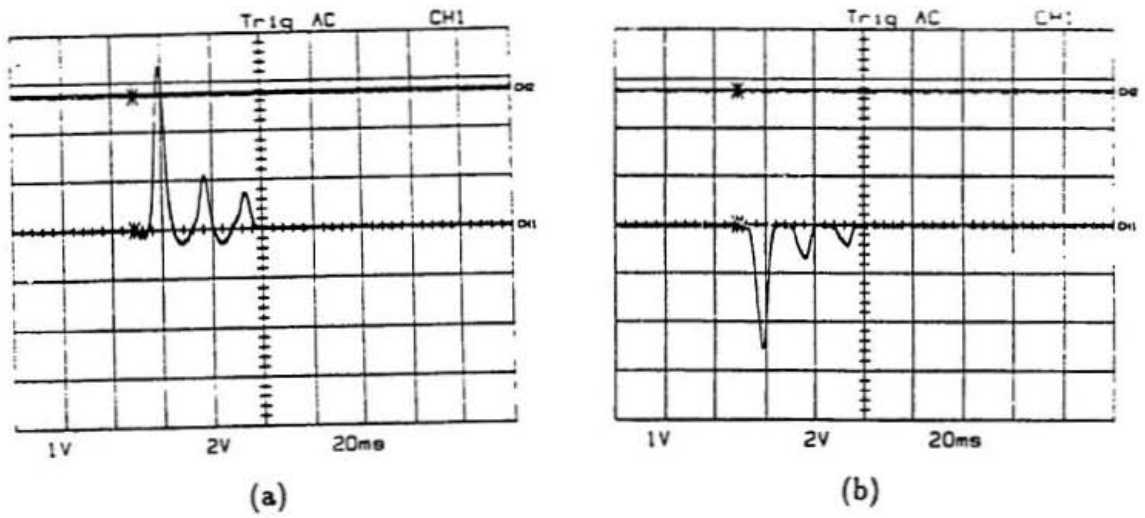

Figure 5.7: ANN responses (one phase implementation) to different inrushes: (a) without load, (b) with load; (Y-scale 1V = 12.5 A).

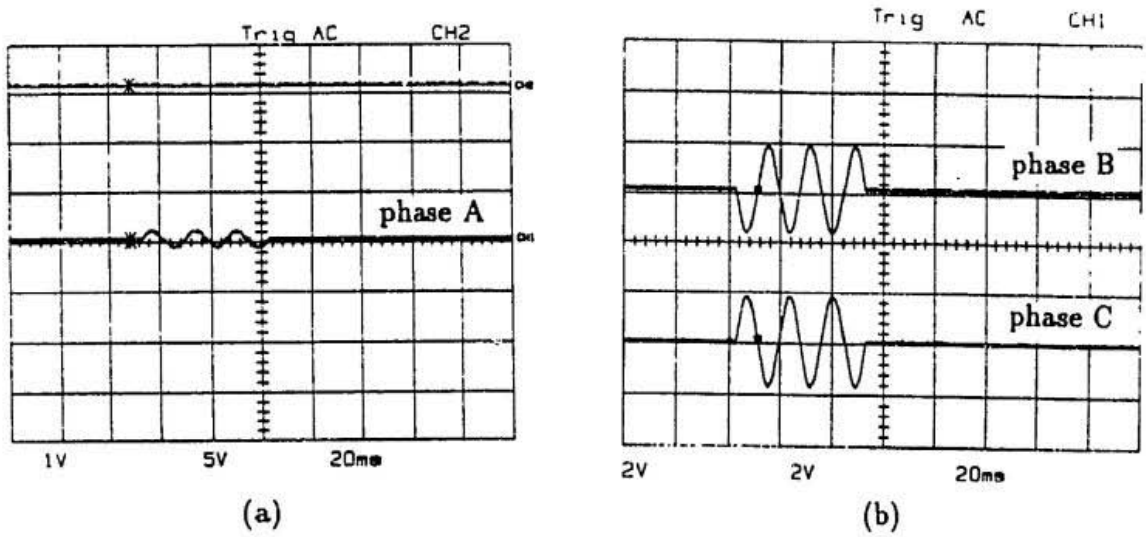

Figure 5.8: ANN responses (one phase implementation) to primary side phase B to phase C fault - (a) control voltage and differential current in phase A, (b) differential currents in phase B and phase C; (Y-scale 1V = 12.5 A).

The next step is to implement the complete scheme for the three phases such that if the fault occurs involving one or more phases, the ANN should be able to detect the fault. This can be done in a number of different ways as described in the following sections.

5.5 On-line Test Results for Three Phases

It is possible to take the current samples for all three phases at each instant and work with three sets of data for processing by the ANN. However, that might increase considerably the computational burden of the DSP. Alternatively, a combination of the three phase currents can be generated either in hardware or software and the resulting current can be used by the ANN for processing in order to decide whether there is a fault or not. There are other possibilities too. In this work, four such methods were attempted and successfully implemented. The results in all four methods are quite similar for most of the cases that have been investigated. However, the time requirement slightly varies. In the first method, three current samples are taken using the D/A of the DSP at each instant and used by the ANN. The algorithm keeps track of three sets of data window of length 16 corresponding to the three currents $\delta i_1, \delta i_2$ and δi_3, and passes the data windows one after another through the same ANN until a trip signal is obtained. If a trip signal is obtained, without checking any further, it sends the trip signal through the DSP's D/A channel. This takes more than one cycle time period to identify a fault in the worst cases. The time requirement varies as it depends on the phases involved in the fault. Thus, the method is not unbiased. Also, the computational burden for the DSP is increased considerably.

However, the second method is based on a addition of three current samples. All

three currents are taken and added in the software. It only keeps track of one data window. The method is unbiased but the computational burden is still high.

The third method involves measurement and calculation using two sets of current samples instead of three. This is based on the assumption that any two of the three currents will bear enough information about the fault and thus, the calculation involving the third current can be avoided. Two phase currents was added in hardware and taken through the A/D channel of the DSP. The added value is used as the input of the ANN. This works quite satisfactorily. Faults are detected within a cycle time period in most of the time. However, as it takes only two out of three phases, the method is biased.

Finally, an unbiased method is chosen in which three current samples are taken and an electronic circuit is designed to add these three currents. The added current sample is taken as the ANN's input. The method is unbiased and faster because it is a less burden to the DSP. All tests were performed using this method for different inrush, fault and over-excitation conditions and the results are described with experimental figures in the following sections. The figures used are plotted directly from the oscilloscope. The differential currents in three phases and the control signal for switch SW4 which is derived from the ANN's output, are shown in the plots.

5.5.1 Magnetizing Inrush

This magnetizing inrush test was performed by switching SW2, while switch SW1 remained closed. The order of the switching sequence is given in Table 5.1. Several hundred tests were performed by random switching and it has been observed that the ANN never gives a trip signal output. The tests were performed both at load and no load conditions. Some of the sample results are shown in Figs. 5.9 and 5.10. It

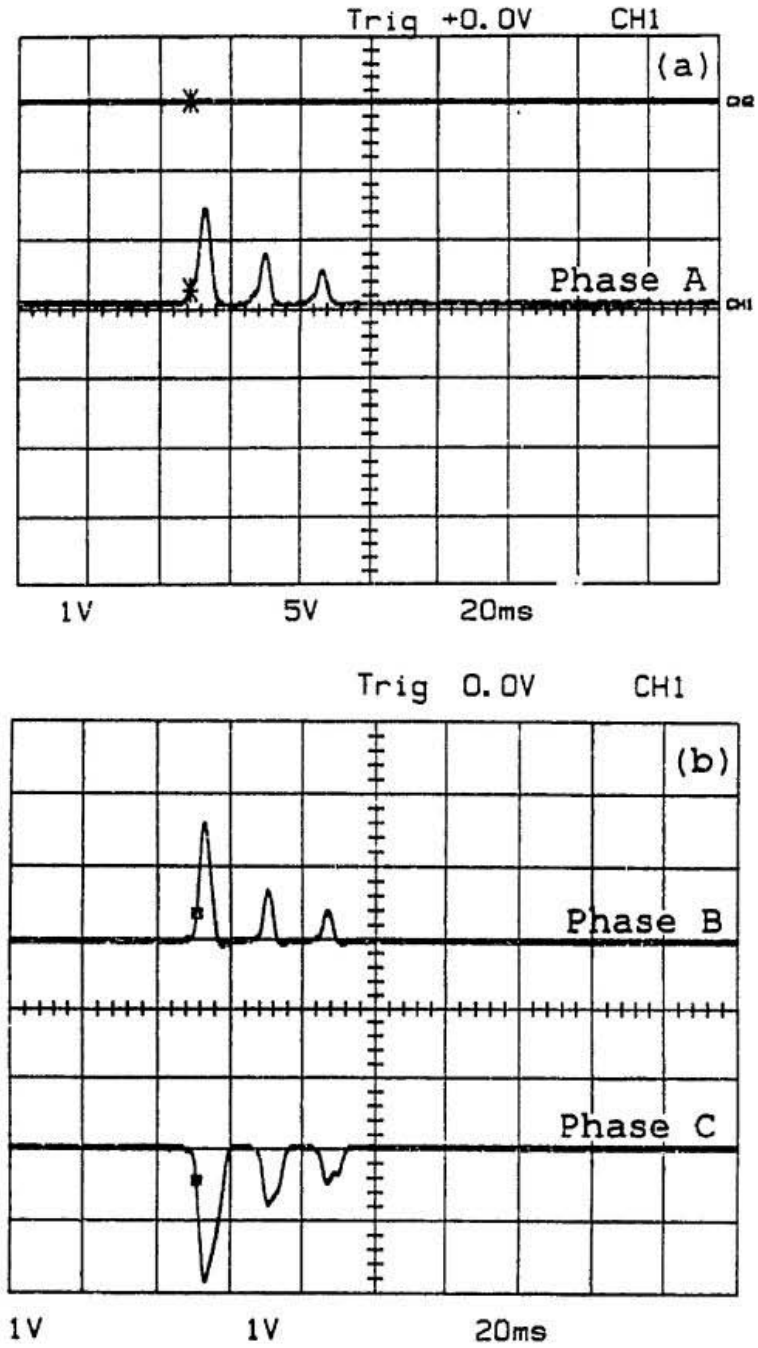

Figure 5.9: ANN response to an inrush with positive peak in phase A without load: (a) control voltage and differential current in phase A, (b) differential currents in phase B and phase C. (Y-scale 1V = 12.5 A).

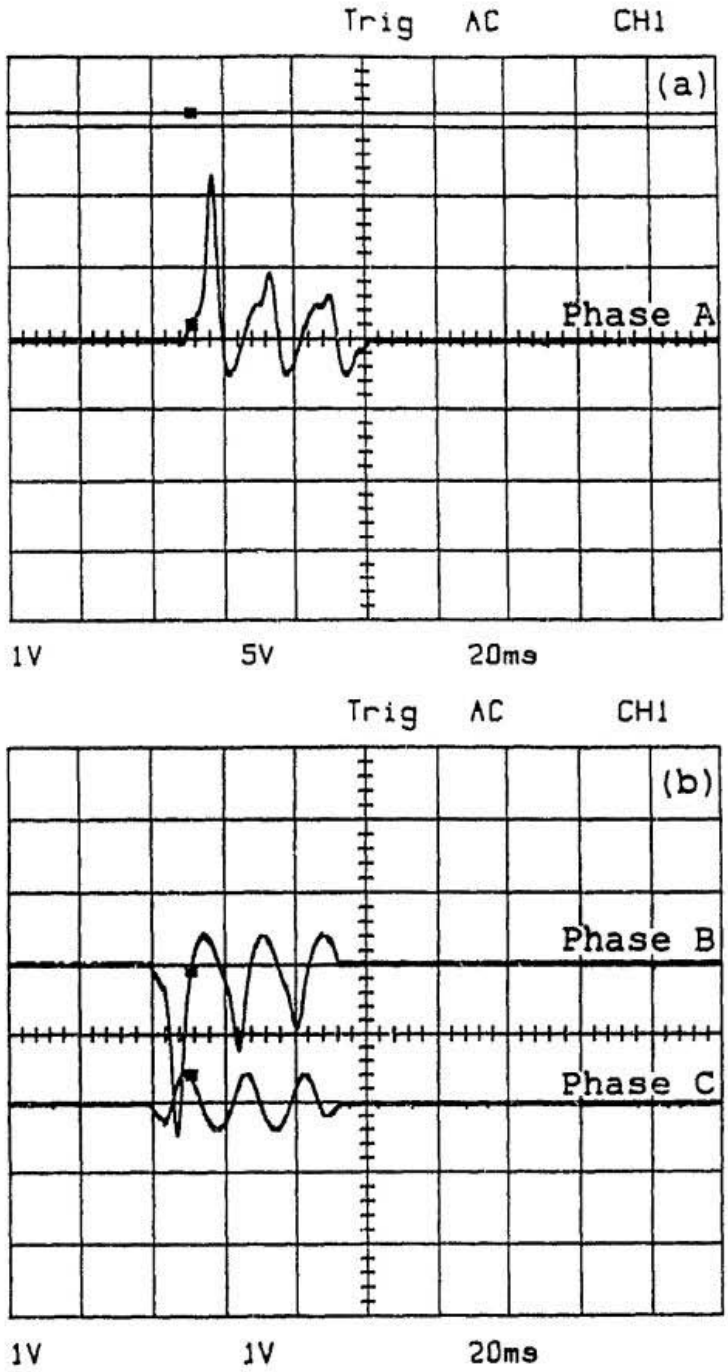

Figure 5.10: ANN response to an inrush with a positive peak in phase B with load: (a) control voltage and differential current in phase A, (b) differential currents in phase B and phase C. (Y-scale 1V = 12.5 A).

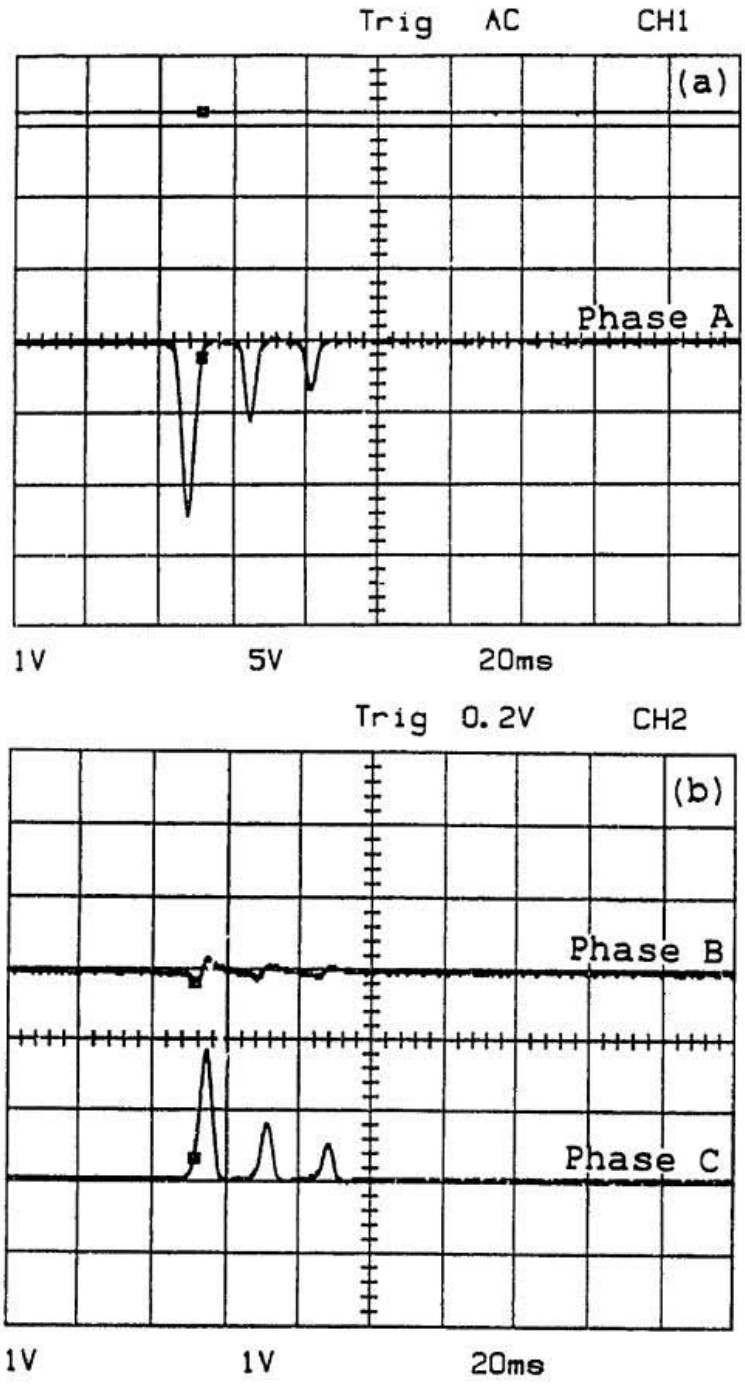

Figure 5.11: ANN response to an inrush with a negative peak in phases A without load: (a) control voltage and differential current in phase A, (b) differential currents in phase B and phase C. (Y-scale 1V = 12.5 A).

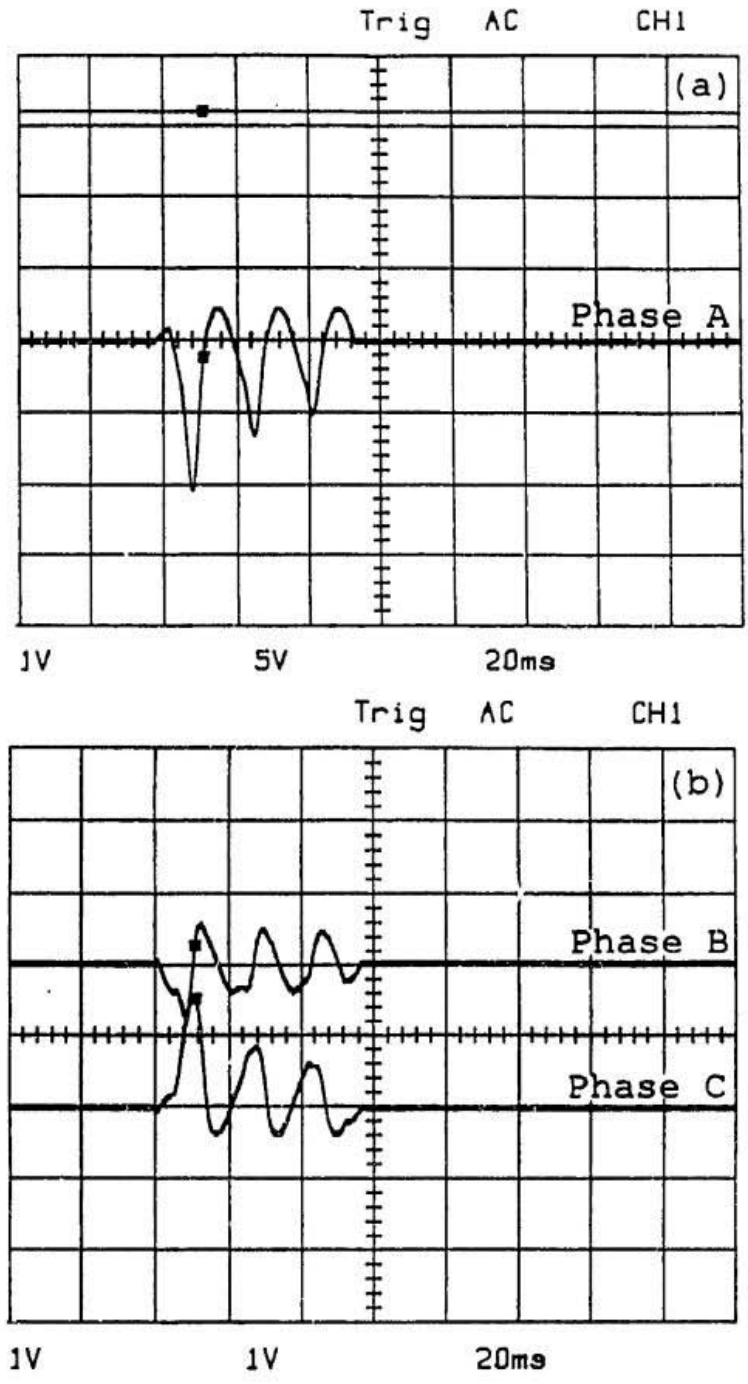

Figure 5.12: ANN response to a negative inrush in phases A with load: (a) control voltage and differential current in phase A, (b) differential currents in phase B and phase C. (Y-scale 1V = 12.5 A).

is clear from the Figs. 5.9 and 5.10 that although the current magnitudes are quite high, at least in two phases, the ANN is able to recognize it as a no fault condition and hence, there was no trip signal output. Fig. 5.9(a) shows the control voltage derived from the decision of the ANN and the differential current in phase A for an inrush without load. It should be noted that like the fault cases, the inrush currents were also not allowed to flow for more than three cycles. Figure 5.9(b) shows the currents in other two phases for the same inrush condition. Figures 5.10(a) and (b) illustrate the control voltage generated from the ANN decision and the three phase currents for an inrush with load.

An example of negative inrush in phase A and without load is also illustrated in Figs. 5.11(a) and (b). It is observed during hundreds of switching of the transformer that the directions and shapes of the currents in three phases are difficult to predict beforehand [77]. However, it does not affect the operation of the ANN as it works with the absolute values of the current samples. A negative inrush condition with load are illustrated in Figs. 5.11(a) and (b). The inrushes with load have quite different patterns than those with no load. Nevertheless, the ANN had no problem identifying them as inrushes; the control voltages remained high all the time as indicated in Figs. 5.12(a) and (b). The ANN worked perfectly both for no load and with load conditions. Simulated data for training may cause mal-operation of the relay as it is quite difficult to accurately simulate different types of inrushes.

5.5.2 Internal faults

All fault tests were performed by connecting the faulty branch between the two points in the transformer involved in the fault. The test results are presented for four different conditions which include whether the fault has occurred before or after

switching the transformer, and the loading conditions. The figures for the fault tests of the three phase implementation are presented throughout the thesis, unless otherwise stated, in the following manner:

(a) control voltage and differential current in phase A,

(b) differential currents in phase B and phase C,

for faults occurred

i) after energizing the transformer without load, ii) after energizing the transformer with load, iii) before energizing the transformer without load, iv) before energizing the transformer with load.

All fault tests were performed in all three phases and they were found to be consistent. Of the three sets of results obtained, one set of results is presented in this chapter. The remaining test results are given in Appendix-C.

i) Primary side Phase-to-Phase Fault

This test was performed by connecting the faulty branch between phase A and phase B in primary side. Figures. 5.13(a) and (b) depict the differential currents in three phases and the control voltage for no load. In this figure, the fault occurred long after the transformer was energized and therefore, there is no inrush effect on the fault. As can be seen from Fig. 5.13(a) the control voltage goes down to zero in about 16 ms after the inception of the fault. It should be noted here that there is a delay between the trip signal output from the ANN and the interruption of the current in the circuit. This is because of the fact that the triac switches cannot be turned off until the current through them goes to zero even if the control signal is withdrawn. This is not a problem for practical applications, because, these switches will be replaced by modern circuit breakers. It has been observed that the ANN produces the trip signal output within a cycle time period and thereby protects the

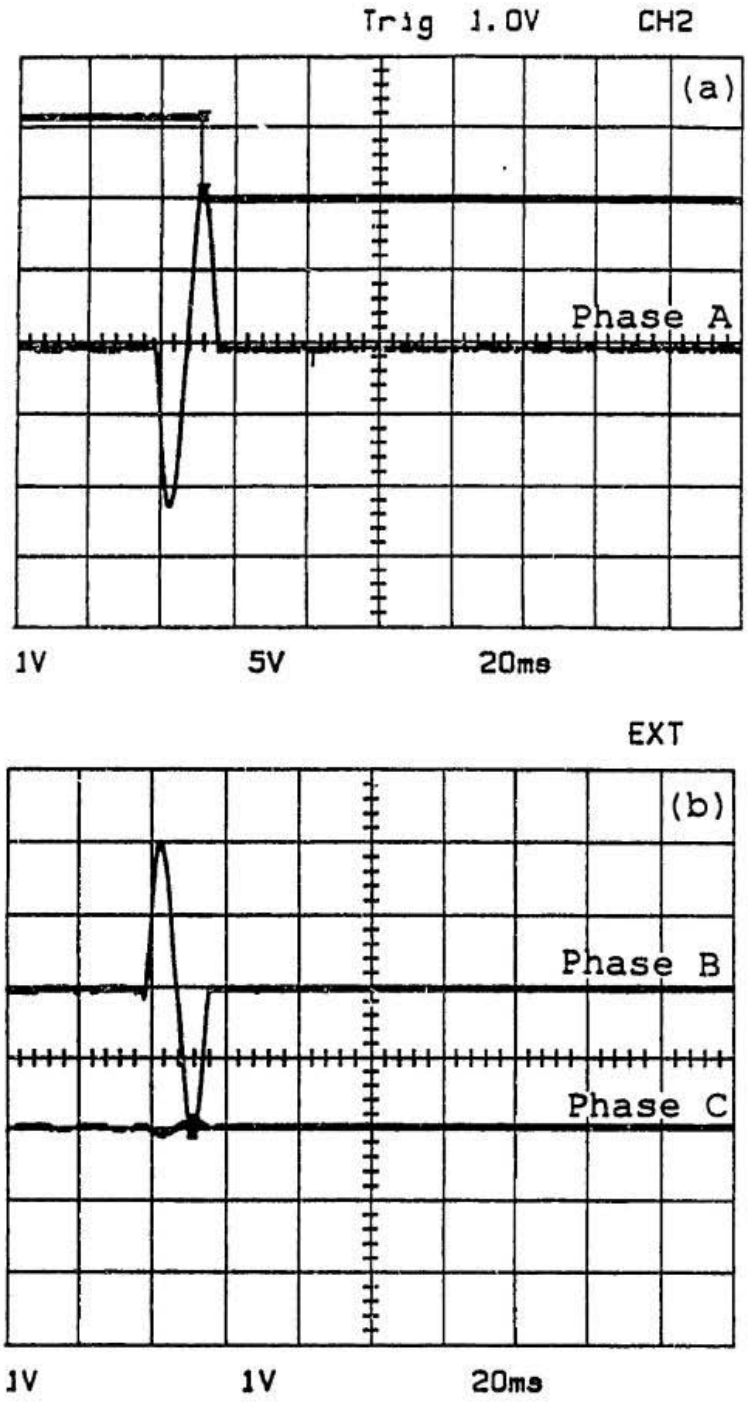

Figure 5.13: ANN responses to a primary side phase A to phase B fault without load and occurred after inrush: (a) control voltage and differential current in phase A, (b) differential currents in phase B and phase C. (Y-scale 1V = 12.5 A).

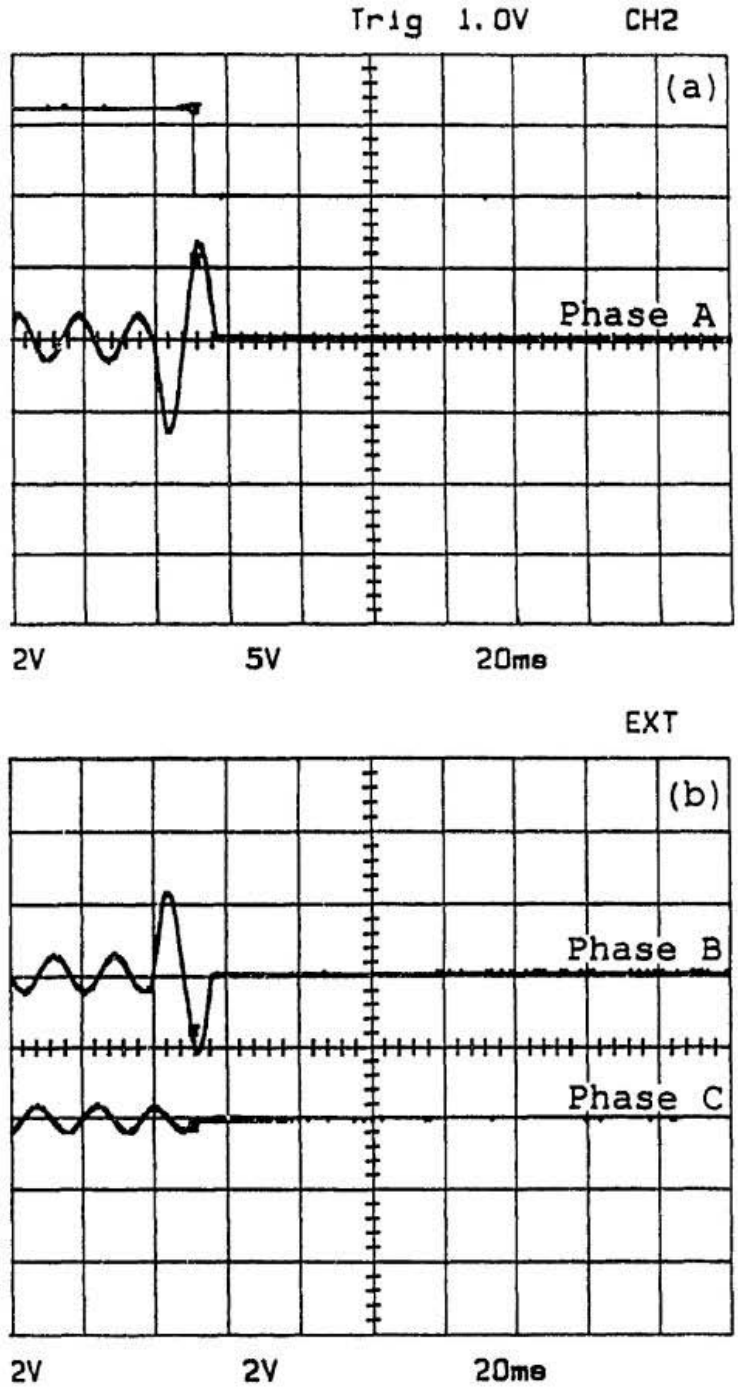

Figure 5.14: ANN responses to a primary side phase A to phase B fault with load and occurred after inrush: (a) control voltage and differential current in phase A, (b) differential currents in phase B and phase C. (Y-scale 1V = 12.5 A).

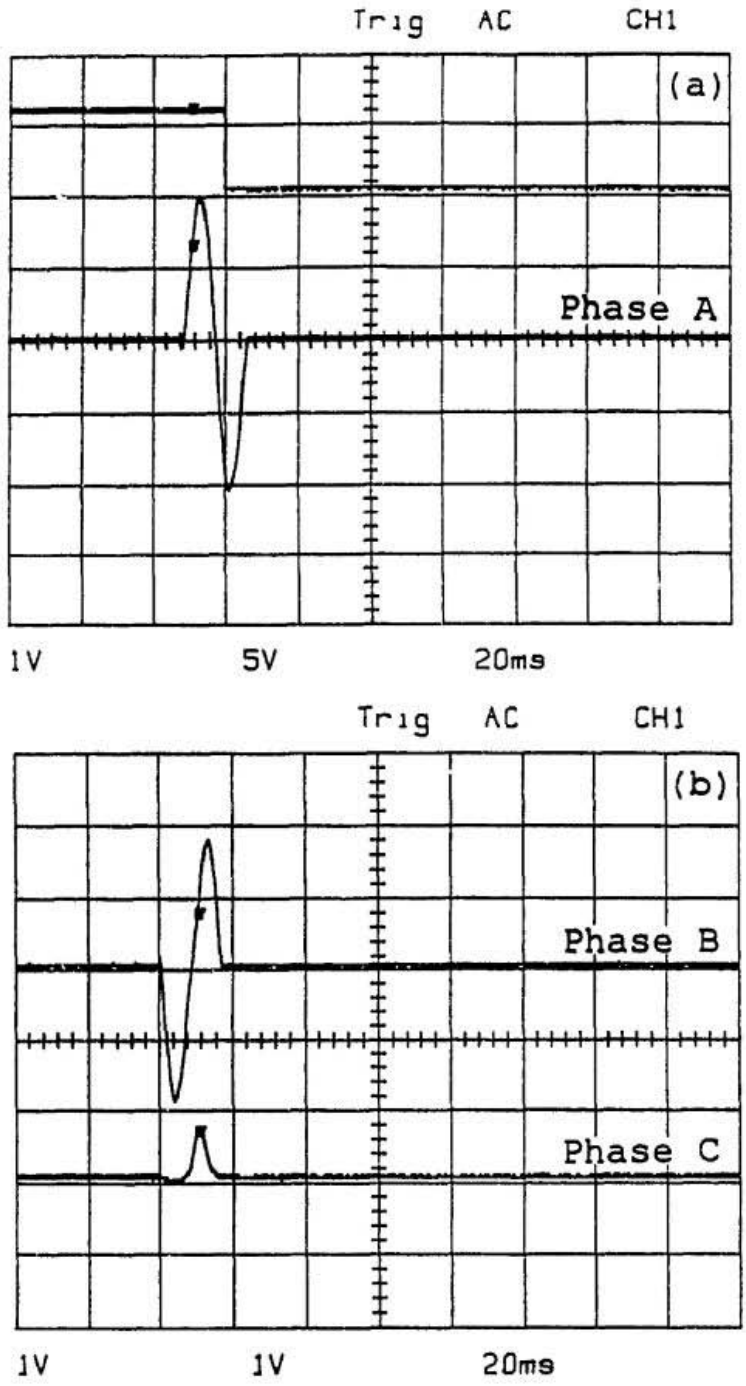

Figure 5.15: ANN responses to a primary side phase A to phase B fault without load and occurred before inrush: (a) control voltage and differential current in phase A, (b) differential currents in phase B and phase C. (Y-scale 1V = 12.5 A).

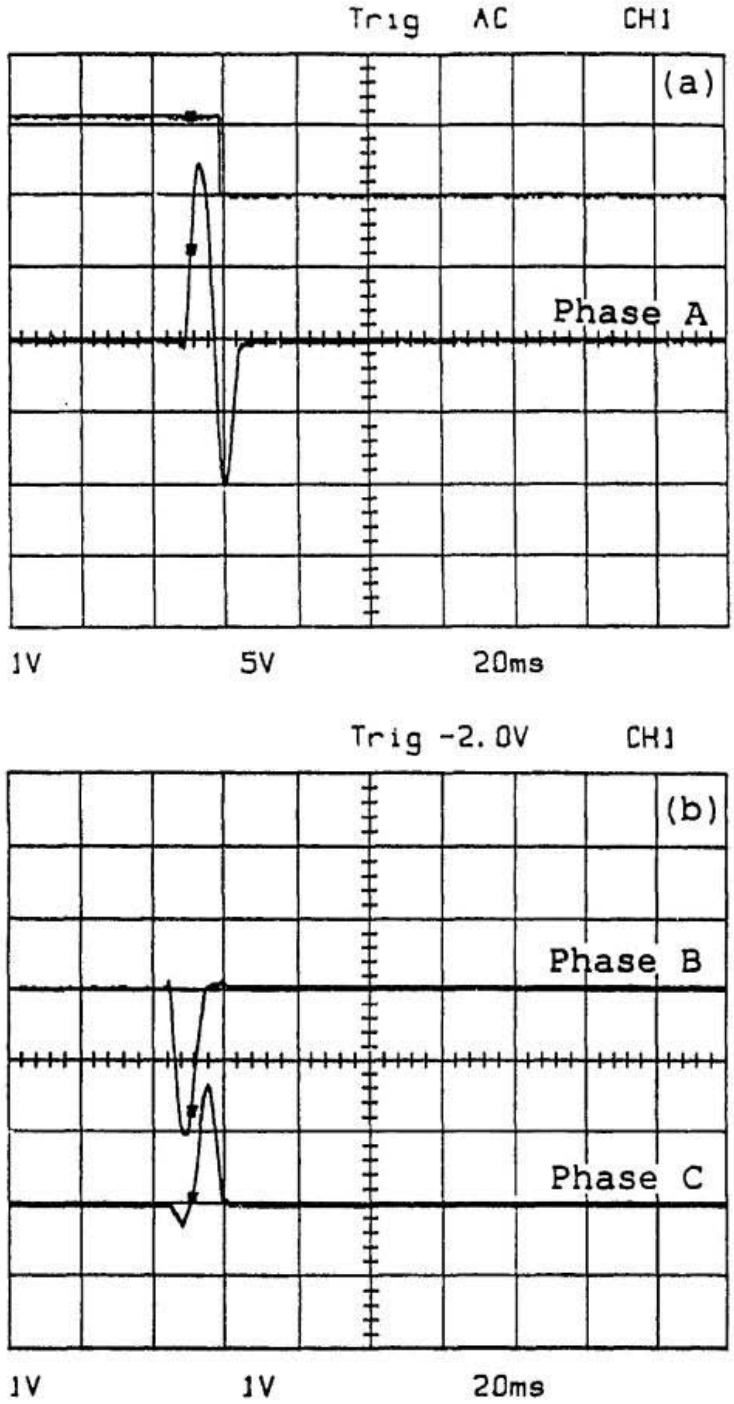

Figure 5.16: ANN responses to a primary side phase A to phase B fault with load and occurred before inrush: (a) control voltage and differential current in phase A, (b) differential currents in phase B and phase C. (Y-scale 1V = 12.5 A).

transformer against the fault.

Also, it is important to test the performance of the ANN with load. This has been done as shown in Figs. 5.14(a) and (b). As expected, the ANN again sent the trip signal output and thus the control signal went to zero. The performance of the ANN was also tested while switching on a fault with both no load and load. The results are as shown in Figs. 5.15 and 5.16. Again the ANN detected the fault within one cycle time period. The above four tests were also carried out in the other two pairs of phases i.e. phase to phase fault between phases B and C, and between phases C and A. The results are shown in Appendix-C. The ANN was able to respond properly in all cases and in most of the cases, the response is within one cycle of the fault inception.

ii) Secondary side phase to ground fault

This test was carried out by connecting the faulty branch between phase A and ground in secondary side. The switchings are done using Table-5.1 according to the corresponding test conditions. Figures 5.17 (a) and (b) illustrate the results for the fault which has occurred after the transformer was energized without load. The results for the same fault with load is shown in Fig. 5.18(a) and (b). The results for the same fault, but already existed when the transformer was switched on, are presented in Figs. 5.19 and 5.20 for both no load and loading conditions, respectively. The ANN again took the right decisions and sent trip signals within one cycle in all cases. Similar results were obtained when the tests were performed in the other two phases i.e. phase to ground faults in phases B and C. The results for these two phases are illustrated in Appendix-C. The control signal went down to zero within a cycle time period and thus interrupted the fault current through the transformer.

iii) Secondary side phase-to-phase fault

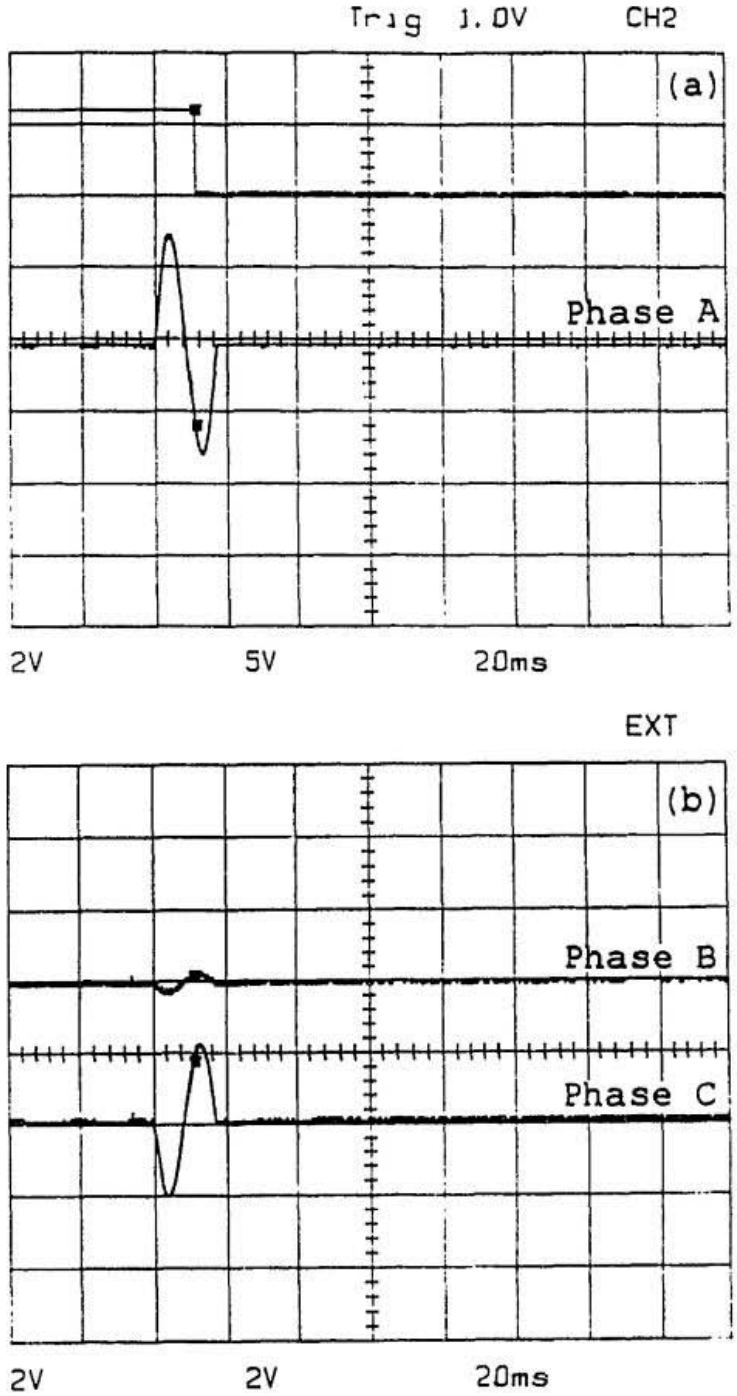

Figure 5.17: ANN responses to a secondary side phase A to ground fault without load and occurred after inrush: (a) control voltage and differential current in phase A, (b) differential currents in phase B and phase C. (Y-scale 1V = 12.5 A).

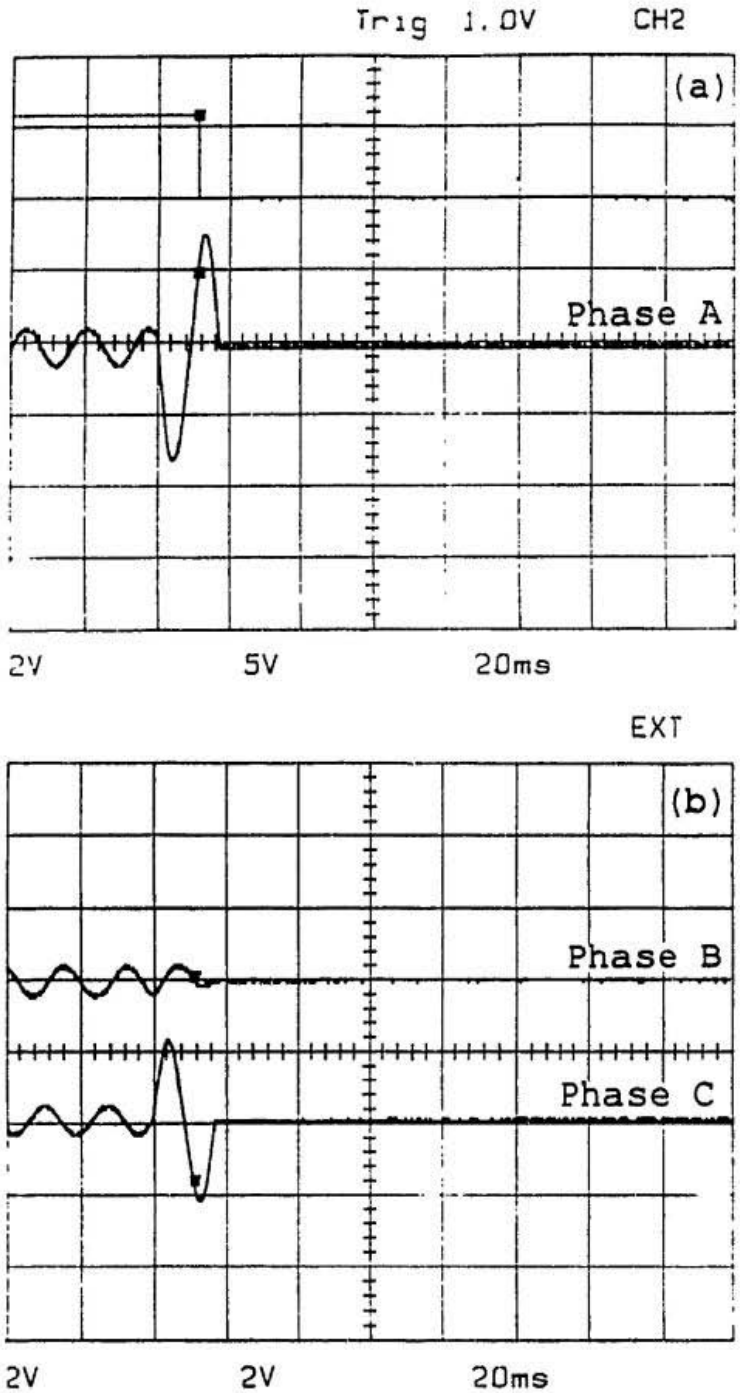

Figure 5.18: ANN responses to a secondary side phase A to ground fault with load and occurred after inrush: (a) control voltage and differential current in phase A, (b) differential currents in phase B and phase C. (Y-scale 1V = 12.5 A).

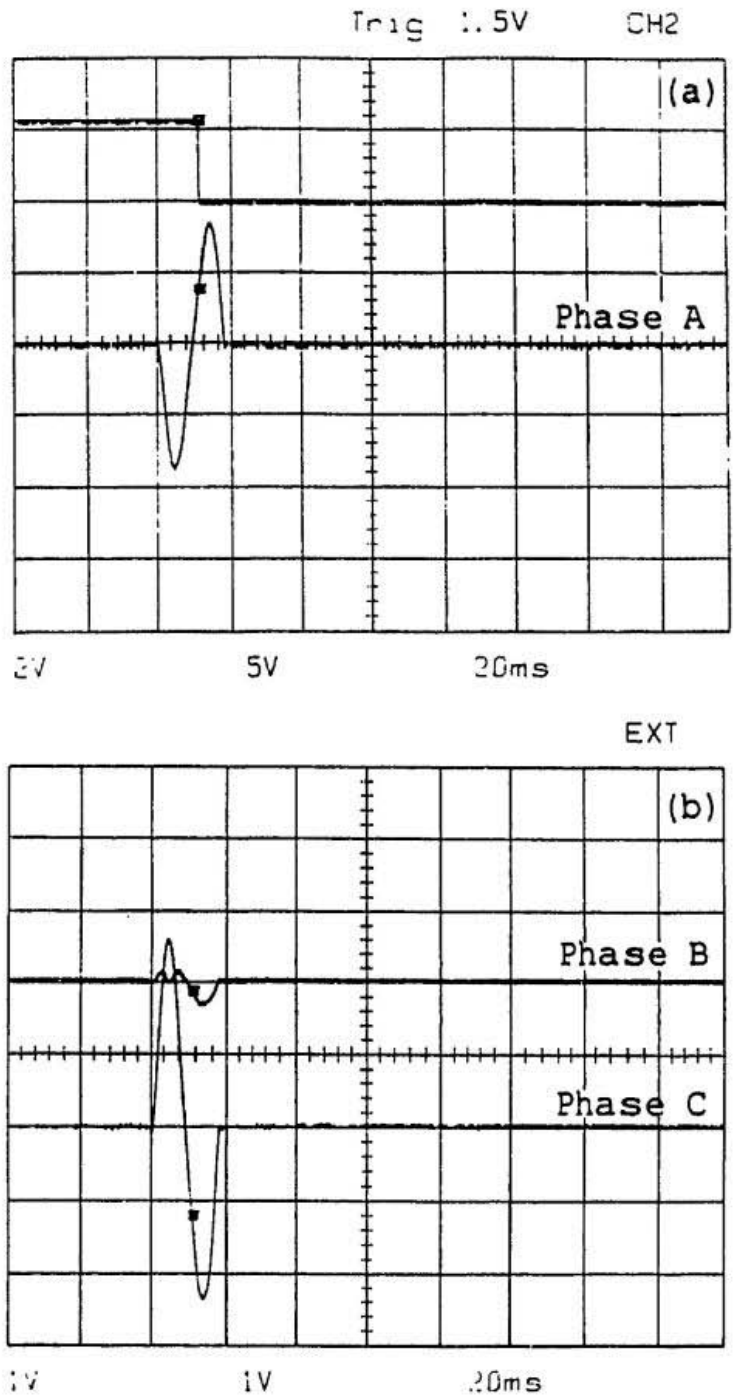

Figure 5.19: ANN responses to a secondary side phase A to ground fault without load and occurred before inrush: (a) control voltage and differential current in phase A, (b) differential currents in phase B and phase C. (Y-scale 1 V = 12.5 A).

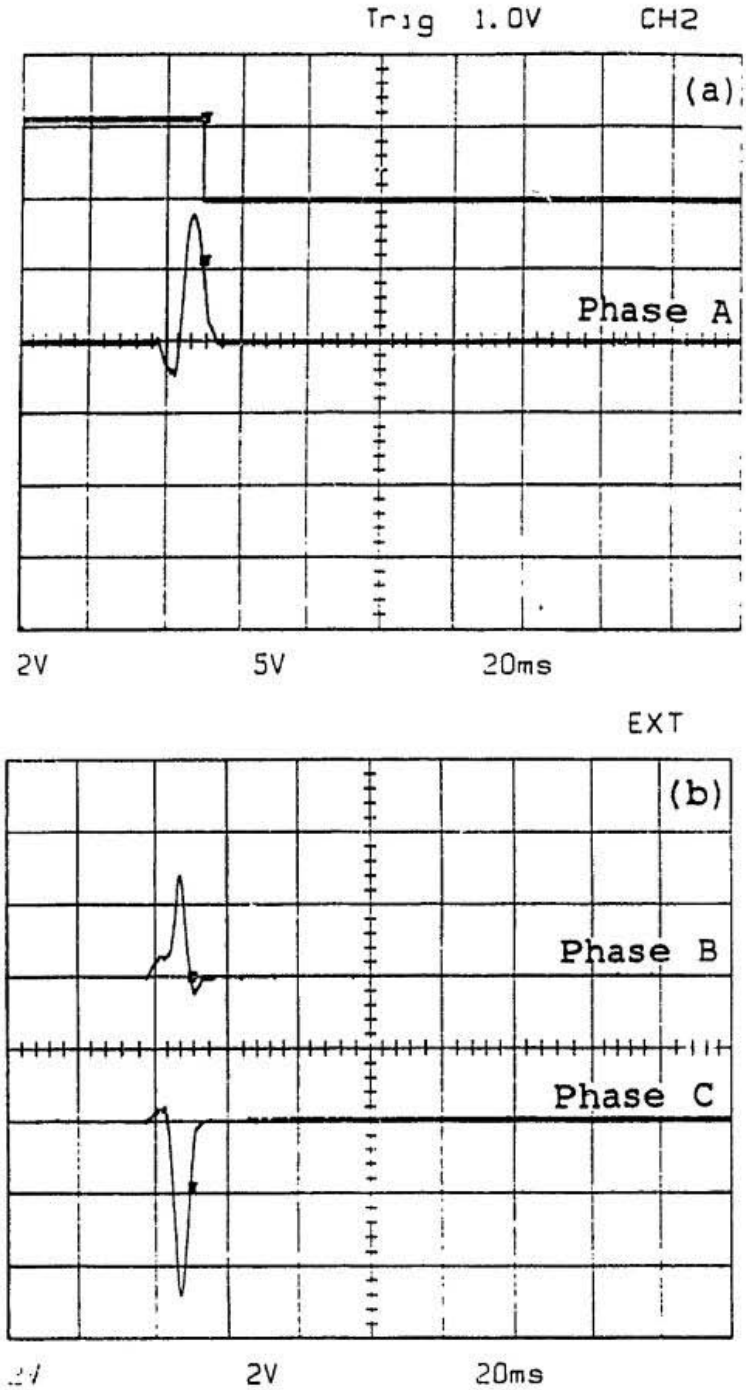

Figure 5.20: ANN responses to a secondary side phase A to ground fault with load and occurred before inrush: (a) control voltage and differential current in phase A, (b) differential currents in phase B and phase C. (Y-scale 1V = 12.5 A).

Tests were carried out by connecting the faulty branch between phases A and B. The switchings are done according to Table 5.1 for the four test conditions. At first, the transformer was energized and then the fault has occurred. The results are shown both for no-load and with load in Figs. 5.21 and 5.22, respectively. Also, the switching of the transformer was performed on the fault with both load and no load. The results are illustrated in Figs. 5.23 and 5.24 for no load and loading conditions, respectively. In all cases, the responses of the ANN are accurate, as expected. It was able to recognize the fault in about three-quarter of a cycle after the fault inception. The tests were also carried out for the other two pairs of phases i.e. between phases B and C, and phases C and A. The results are given in Appendix-C.

iv) Secondary side fault between taps

This test procedure was done by connecting the faulty branch in between the 550 and 600 V taps in phase A. Switching sequences are given in Table 5.1 for different conditions. The results are illustrated in Figs. 5.25 - 5.28. It should be noted that the fault magnitude is quite low in this type of fault. However, the ANN was able to recognize the fault and sent appropriate signal to the control circuit. Figures 5.25 and 5.26 show the ANN responses and the differential currents in three phases for the faults between tap without and with load, respectively, and the faults occurred after energizing the transformer. The same fault, which has occurred before the energization of the transformer with no load and load are also illustrated in Figs. 5.27 and 5.28. It is worth noting that the margin between pre-fault and post-fault currents are quite low in Figs. 5.26(a) and (b). However, like all other fault cases, the ANN was able to recognize the fault, within a cycle of the fault inception.

Similar results were found while performing the experiments in the other two phases. The results are shown in Appendix-C.

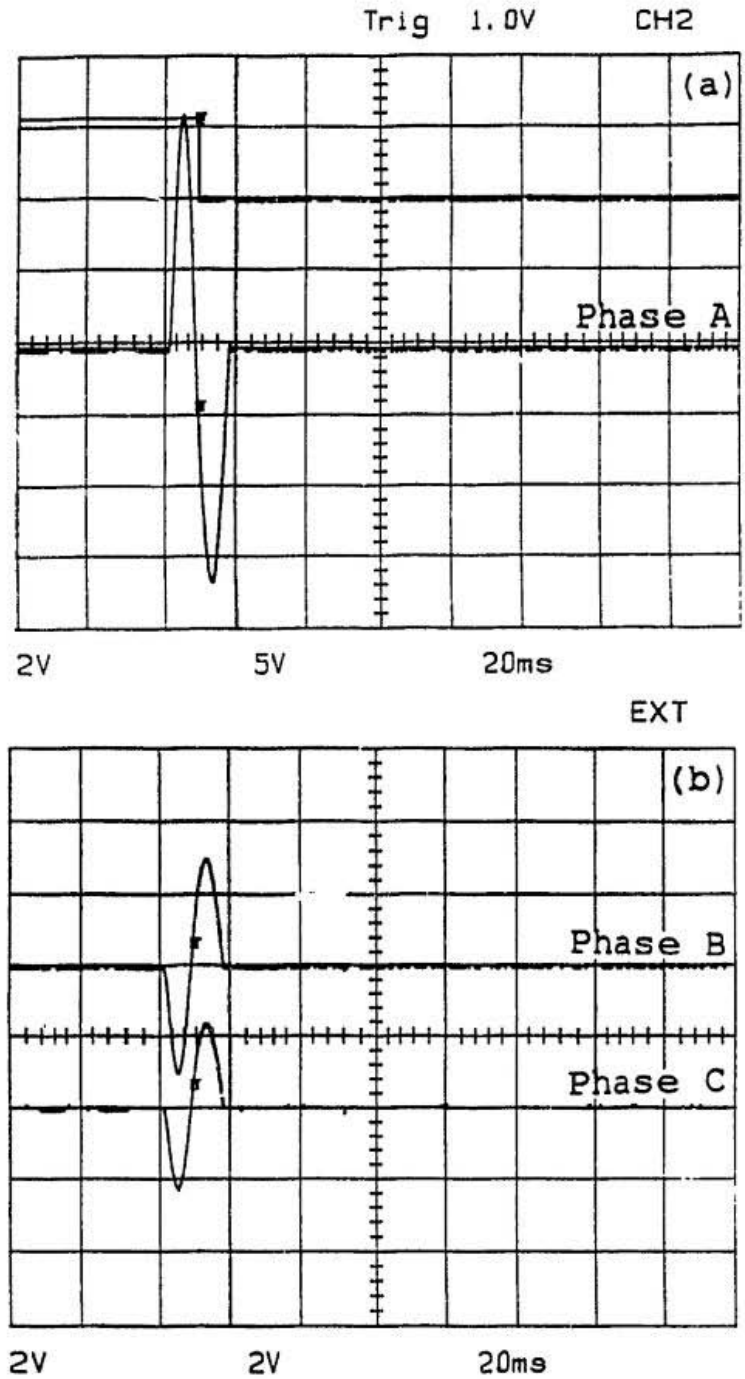

Figure 5.21: ANN responses to a secondary side phase A to phase B fault without load and occurred **after** inrush: (a) control voltage and differential current in phase A, (b) differential currents in phase B and phase C. (Y-scale 1V = 12.5 A).

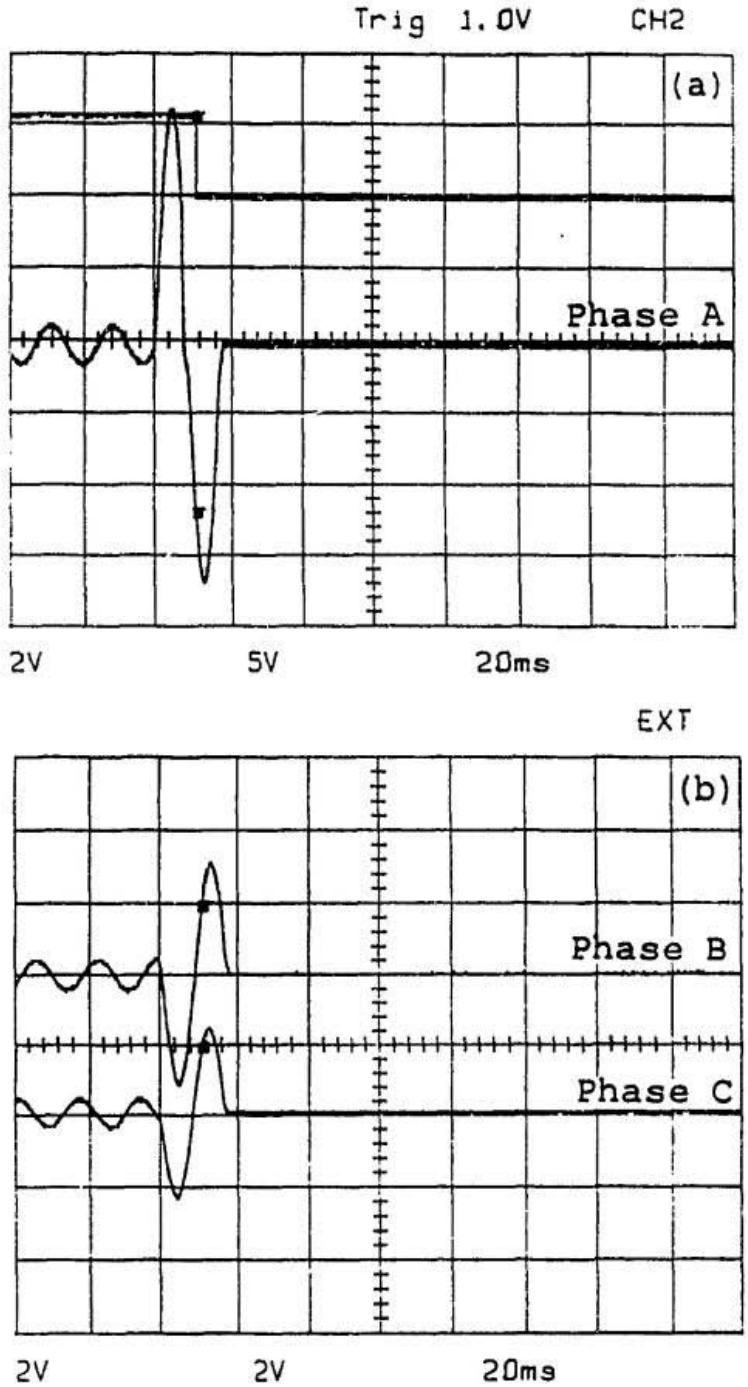

Figure 5.22: ANN responses to a secondary side phase A to phase B fault with load and occurred after inrush: (a) control voltage and differential current in phase A, (b) differential currents in phase B and phase C. (Y-scale 1V = 12.5 A).

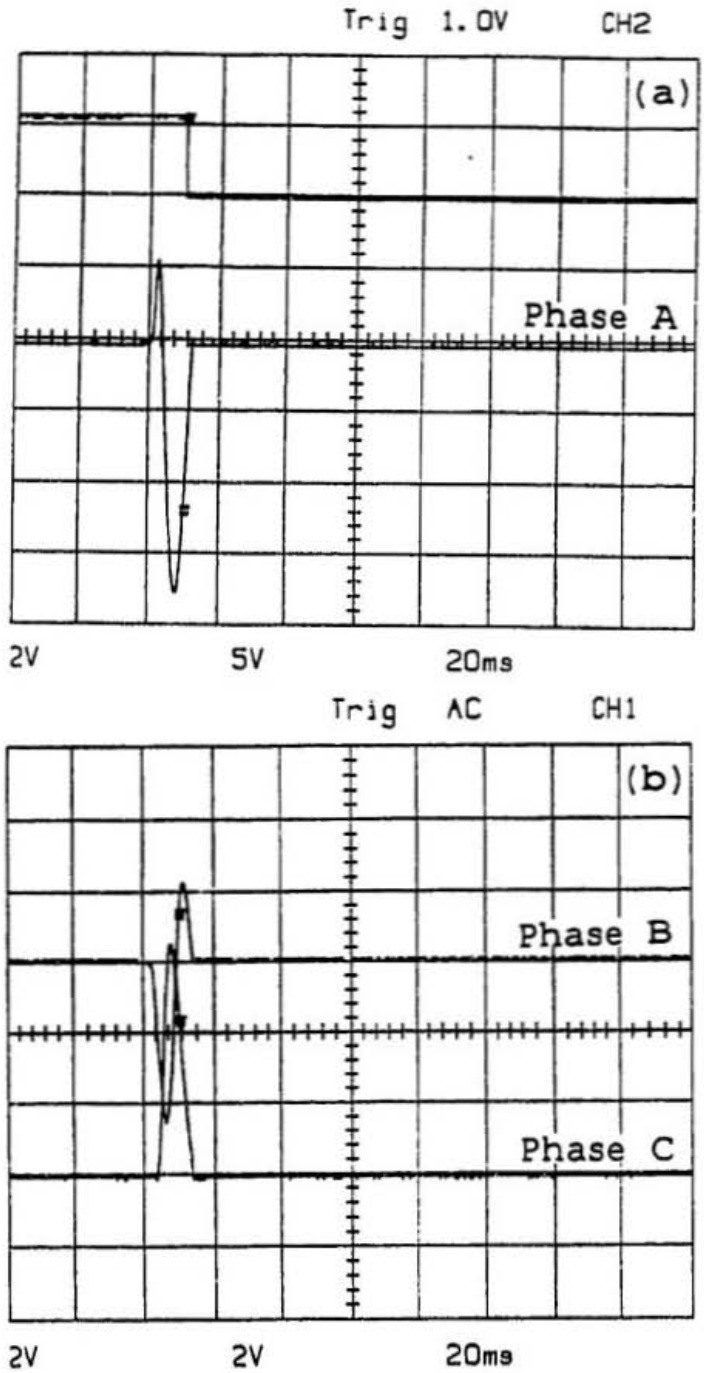

Figure 5.23: ANN responses to a secondary side phase A to phase B fault without load and occurred before inrush: (a) control voltage and differential current in phase A, (b) differential currents in phase B and phase C. (Y-scale 1V = 12.5 A).

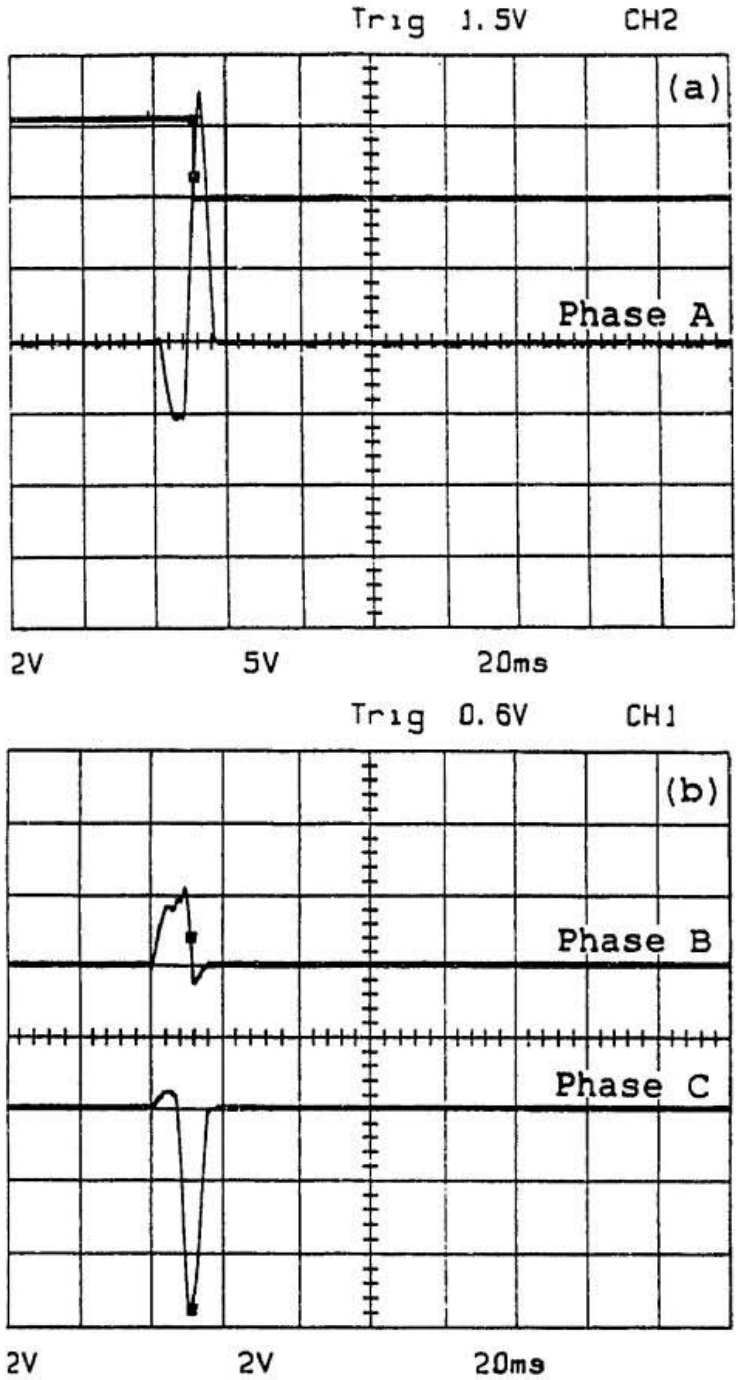

Figure 5.24: ANN responses to a secondary side phase A to phase B fault with load and occurred before inrush: (a) control voltage and differential current in phase A, (b) differential currents in phase B and phase C. (Y-scale 1V = 12.5 A).

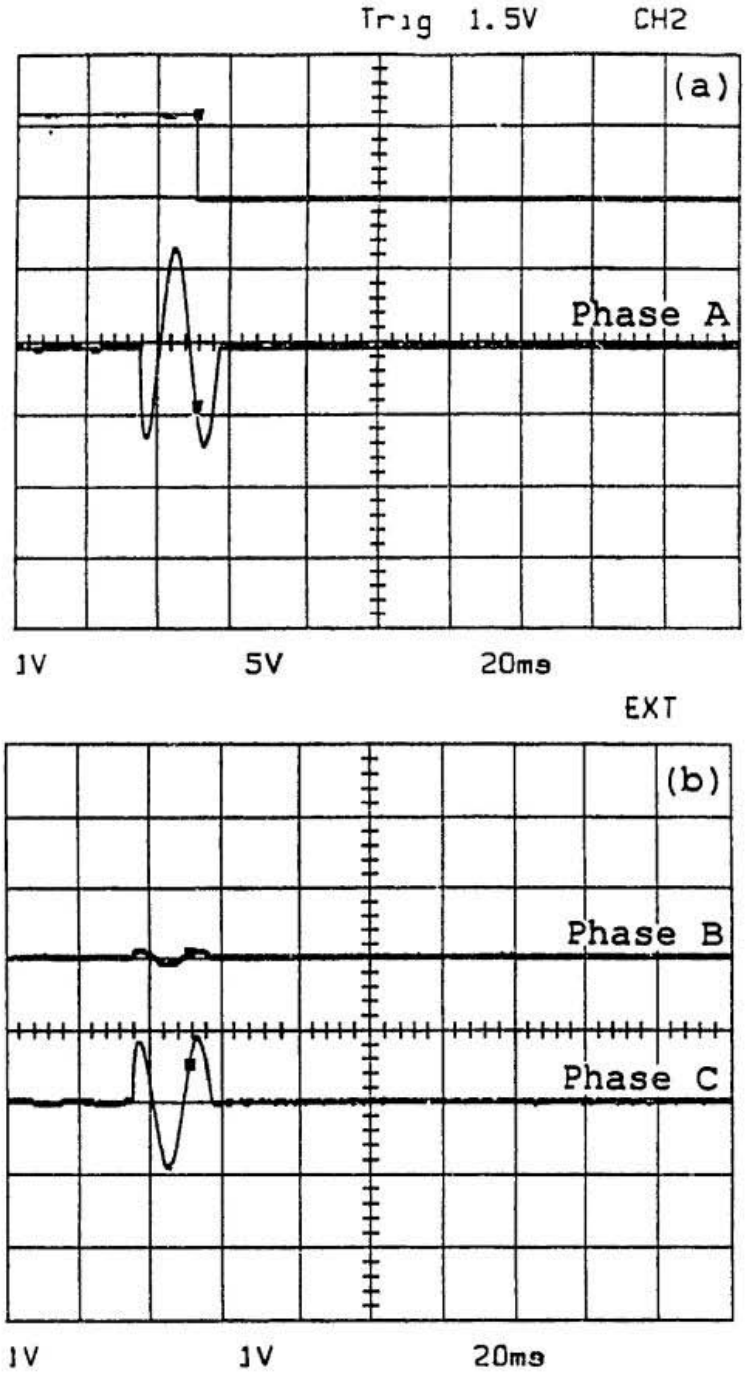

Figure 5.25: ANN responses to a secondary side between tap fault in phase A without load and occurred after inrush: (a) control voltage and differential current in phase A, (b) differential currents in phase B and phase C. (Y-scale 1V = 12.5 A).

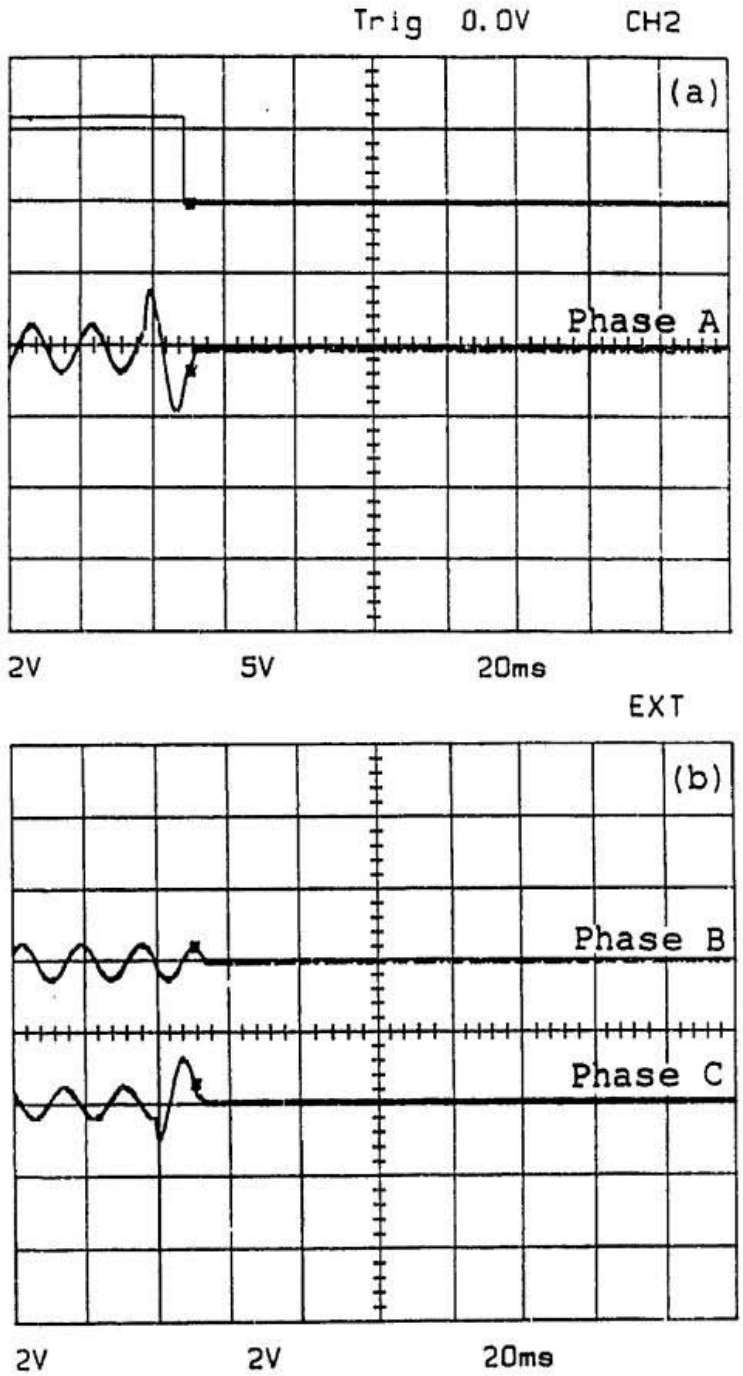

Figure 5.26: ANN responses to a secondary side between tap fault in phase A with load and occurred after inrush: (a) control voltage and differential current in phase A, (b) differential currents in phase B and phase C. (Y-scale 1V = 12.5 A).

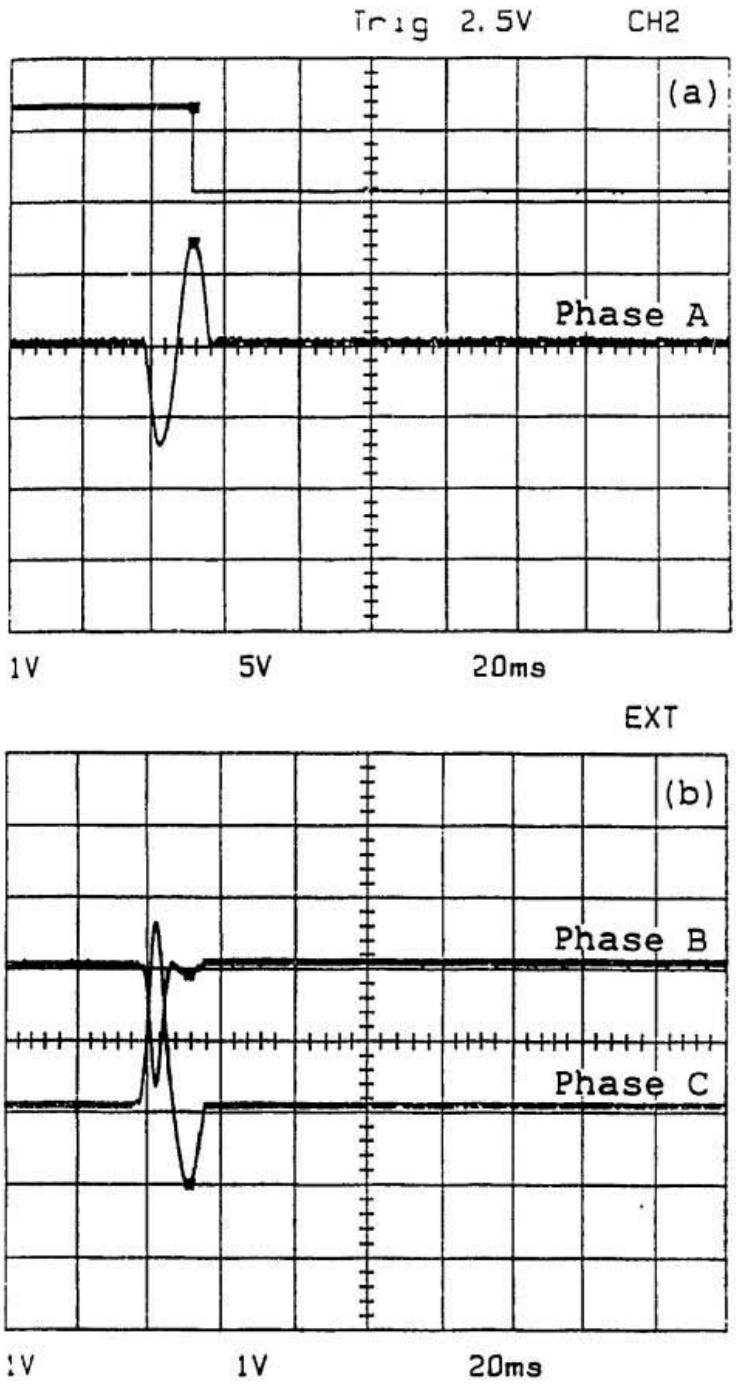

Figure 5.27: ANN responses to a secondary side between tap fault in phase A without load and occurred before inrush: (a) control voltage and differential current in phase A, (b) differential currents in phase B and phase C. (Y-scale 1V = 12.5 A).

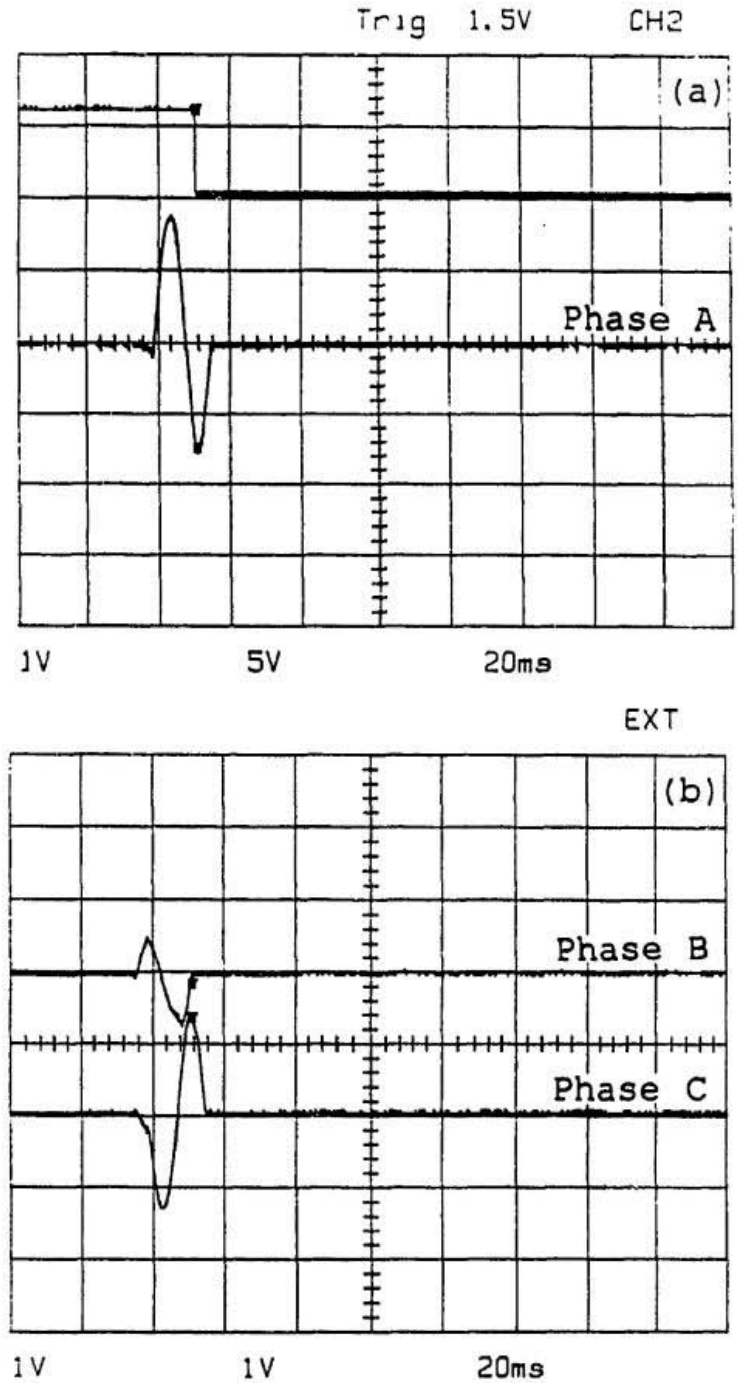

Figure 5.28: ANN responses to a secondary side between tap fault in phase A with load and occurred before inrush: (a) control voltage and differential current in phase A, (b) differential currents in phase B and phase C. (Y-scale 1V = 12.5 A).

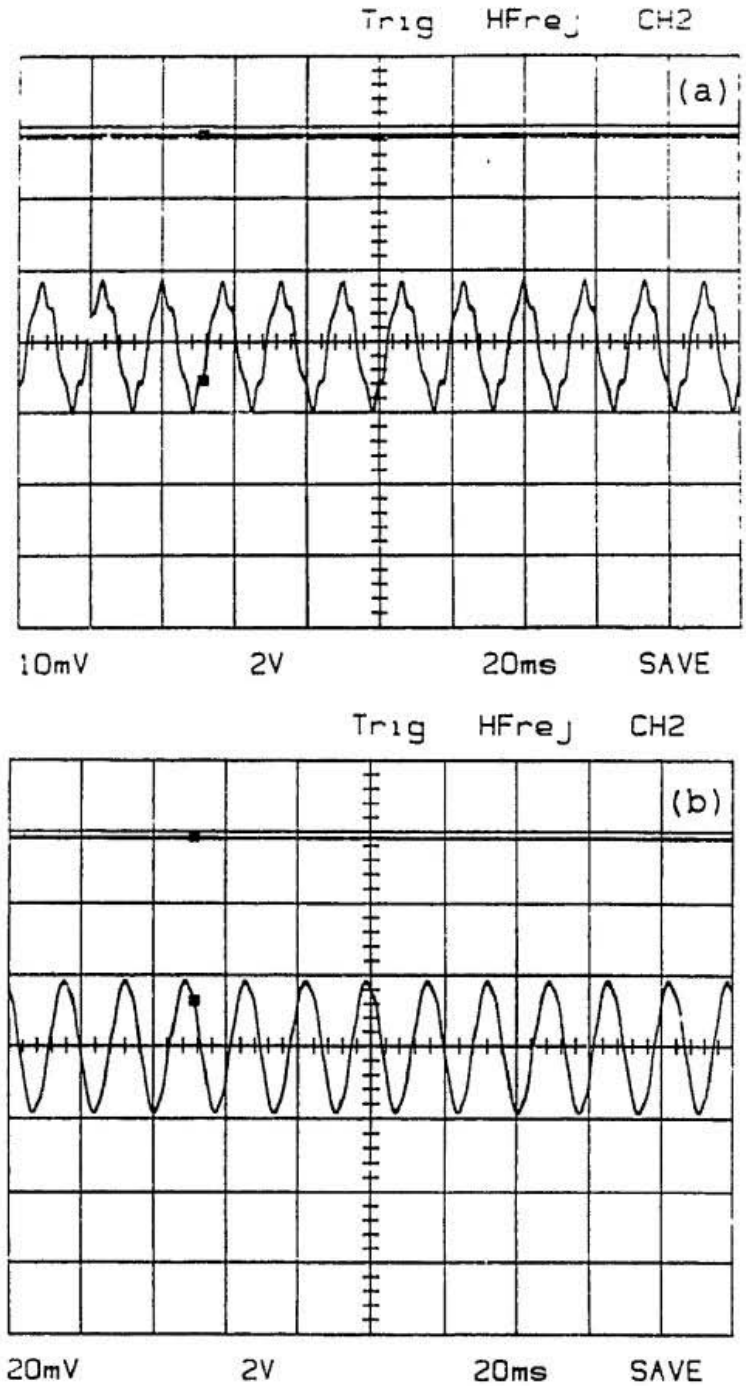

Figure 5.29: ANN responses to steady-state over-excitation: (a) without load, (b) with load; (Y-scale 1mv = 0.5 A).

5.5.3 Steady state over-excitation

This test was carried out by increasing the supply voltage to about 128% of its rated voltage. Since the laboratory cannot supply more than 230 V directly, the voltage was stepped up by another step-up transformer which was connected in series with the test transformer. As can be seen from Fig. 5.29(a), under no load condition, the current is quite distorted. This is because of the presence of strong fifth harmonic component. The ANN does not have any difficulty in maintaining the control signal i.e. it recognizes the current as a no fault situation and therefore restrains from tripping. This strong fifth harmonic component is used in other digital relaying techniques [48]. However, unlike the other methods, the ANN relies on the overall pattern of the current waveform to take the decision. The advantages of this method over the other methods is that the decision of the ANN does not depend directly on the harmonic contents of the current as explained in the previous chapter. The same test was also performed with load as shown in Fig. 5.29(b).

The proposed ANN based algorithm is successfully implemented in real time using the digital signal processor, DS-1102. The on-line test results are very consistent with the off-line test results. The response of the ANN is accurate and prompt in all cases. In most of the fault cases, the trip signal is delivered within a cycle. In the worst case, the ANN takes about one and half cycle time period to detect the fault. The ANN has its ability to generalize and thus even if the waveform is distorted to some extent due to many practical reasons such as CT saturation, dc offsets etc., it should work accurately.

The next chapter provides a brief summary of this thesis work. The major contributions are also presented in Chapter 6. Finally, the thesis is concluded by pointing out some future directions for this work.

Chapter 6

Summary and Conclusions

6.1 Summary

Transformer protection is generally more difficult than protecting other parts of the power system. This is primarily due to the presence of magnetizing inrush phenomenon in a transformer. The differential protection scheme with harmonic restraint is commonly used for power transformer protection. The harmonic restraint is required to prevent the mal-operation which may occur due to high magnetizing inrush current. There exist many digital algorithms based on the harmonic restraint principle. These algorithms work quite satisfactorily under the assumption that the magnetizing current contains a much higher second harmonic component than that present in the fault current. This assumption is no longer as valid as it was before the introduction of modern transformers which use low-loss amorphous materials. It has been reported that modern transformers do not exhibit significant amount of the second harmonic component in the inrush current [59]. The harmonic restraint algorithms are also based on the fact that the fundamental component present in the fault current is much higher than that present in the inrush current which may not

be the case for all types of faults, e.g., the winding fault. The existing methods based on the harmonic restraint are not quite so reliable for modern transformer protection.

The recent trend for power transformer protection deviates from the harmonic restraint concept. Voltage and flux restraint algorithms have been developed. However, these algorithms are also found to be ineffective. Some recent techniques have been developed which use the transformer equivalent circuit model. In such methods, the transformer parameters are determined from tests and/or taken from design data. The parameters usually change their values under different operating conditions. Therefore, these algorithms are susceptible to parameter variations and hence not quite reliable.

Realizing the limitations of the harmonic and model based techniques for three phase power transformer protection, an alternative method is searched for. In recent years, the artificial neural network has been successfully used in many applications, particularly in pattern recognition. Distinguishing between the magnetizing inrush current and the internal fault current can be considered as a pattern recognition problem. In this study, an ANN based three phase power transformer protection scheme is developed. The protection algorithm is implemented and tested both off-line and on-line.

In chapter 1, an extensive literature survey on many existing digital relaying algorithms for transformer protection is carried out. A critical review of these algorithms gives a clear picture of the problem. The problem involving transformer protection is identified and a solution approach using artificial neural network is proposed.

The complex but unavoidable magnetizing inrush phenomenon is described elaborately for both the single phase and three phase transformers in Chapter 2. Some other features, namely CT saturation and over-excitation, etc. which are important

considerations in designing relays for transformer protection are also included in chapter 2. The basic principle of the harmonic restraint differential relaying is described using a typical analogue relay. An efficient digital relaying algorithm using the digital Fourier transform (DFT) is studied thoroughly. The DFT algorithm is implemented on a three phase laboratory power transformer using the digital signal processor board DS-1102. On-line test results for the DFT algorithm on different magnetizing inrush and fault conditions are also presented in Chapter 2.

In Chapter 3, the concept and some applications of artificial neural network are introduced. In recent years, applications of artificial neural network in various power system areas are becoming increasingly popular. It is, however, important to choose a proper ANN structure and suitable training algorithm in the case of supervised learning. Multi-layer perceptron (MLP) is the main-stream of the ANN structure used in power system applications. A multi-layer feed-forward neural network is used in this work. At first, the general structure and characteristics of the network are described and then the design of the ANN for current signature verification for the transformer protection is presented. A back-propagation algorithm is used to train the network. The algorithm is also described in detail in Chapter 3. The training of the ANN for this work is performed using experimental data for large number of fault, inrush and over-excitation currents.

The experimental setup for data acquisition is presented in Chapter 4 where different fault and inrush tests are carried out. In order to take into account the various characteristics of inrush currents, the transformer is randomly switched on many times using electronically controlled triac switches. It is ensured that under no circumstances can the fault current flow through the transformer for more than five cycle time period. Five cycle data are taken in all inrush and fault cases which were

processed later on for use in training and testing the ANN. Following data acquisition and processing, the training of the ANN is presented in detail. The ANN is tested with some of the experimental data and the results are presented in the latter part of Chapter 4. A study is performed to investigate the sensitivity of the ANN algorithm to harmonic distortion. The original inrush, fault and over-excitation current data are distorted by varying different harmonic contents. The performances of the ANN under such conditions are compared with those for the DFT algorithm. The comparative results are also presented.

The real time implementation of the proposed ANN based algorithm using the digital signal processor board DS-1102 is presented in Chapter 5. The on-line experimental results are consistent with the off-line test results. The test is first performed for the single phase case and then extended for three phases. The three phase implementation is done in four different ways. In all test cases, the responses of the ANN are found accurate and prompt. In most of the fault cases, the trip signal is delivered within one cycle time period. In no case, did the ANN take more than one and half cycle time period to detect the fault.

6.2 Contributions

The major contributions of this thesis are

- A novel method for transformer protection using an artificial neural network (ANN) is developed.
- An innovative ANN structure has been designed.
- An experimental set-up for acquiring inrush and fault current data is developed.

- An efficient digital relaying algorithm based on the discrete Fourier transform (DFT) is implemented in real time using the DS-1102 digital signal processor.
- The proposed innovative ANN algorithm is successfully implemented in real-time on a laboratory three phase transformer protection.
- A critical discussion of the ANN and DFT algorithms under various harmonic distortions is presented.

6.3 Conclusions

- The artificial neural network (ANN) is a fairly new concept in the power system protection. In this thesis, an innovative application of the ANN in a three phase transformer protection is successfully established for the first time.
- The inrush characteristic in a three phase transformer is quite difficult to model. Thus it is better to train the ANN using experimental data rather than using simulated data for realistic protection of a power transformer. The ANN algorithm trained with the experimental data worked satisfactorily for the protection of a three phase laboratory power transformer protection.
- Unlike conventional relaying algorithms, the ANN algorithm does not depend directly on the harmonic contents of the current waveform. Therefore, it is less sensitive to the harmonic distortion of the current and/or dc offset. In modern transformers with low-loss amorphous materials, there is less second harmonic component in magnetizing inrush current. The ANN based algorithm is expected to be reliable for the protection of these modern power transformers.

- The ANN algorithm is easy to implement, simple and accurate. The ANN is prompt as it detects most of the faults within one cycle. At no time is the response in excess of one and half cycle time period.

- Since the training data for the proposed ANN is obtained through experiments, the algorithm is insensitive to parameter variations, CT saturation and other system disturbances.

6.4 Suggestion for the Future Work

The ANN used in this study is a multi-layer perceptron (MLP) which is trained with the back-propagation algorithm. The MLP with back-propagation is successful in many applications. The main attractive feature of the MLP is its simplicity, which is very important in relaying applications. Limitation of this type of network is that if there is new data, the network has to be retrained with all data, which is time-consuming. There is a wide scope for research in this area. Some suggestions for further works are

- Investigations of other types of neural networks, such as adaptive resonance theory (ART), recurrent neural networks (RNNs), radial basis neural networks (RBNNs), etc. that can overcome the limitation of extensive training time could be made. However, it should be mentioned that these type of networks are complex which may cause an extensive computational burden on the available digital signal processors.

- Experimental investigations of the effects of some other power system disturbances on the ANN based algorithm need to be carried out.

- Field testing of the ANN based stand-alone transformer relay should be undertaken.

- Electromagnetic transient program (EMTP) simulation package is one of the standard tools in power system analysis and protection studies. Incorporation of the ANN in the EMTP program may improve the usefulness of the computer software packages for power system protection.

References

[1] *Applied Protective Relaying*, Westinghouse Electric Corporation, Newark, N.J., 1976.

[2] Rahman, M.A. and Gangopadhyay, A., "Digital Simulation of Magnetizing Inrush Currents In Three Phase Transformers", *IEEE Trans. on Power Delivery*, Vol. PWRD-1, No. 4, 1986, pp. 232-242.

[3] Specht., T.R., "Transformer Inrush and Rectifier Transient Currents", *IEEE Trans. on Power Apparatus and Systems*, Vol. PAS-88, No-4, 1969, pp. 269-276.

[4] Blume, L.F., Camilli, G., Farnham, S.B. and Peterson, H.A., "Transformer Magnetizing Inrush Currents and Influence on System Operation", *AIEE Transaction*, Vol. 63, 1944, pp. 366-375.

[5] Finzi, L.A. and Mutschler, W.H., "The Inrush of Magnetizing Current in Single-Phase Transformers", *AIEE Transaction*, Vol. 70, 1951, pp. 1436-1438.

[6] Sonnemann, W.K., Wagner, C.L. and Rockfeller, G.D., "Magnetizing Inrush Phenomenon in Transformer Banks", *AIEE Transaction*, Vol. 77, 1958, pp. 884-892.

[7] Dick, E.P. and Watson, W., "Transformer Models for Transient Studies Based on Field Measurements", *IEEE Trans. on Power Apparatus and Systems*, Vol. PAS-100, No. 1, pp. 409-418.

[8] Fergestad, P.I. and Henriksen, T., "Inductances for the Calculation of Transient Oscillation in Transformers", *IEEE Trans. on Power Apparatus and Systems*, Vol. PAS-93, 1974, pp. 510-517.

[9] Keyhani, A., Miri, S.M. and Hao, S., "Parameter Estimation for Power Transformer Models from Time Domain Data", *IEEE Trans. on Power Delivery*, Vol. 1, No. 3, 1986, pp. 1070-1078.

[10] Keyhani, A., Chua, S.W. and Sebo, S.A., "Maximum Liklihood Estimation of Transformer High Frequency Parameters from Test Data", *IEEE Trans. on Power Delivery*, Vol. 6, No. 2, 1991, pp. 858-865.

[11] Leon, F. and Semlyen, A., "Reduced Order Model of Transformer Transients", *IEEE Trans. on Power Delivery*, Vol. 7, No. 1, 1992, pp. 361-369.

[12] Leon, F. and Semlyen, A., "Efficient Calculation of Elementary Parameters of Transformers", *IEEE Trans. on Power Delivery*, Vol. 7, No. 1, 1992, pp. 376-383.

[13] Leon, F. and Semlyen, A., "Complete Transformer Model for Electromagnetic Transients", *IEEE Trans. on Power Delivery*, Vol. 9, No. 1, 1994, pp. 231-239.

[14] Kennedy, L.F. and Hayward, C.D., "Harmonic-Current-Restrained Relays for Differential Protection", *AIEE Transaction*, Vol. 57, 1938, pp. 262-271.

[15] Hayward, C.D., "Harmonic-Current-Restrained Relays for Transformer Differential Protection", AIEE Trans., Vol. 60, 1941, pp. 377-382.

[16] Mathews, C.A., "An Improved Transformer Differential Relay", *AIEE Transaction*, Vol. 73, 1954, pp. 645-649.

[17] Sharp, R.L. and Glassburn, W.E., "A Transformer Differential Relay with Second-Harmonic Restraint", *AIEE Transaction*, Vol. 77, 1958, pp. 913-918.

[18] Einvall, C.H. and Linders, J.R., "A Three-Phase Differential Relay for Transformer Protection", *IEEE Trans. on Power Apparatus and Systems*, Vol. PAS-94, No. 6, 1975, pp. 1971-1980.

[19] Rockfeller, G.D., "Fault Protection with a Digital Computer", *IEEE Trans. on Power Apparatus and Systems*, Vol. PAS-88, No. 4, 1969, pp. 438-461.

[20] Mann, B.J. and Morrison, I.F., "Digital Calculation of Impedance for Transmission Line Protection", *IEEE Trans. on Power System and Apparatus*, Vol. PAS-90, No. 1, 1971, pp. 270-279.

[21] Mann, B.J. and Morrison, I.F., "Relaying a Three-Phase Transmission Line with a Digital Computer", *IEEE Trans. on Power Apparatus and Systems*, Vol. PAS-90, No. 2, 1971, pp. 742-750.

[22] Cheetham, W.J., "Computerized Protection or Not ? - Primary and Local Backup Protection", *IEE Conference*, Vol. 125, 1975, pp. 291-296.

[23] Cheetham, W.J., "Computerized Protection or Not ? - Remote Backup Protection", *IEE Conference*, Vol. 125, 1975, pp. 297-303.

[24] "Microprocessor Relays and Protection Systems", *IEEE Tutorial Course Text*, 88EH0269-1-PWR, 1988.

[25] Sykes, J.A. and Morrison, I.F., "A Proposed Method of Harmonic Restraint Differential Protection Relay for Power Transformers", *IEEE Trans. on Power Apparatus and Systems*, Vol PAS-91, No. 3, 1972, pp. 1266-1272.

[26] Malik, O.P., Dask, P.K. and Hope, G.S., "Digital Protection of a Power Transformer", *IEEE Power Engineering Winter Meeting*, A 76 191-7, 1976.

[27] Schweitzer, E.O., Larson, R.R. and Flechsig, A. J., "An efficient Inrush Current- Detection Algorithm for Digital Computer Relay Protection of Transformers", *IEEE Power Engineering Summer Meeting*, Mexico City, Mexico, A 77 510-1, 1977.

[28] Larson, R.R., Flechsig, A.J. and Schweitzer, E.O., "The Design and Test of a Digital Relay for Transformer Protection", *IEEE Trans. on Power Apparatus and Systems*, Vol. PAS-98, No. 3, 1979, pp. 795-804.

[29] Ramamoorty, M., "Applications of Digital Computer to Power System Protection", *Journal of Institute of Engineering (India)*, Vol. 52, No. 10, 1972, pp. 235-238.

[30] Thorp, J.S. and Phadke, A.G., "A Microprocessor Based Three-Phase Transformer Differential Relay", *IEEE Trans. on Power Apparatus and Systems*, Vol. PAS-101, No. 2, 1982, pp. 426-432.

[31] Rahman, M.A. and Dash, P.K., "Fast Algorithm for Digital Protection of Power Transformer", *IEE Proc.*, Vol. 129, Pt. C, No. 2, 1982, pp. 79-85.

[32] Horton, J.H., "Walsh Function for Digital Impedance relaying for Power Lines", *IEEE Power Engineering Society Summer Meeting*, San Francisco, 1975, pp. 530-541.

[33] Jeyasurya, B. and Rahman, M.A.,"Applications of Walsh Functions for Microprocessor-Based Transformer Protection", *IEEE Trans. on Electromagnetic Compatibility*, Vol. EMC-27, No. 4, 1985, pp. 221-225.

[34] Beauchamp, K.G., *Walsh Functions and Their Applications*, Academic Press, London, 1975.

[35] Fakruddin, D.B., Parthasarathy, K., Jenkins, L. and Hogg, B.W., "Applications of Harr Functions for Transmission Line and Transformer Differential Protection", *Electrical Power & Energy Systems*, Vol. 6, No. 3, 1984, pp. 169- 180.

[36] Murty, Y.V.V.S. and Smolinski, W.J., "Design and Implementation of a Digital Differential Relay for a 3-Phase Power Transformer Based on Kalman Filtering Theory", *IEEE Trans. on Power Delivery*, Vol. 3, No. 2, 1988, pp. 525-533.

[37] Murty, Y.V.V.S. and Smolonski, W.J., "A Kalman Filter Based Digital Percentage Differential and Ground Fault Relay for a 3-Phase Power Transformer", *IEEE Trans. on Power Delivery*, Vol. 5, No. 3, 1990, pp. 1299-1308.

[38] Degens, A.J., "Algorithm for a digital transformer differential protection based on a least-square-curve-fitting", *IEE Proceedings*, Vol. 128, Part C, 1981, pp. 155-161.

[39] Degens, A.J., "Microprocessor-implemented digital filters for inrush current detection", *Electrical Power and Energy System*, Vol. 4, No. 3, 1982, pp. 196- 205.

[40] Rahman, M.A., Dash, P.K. and Downton, E.R., "Digital Protection of Power Transformer Based on Weighted Least Square Algorithm", *IEEE Trans. on Power Apparatus and Systems*, Vol. PAS-101, No. 11, 1982, pp. 4204-4210.

[41] Sachdev, M.S. and Sidhu, T.S., "A Least Squares Technique and Differential Protection of Three-Phase Transformers", *Transaction of the Engineering and Operating Division of Canadian Electrical Association, Power System Planning and Operation Section*, 90-SP-158, 1990.

[42] Dash, P.K. and Rahman, M.A., "A New Algorithm for Digital Protection of Power Transform[illegible]", *Transaction of the Engineering and Operating Division of Canadian Electrical Association, Power System Planning and Operation Section*, 89-SP-169, 1987.

[43] Lihua, H., Yilin, Y., Rahman, M.A., Chan, D.T.W. and Ong, P.K.S., "A Novel Algorithm For Digital Protection of Power Transformers", *Transaction of the Engineering and Operating Division of Canadian Electrical Association, Power System Planning and Operation Section*, 92-SP-165, 1992.

[44] Hermanto, I., Murty, Y.V.V.S. and Rahman, M.A., "A stand-Alone Digital Protective Relay for Power Transformers", *IEEE Trans. on Power Delivery*, Vol. 6, No. 1, 1991, pp. 85-95.

[45] Habib, M. and Martin, M.A., "A Comparative Analysis of Digital Relaying Algorithms for Differential Protection of Three Phase Transformers", *IEEE Trans. on Power Systems*, Vol. 3, No. 3, 1988, pp. 1378-1384.

[46] Rahman, M.A. and Jeyasurya, B., "A State-of-the-Art Review of Transformer Protection Algorithms", *IEEE Trans. on Power Delivery*, Vol. 3, No. 2, 1988, pp. 534-544.

[47] So, B., "Experimental Testing of Stand-Alone Digital Relay for Power Transformers", *Master of Engineering Thesis*, Memorial University of Newfoundland, St. John's, Newfoundland, January, 1993.

[48] So, B., and Rahman, M.A., "Experimental Testing of Stand-Alone Digital Relay for Power Transformers", *Transaction of the Engineering and Operating Division of Canadian Electrical Association, Power System Planning and Operation Section*, 93-SP-104, 1993.

[49] Rahman, M.A., So., B. and Zaman, M.R., "Testing of Algorithms for a Stand-Alone Digital Relay for Power Transformer", *Accepted for presentation at the 1997 IEEE Winter Meeting, Power Engineering Society*, Paper No. 96 5M 397, New York, USA.

[50] Liu, P., Malik, O.P., Chen, D., Hope, G.S. and Guo, Y., "A Novel Algorithm for Digital Protection of Power Transformer", *IEEE Trans. on Power Delivery*, Vol. 7, No. 4, 1992, pp. 1912-1919.

[51] Sachdev, M.S., Sidhu, T.S. and Wood, H.C., "A Non-linear Modeling Approach for Detecting Winding Faults in Power Transformers", *Transaction of*

the Engineering and Operating Division of Canadian Electrical Association, Power System Planning and Operation Section, 89-SP-142, 1989.

[52] Liu, P., Malik, O.P., Chen, D. and Hope, G.S., "Study of Non-operation for Internal Faults of Second Harmonic Restraint Differential Protection of power Transformers", *Transaction of the Engineering and Operating Division of Canadian Electrical Association, Power System Planning and Operation Section*, 89-SP-141, 1989.

[53] Sidhu, T.S. and Sachdev, M.S., "On-line Identification of Magnetizing Inrush and Internal Faults in Three-Phase Transformers", *IEEE Trans. on Power Delivery*, Vol. 7, 1992, pp. 1885-1891.

[54] Inagaki, K., Higaki, M., Kurita, K., Suzuki, M., Yoshida, K. and Maeda, T., "Digital Protection Method for Power Transformers Based on An Equivalent Circuit Composed of Inverse Inductance", *IEEE Trans. on Power Delivery*, Vol. 3, No. 4, 1988, pp. 1501-1510.

[55] Phadke, A.G. and Thorp, J.S., "A New Computer-Based, Flux Restrained, Current Differential Relay for Power Transformer Protection", *IEEE Trans. on Power Apparatus and Systems*, Vol. PAS-102, No. 11, 1983, pp. 3624-3629.

[56] Sidhu, T.S., Sachdev, M.S., Wood, H.C. and Nagpal, M., "Design, Implementation and Testing of A Micro-processor-based High-speed Relay for Detecting Transformer Winding Faults", *IEEE Trans. on Power Delivery* , Vol. 7, No. 1, 1992, pp. 108-117.

[57] Thorp, J.S. and Phadke, A.G., "A Microprocessor-Based, Voltage-Restrained, Three-Phase Transformer Differential Relay", *Proceedings of the South Eastern Symposium on Systems Theory*, 1982, pp. 312-316.

[58] Sachdev, M.S., Sidhu, T.S. and Wood, H.C., "A Digital Relaying Algorithm for Detecting Transformer Winding Faults", *IEEE Trans. on Power Delivery*, Vol. 4, 1989, pp. 1638-1648.

[59] Sachdev, M.S., Sidhu, T.S. and Wood, H.C., "Detecting Transformer Winding Faults Using Nonlinear Models of Transformers", *Fourth International Conference on Developments in Power System Protection, IEE Publication*, No. 302, 1989, pp. 70-74.

[60] El-Sharkawi, M.A. and Niebur, D., *Tutorial Course: Artificial Neural Networks with Applications to Power Systems*, IEEE Power Engineering Society, Paper No. 96TP112-0, January, 1996.

[61] El-Hawary, M., "Environmental Dispatch using Hopfield Neural Network", *Proceedings of Canadian Electrical Association Conference*, Vancouver, March, 1995.

[62] Dash, P.K, Dash, S., Swain, A.K., Rahman, S. and Chandrasekharaiah, H.S., "Short Term Load Forecasting Using Artificial Neural Network with a Fast Learning Algorithm", *Proceedings of the Fourth Symposium on Expert System*, Melbourne, Australia, Jan. 5, 1993, pp. 169-174.

[63] El-Sharkawi, M.A., Marks II, R.J., Oh, S. and Brace, C.M., "Data Partitioning for Training a Layered Perceptron to Forecast Electric Load", *Proceed-*

ings of the Second International Forum on Applications of Neural Networks to Power Systems, Yokohama, Japan, April 19-22, 1993, pp. 66-68.

[64] Mori, H., Ogasawara, T., "A Recurrent Neural Network for Short Term Load Forecasting", *Proceedings of the Second International Forum on Applications of Neural Networks to Power Systems*, Yokohama, Japan, April 19-22, 1993, pp. 395-500.

[65] Jeyasurya, B., "Artificial Neural Networks for Power System Steady State Voltage Instability Evaluations", *Electric Power Systems Research*, Vol. 29, No. 2, March, 1994, pp. 85-90.

[66] El-Keib, A.A. and Ma, X., "Applications of Artificial Neural Networks in Voltage Stability", *IEEE Power Engineering Society Winter Meeting*, Paper No. WM156-0-PWRS, New York, January-February. 1995.

[67] Ebron, S., Lubkeman, D. and White, M., "A Neural Network Approach to the Detection of Incipent Faults on Power Distribution Feeders", *IEEE Trans on Power Delivery*, Vol. 5, No. 2, 1990, pp. 905-914.

[68] Ebron, S., Lubkeman, D., White, M. and Harper, J., "Neural Network Applications for Data Interpretation and Diagnostic Analysis", *American Power Conference*, May, 1989, pp. 593-597.

[69] Sultan, A., Swift, G. and Fedirchuk, D., "Detection of High Impedance Arcing Faults Using a Multi-Layer Perceptron", *IEEE Trans. on Power Delivery*, Vol. 7, No. 4, 1992, pp. 1871-1877.

[70] Perez, L.G., Flechsig, A.J., Meador, J.L. and Obradovic, Z.,"Training An Artificial Neural Network to Discriminate Between Magnetizing Inrush and

Internal Faults", *IEEE Trans. on Power Delivery*, Vol. 9, No. 1, 1994, pp. 434-441.

[71] Zaman, M.R., Hoque, M.A. and Rahman, M.A., "Artificial Neural Network Based Protection for Transformers", *Proceedings of Canadian Electrical Association Conference, Power System Planning and Operation Section*, Vancouver, April, 1995.

[72] Bastard, P., Meunier, M. and Regal, H.,"Neural Network-based Algorithm for Power Transformer Differential Relays",*IEE Proceedings, Generation, Transmission and Distribution*, Vol 142, No. 4, July, 1995, pp. 386-392.

[73] Zaman, M.R. and Rahman, M.A., "Protection of Power Transformers using Artificial Neural Network", *Presented in the Conference of Engineering and Operating Division of Canadian Electrical Association, Power System Planning and Operation Section*, Montreal, April 28 - May 3, 1996.

[74] Haykin, H., *Neural Networks : A Comprehensive Foundation*, IEEE Press, Macmillan College Publishing Company Inc., 1994.

[75] Baumann, T., Germond, A. and Tschudi, D.,"Impulse Test Fault Diagnosis on Power Transformer Using Kohonen's Self Organizing Neural Network", *Proc. of the Third Symposium on Expert System Application to Power Systems*, Tokyo, April 1-5, 1991, pp. 642-647.

[76] Giuliante, T. and Clough, G., "Advances In The Design of Differential Protection For Power Transformers", *Georgia Tech Relaying Conference*, Atlanta, May, 1991, pp. 1-12.

[77] Slemon, G.R., *Electric Machines and Drives*, Addison Wesley Publishing Company Inc., 1992.

[78] Mori, H., Itou, K., Uematsu, H. and Tsuzuki, S., "An Artificial Neural-Net Based Method for Predicting Power System Voltage Harmonics", *IEEE Trans on Power Delivery*, Vol. 7, No. 1, 1992, pp. 402-409.

[79] Demuth, H. and Beale, M., *Neural Network Toolbox : For Use with MATLAB*, The Math Works Inc., 1994.

[80] Freeman, J.A. and Skapura, D.M., *Neural Networks : Algorithms, Applications, and Programming Techniques*, Addison-Wesley Publishing Company, 1992.

[81] Wood, H.C., Sidhu, T.S., Nagpal, M. and Sachdev, M.S., "A General Purpose Hardware for Microprocessor Based Relays", *Proceedings of International Conference on Power System Protection*, Singapore, 13-14, 1989, pp. 43-59.

Appendix A

Triac switch and control circuit

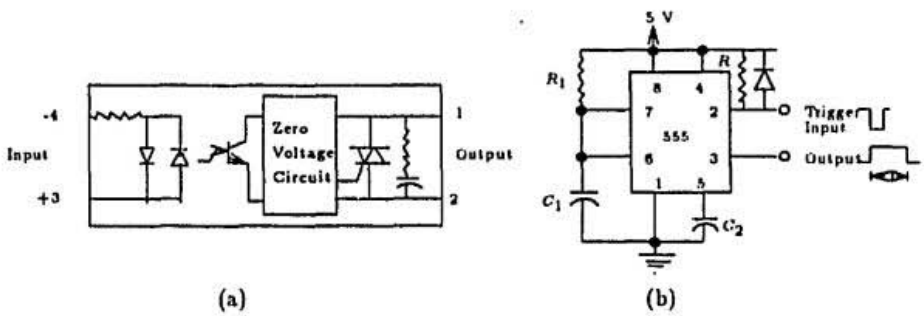

Figure A.1: (a) Equivalent circuit of the triac switch, (b) control circuit to operate the triac switch

In Fig. A.1(a), +3 and −4 are the input voltage terminals fed from the controlling circuit. The output terminals 1 and 2 are open if there is no voltage at the input terminals and shorted if $3 - 32$ volts are applied to the input terminals.

A control circuit is used to operate the triac switches so that it allows the current to flow through the transformer for five cycles for data acquisition purpose and three cycles for on-line testing purpose. The control circuit is shown in Fig. A.1(b). The pulse width of the control voltage is calculated by the formula $T = 1.1\ R_1\ C_1$. In

our case, all switchings are done for 5 cycles i.e. 83.5ms for 60 Hz signal. The design parameters are $R_1 = 100$ KΩ, $C_1 = 1\mu$F, $R = 10$ KΩ, $C_2 = 0.01\mu$F.

Appendix B

Weights and Biases for the ANN

B.1 Hidden layer weights and biases

W1 =

Columns 1 through 7

2.0885	-1.2420	-1.8562	-3.0994	-1.9809	-1.0208	0.7947
2.1140	2.8667	2.5800	1.2313	1.3366	-0.3571	2.1816
-0.1272	-0.5374	2.0195	-1.0126	-0.2421	-1.4579	2.0722

Columns 8 through 14

-2.9266	1.0115	0.2806	-2.3452	-0.6182	-1.1746	-1.1807
2.5816	-0.0171	2.3640	5.0790	0.8606	0.9524	0.8980
1.7.01	1.5374	2.3781	0.27.0	2.6971	0.1068	1.2874

```
  Columns 15 through 16

   -1.6967    0.3633
    2.3383    2.1806
    0.2031   -2.0512

B1 =

    0.0806
  -15.8455
    4.3342
```

B.2 Output layer weights and biases

```
W2 =

    0.0396    2.2585    3.9311

B2 =

   -3.8410
```

Appendix C

On-line test results

As mentioned, the ANN based algorithm for transformer protection is tested on-line on a three phase, 230/550-575-600V, 5 kVA transformer using DS-1102 digital signal processor. The fault tests are done in all three phases and the test results for one of the phases are presented in Chapter 5. This section provides the rest of the on-line test results of the three phase implementation of the ANN based algorithm.

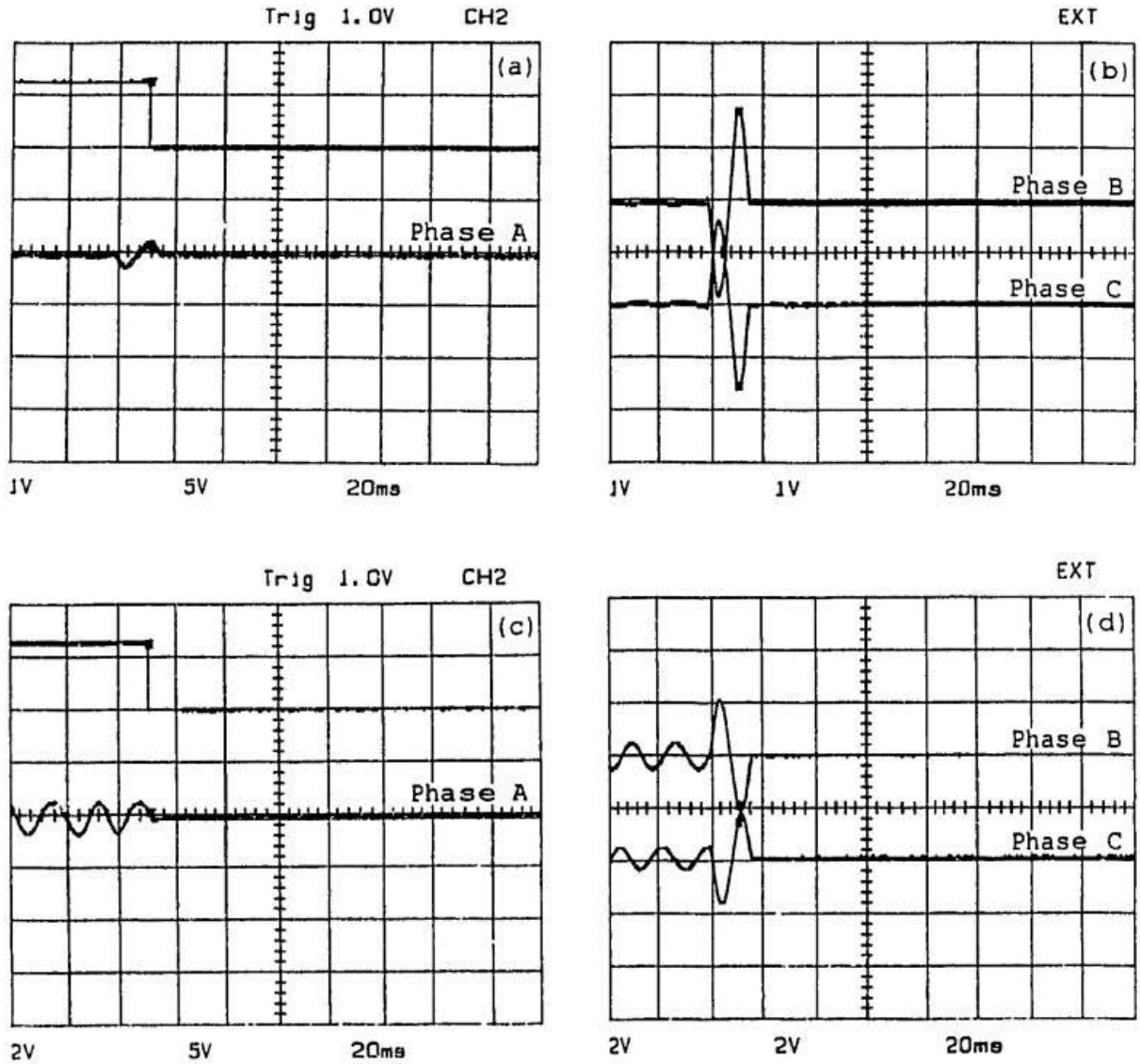

Figure C.1: Primary side phase B to phase C fault, occurred before inrush – (a),(b) without load; (c),(d) with load; (1V = 12.5 A).

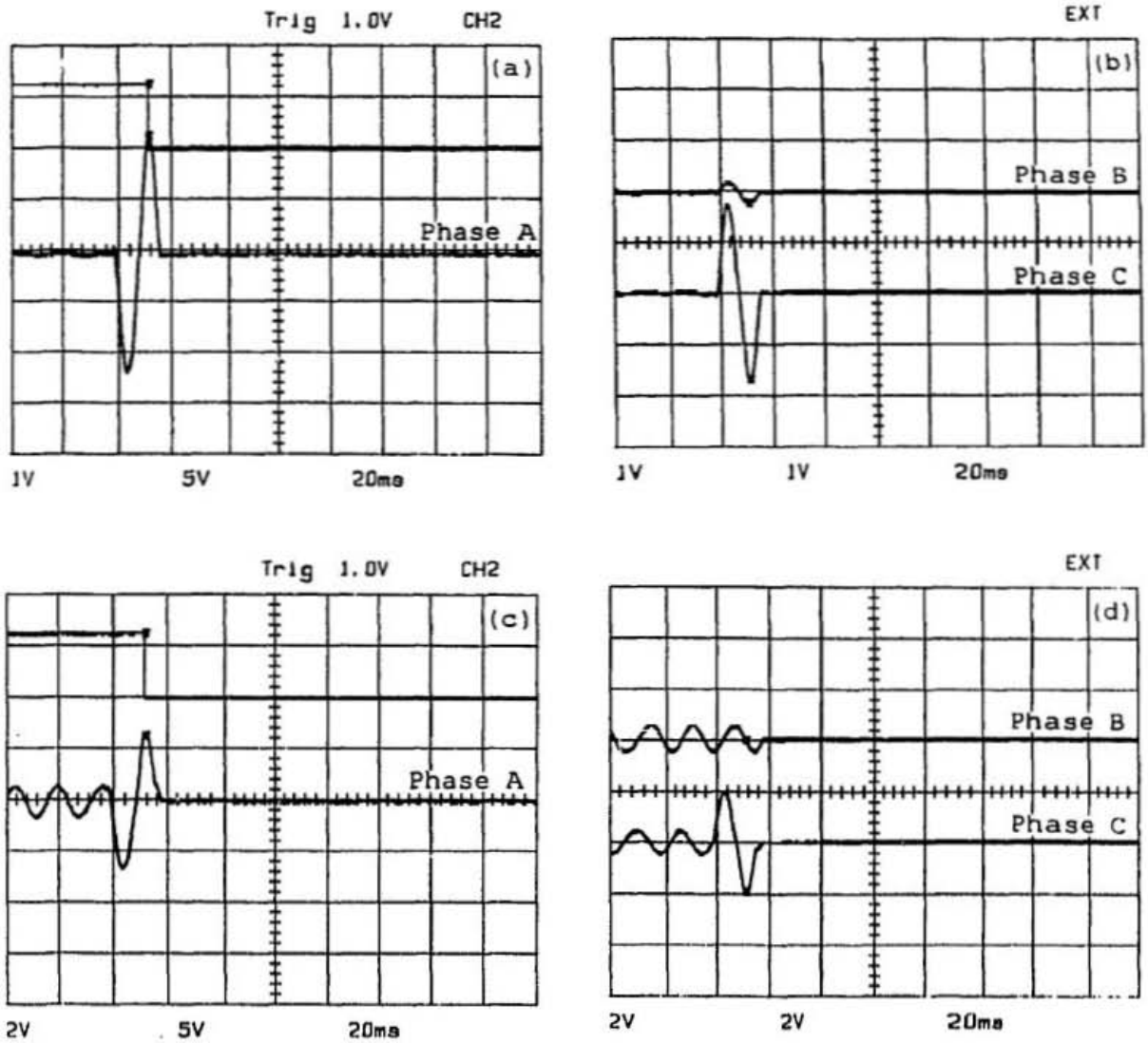

Figure C.2: Primary side phase B to phase C fault, occurred after inrush - (a),(b) without load; (c),(d) with load; (1V = 12.5 A).

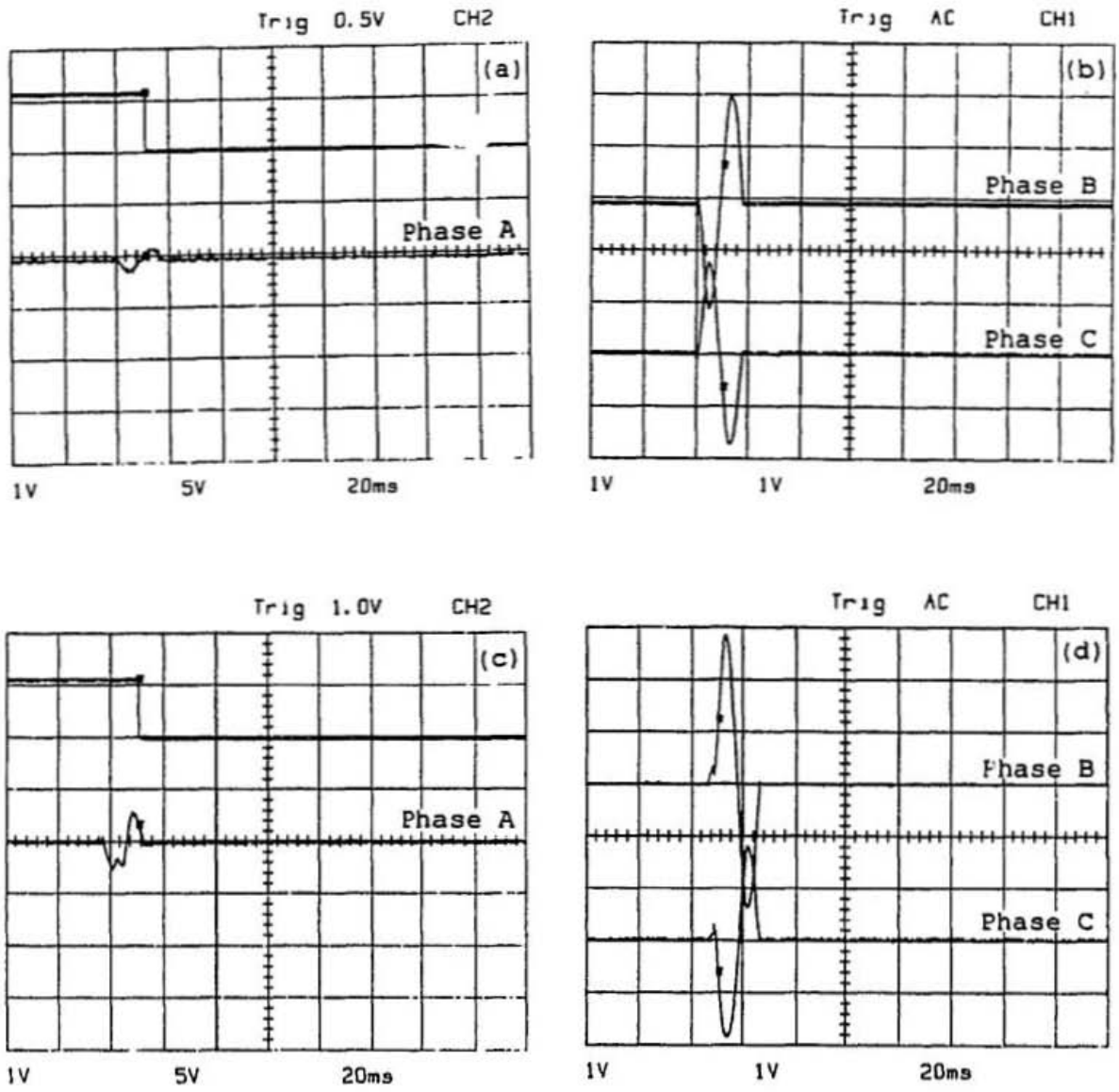

Figure C.3: Primary side phase C to phase A fault, occurred before inrush - (a),(b) without load; (c),(d) with load; (1V = 12.5 A).

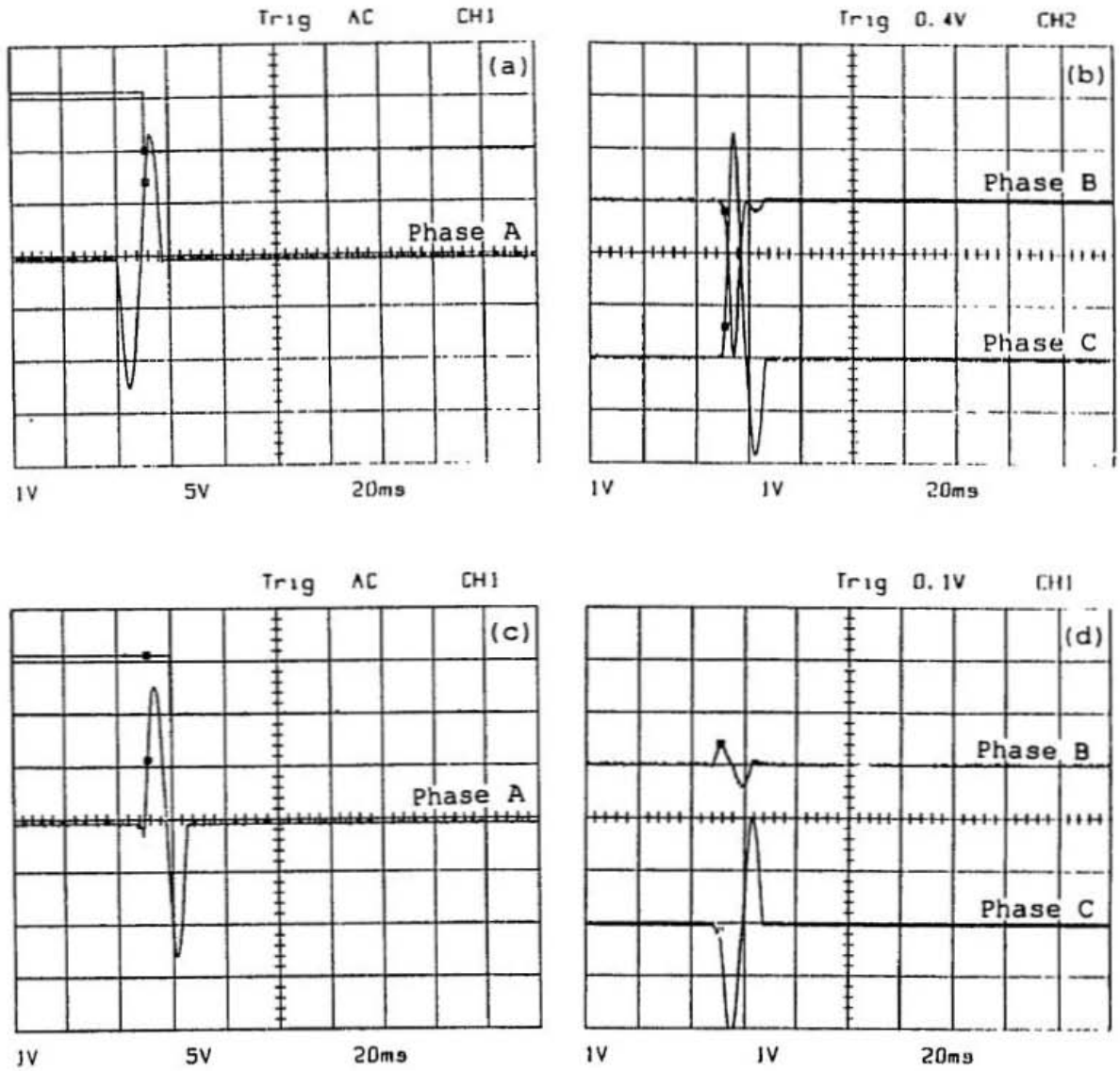

Figure C.4: Primary side phase C to phase A fault, occurred after inrush - (a),(b) without load; (c),(d) with load; (1V = 12.5 A).

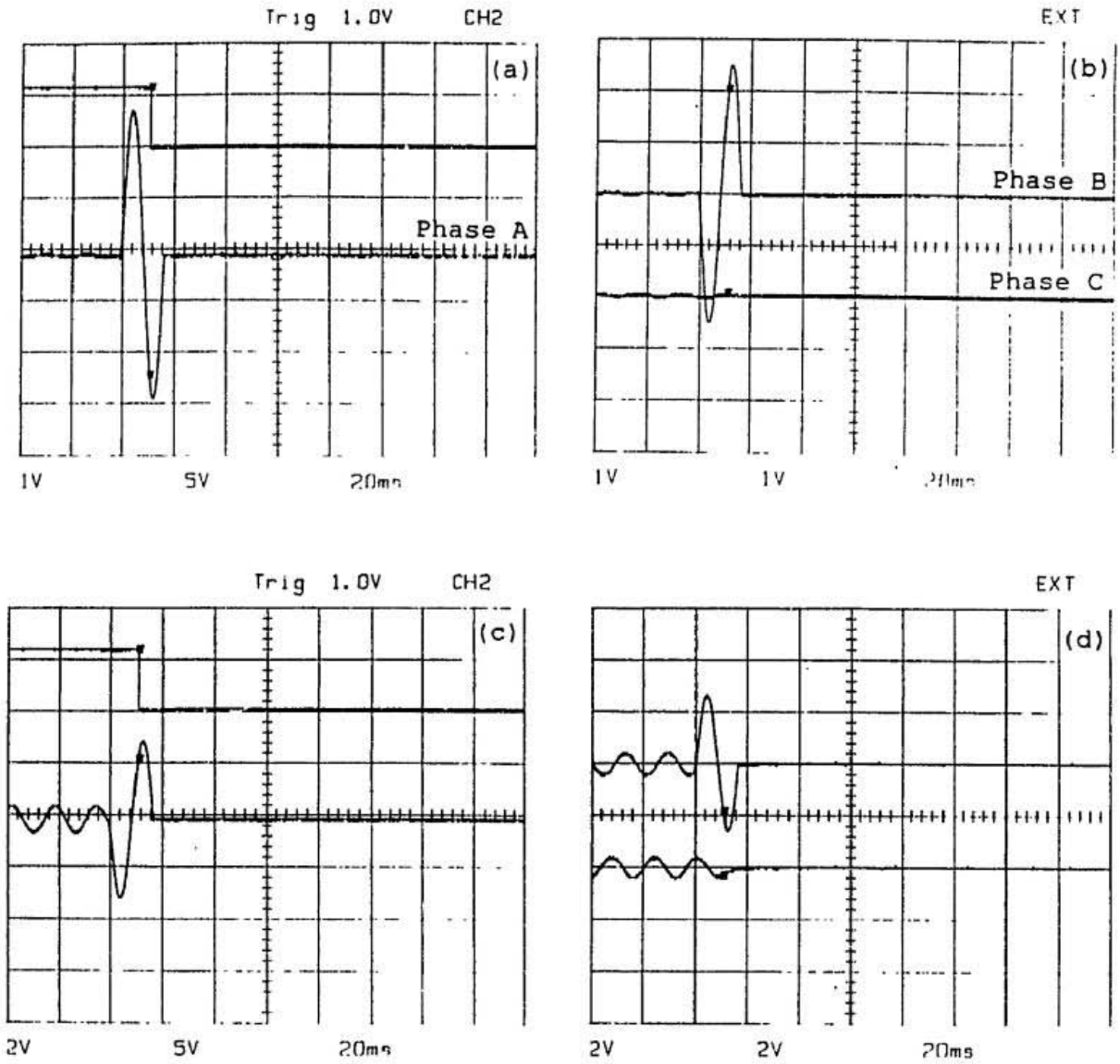

Figure C.5: Secondary side phase B to ground fault, occurred before inrush - (a),(b) without load; (c),(d) with load; (1V = 12.5 A).

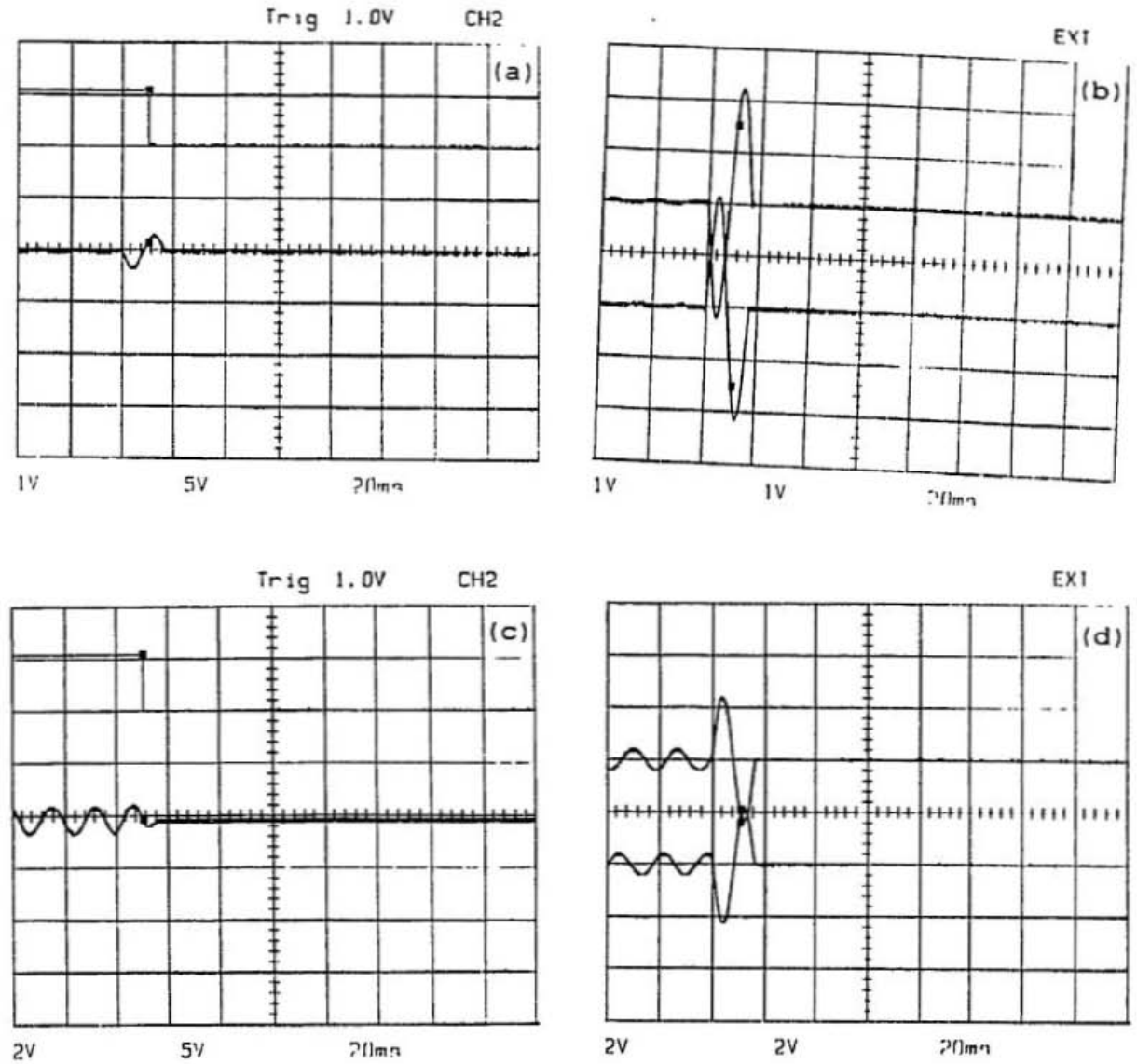

Figure C.6: Secondary side phase B to ground fault, occurred after inrush - (a),(b) without load; (c),(d) with load; (1V = 12.5 A).

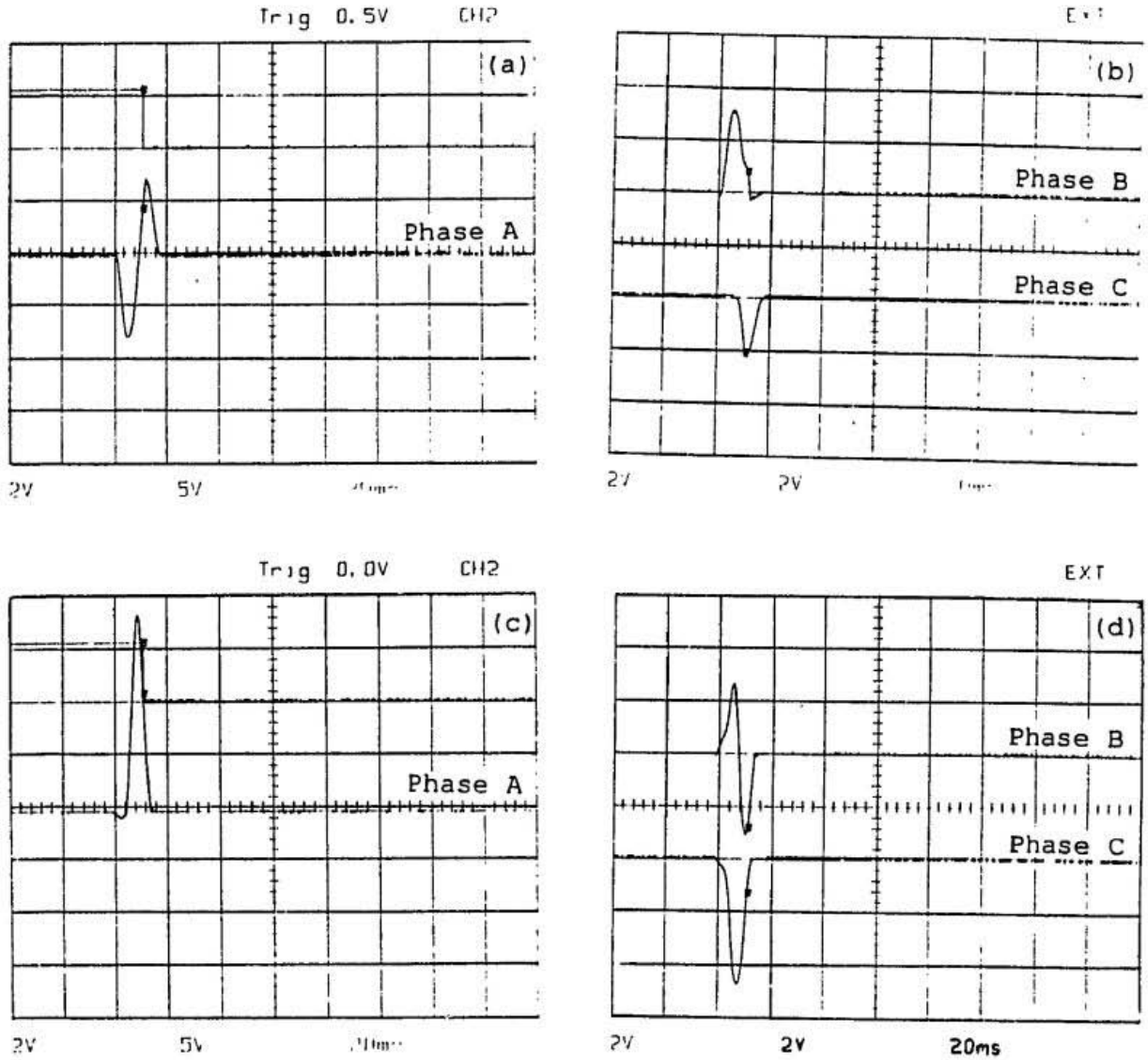

Figure C.7: Secondary side phase C to ground fault, occurred before inrush – (a),(b) without load; (c),(d) with load; (1V = 12.5 A).

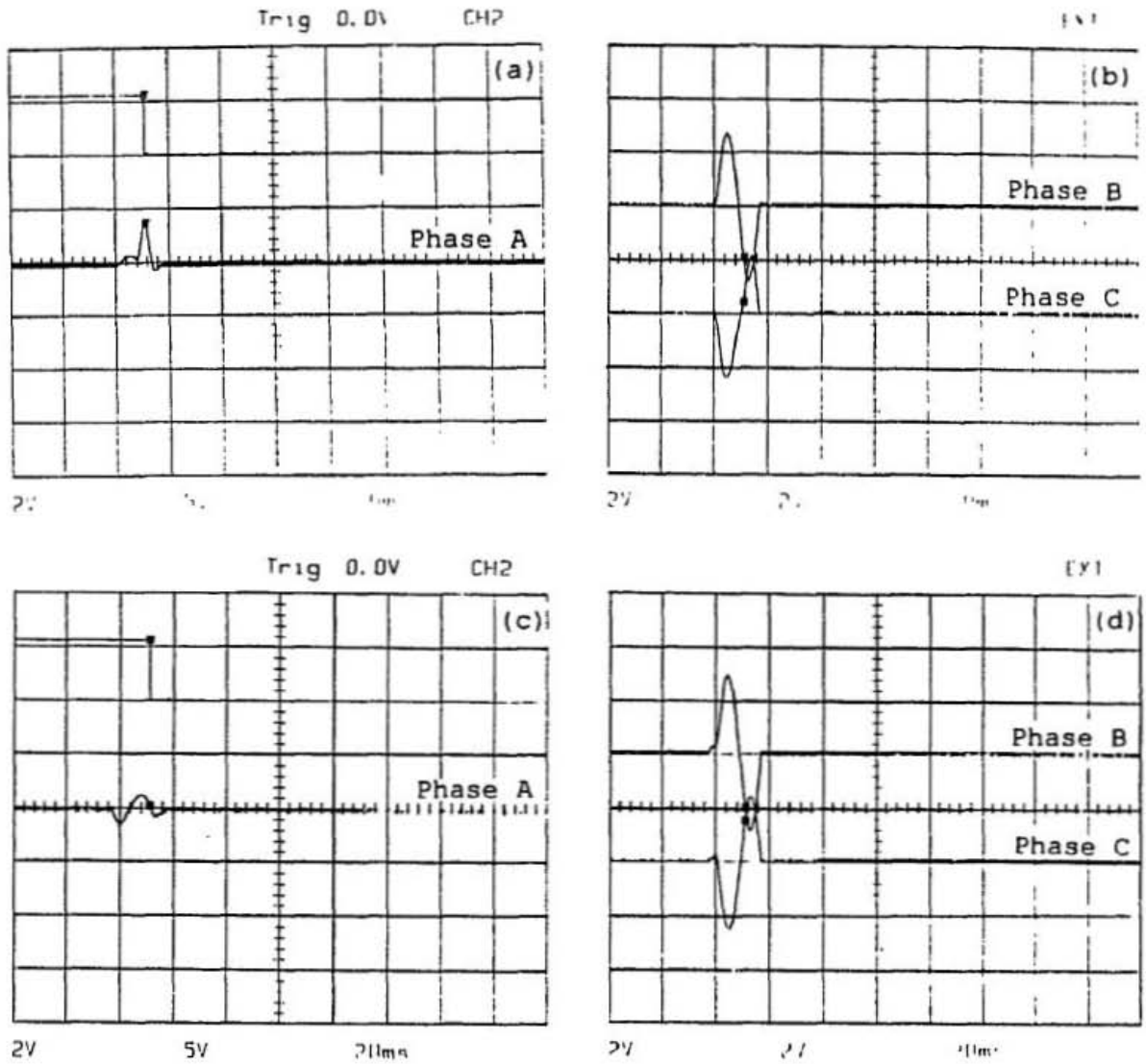

Figure C.8: Secondary side phase C to ground fault, occurred after inrush - (a),(b) without load; (c),(d) with load; (1V = 12.5 A).

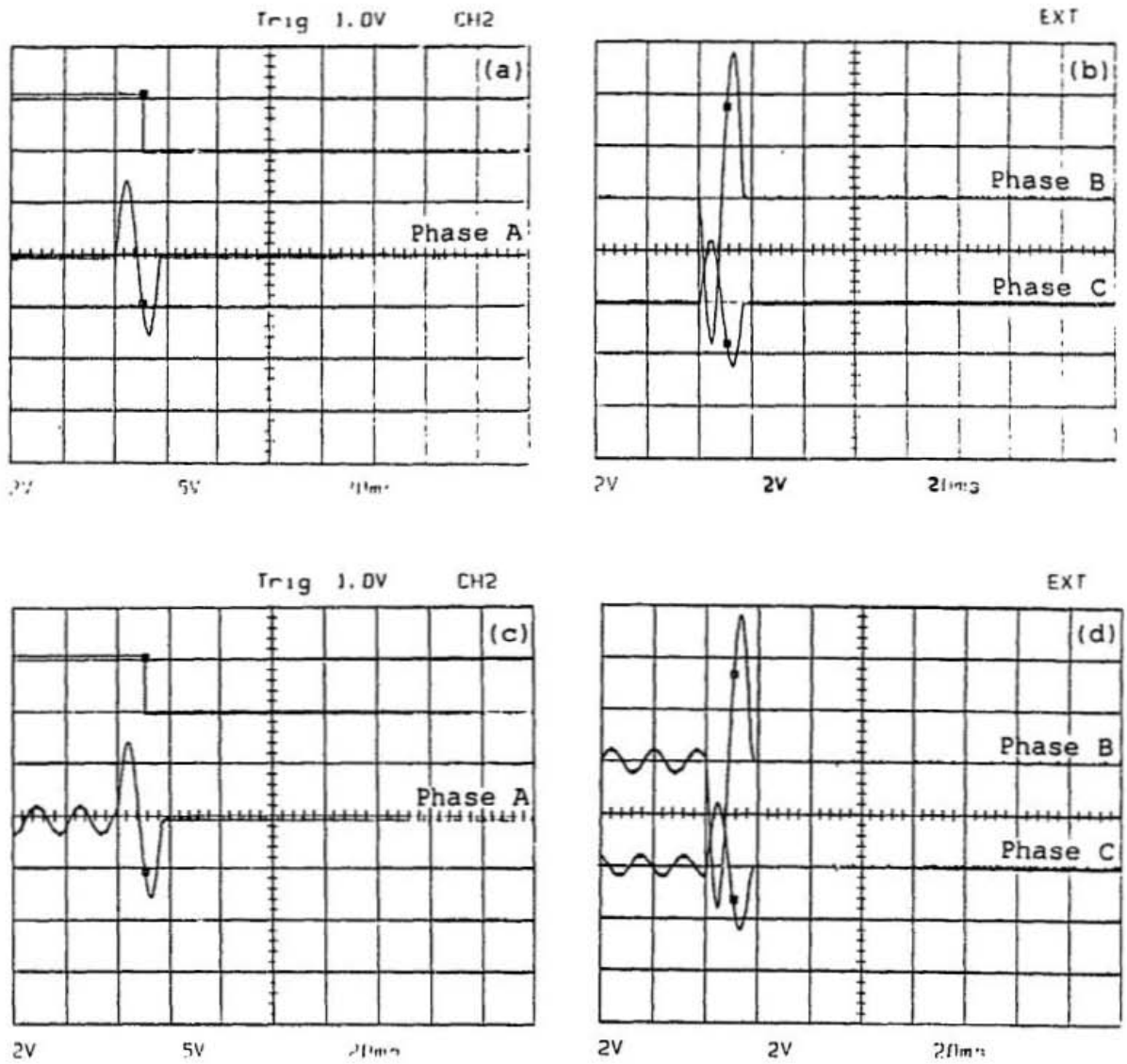

Figure C.9: Secondary side phase B to phase C fault, occurred before inrush – (a),(b) without load; (c),(d) with load; (1V = 12.5 A).

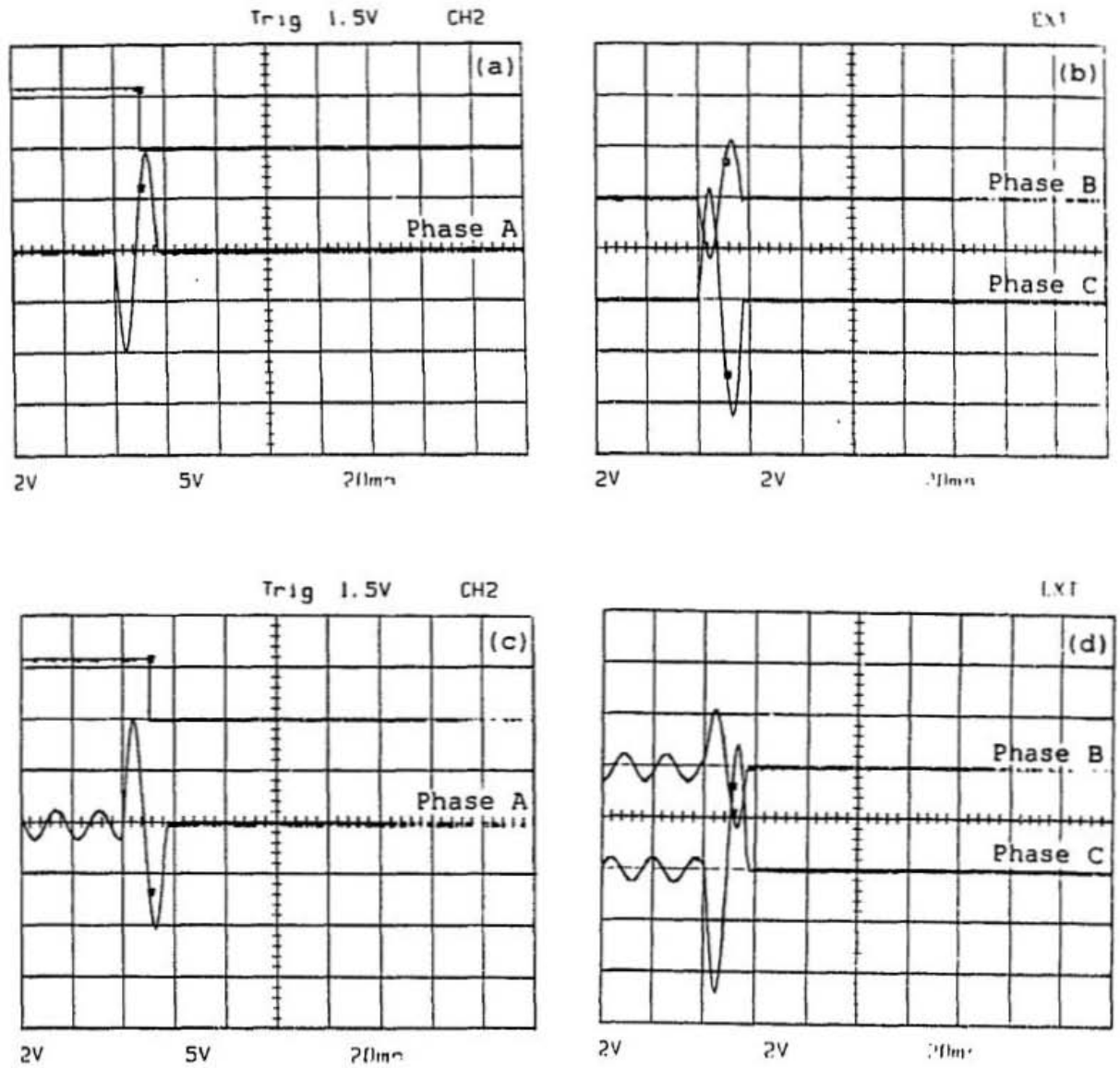

Figure C.10: Secondary side phase B to phase C fault, occurred after inrush – (a),(b) without load; (c),(d) with load; (1V = 12.5 A).

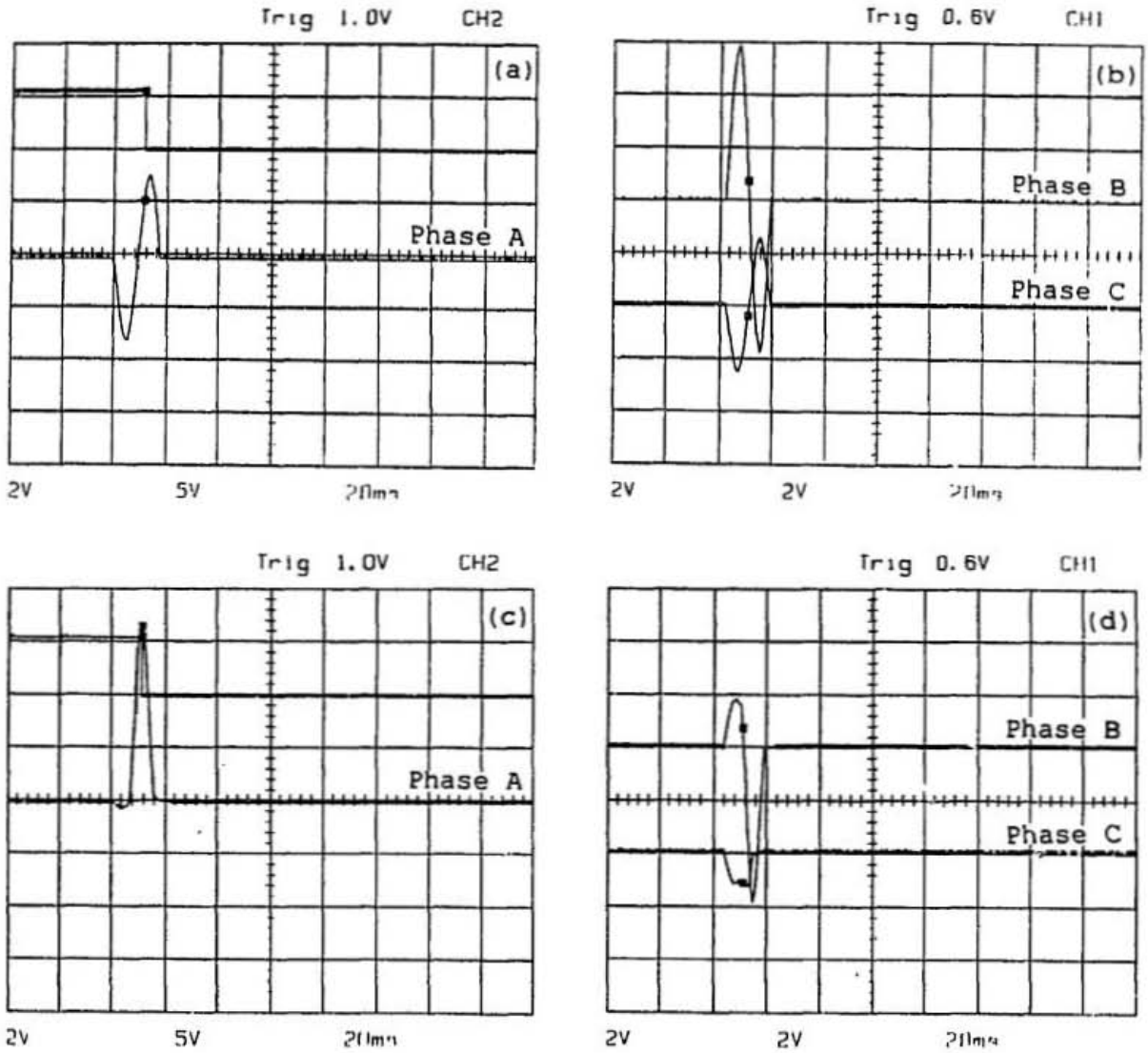

Figure C.11: Secondary side phase C to phase A fault, occurred before inrush – (a),(b) without load; (c),(d) with load; (1V = 12.5 A).

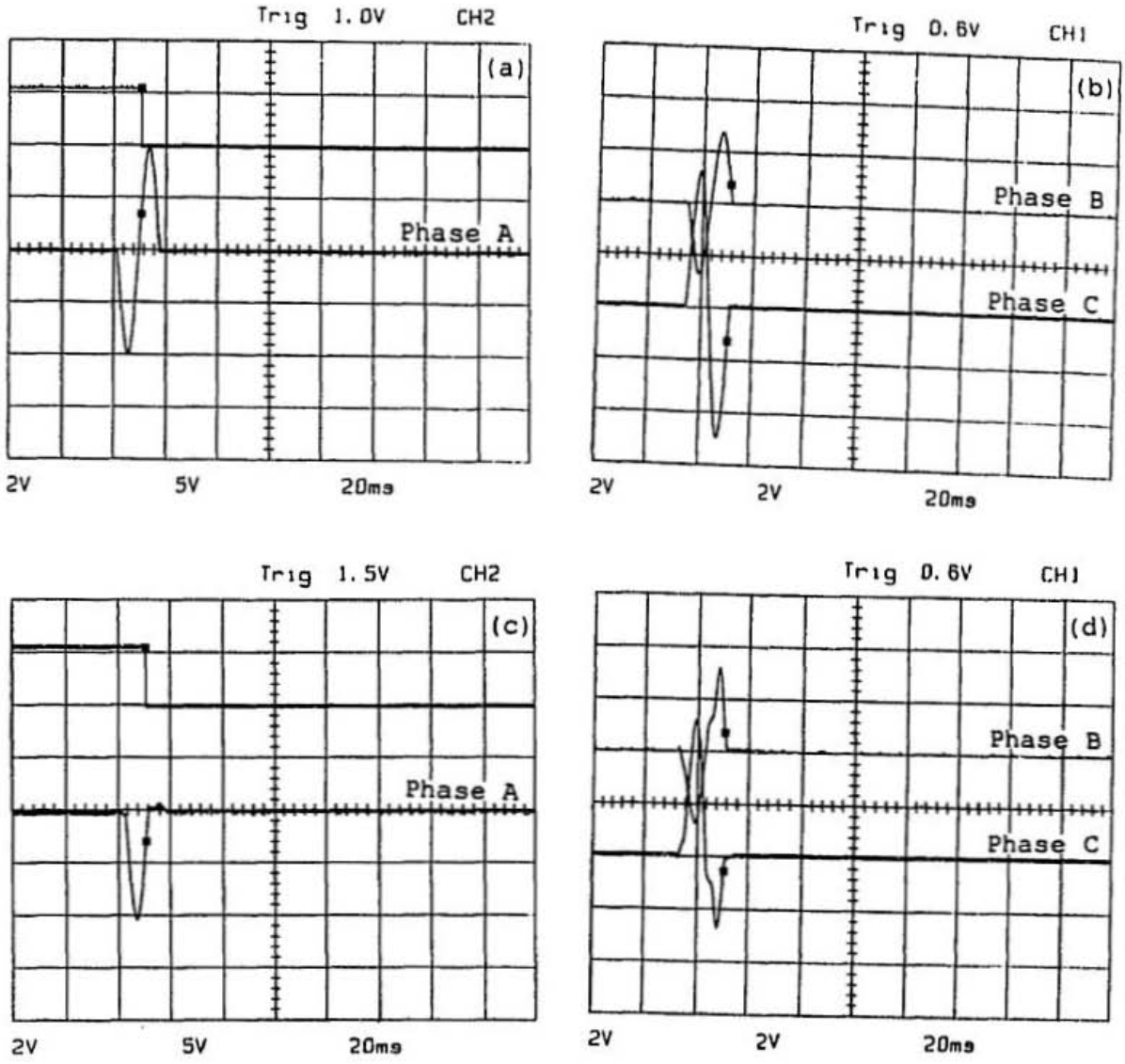

Figure C.12: Secondary side phase C to phase A fault, occurred after inrush – (a),(b) without load; (c),(d) with load; (1V = 12.5 A).

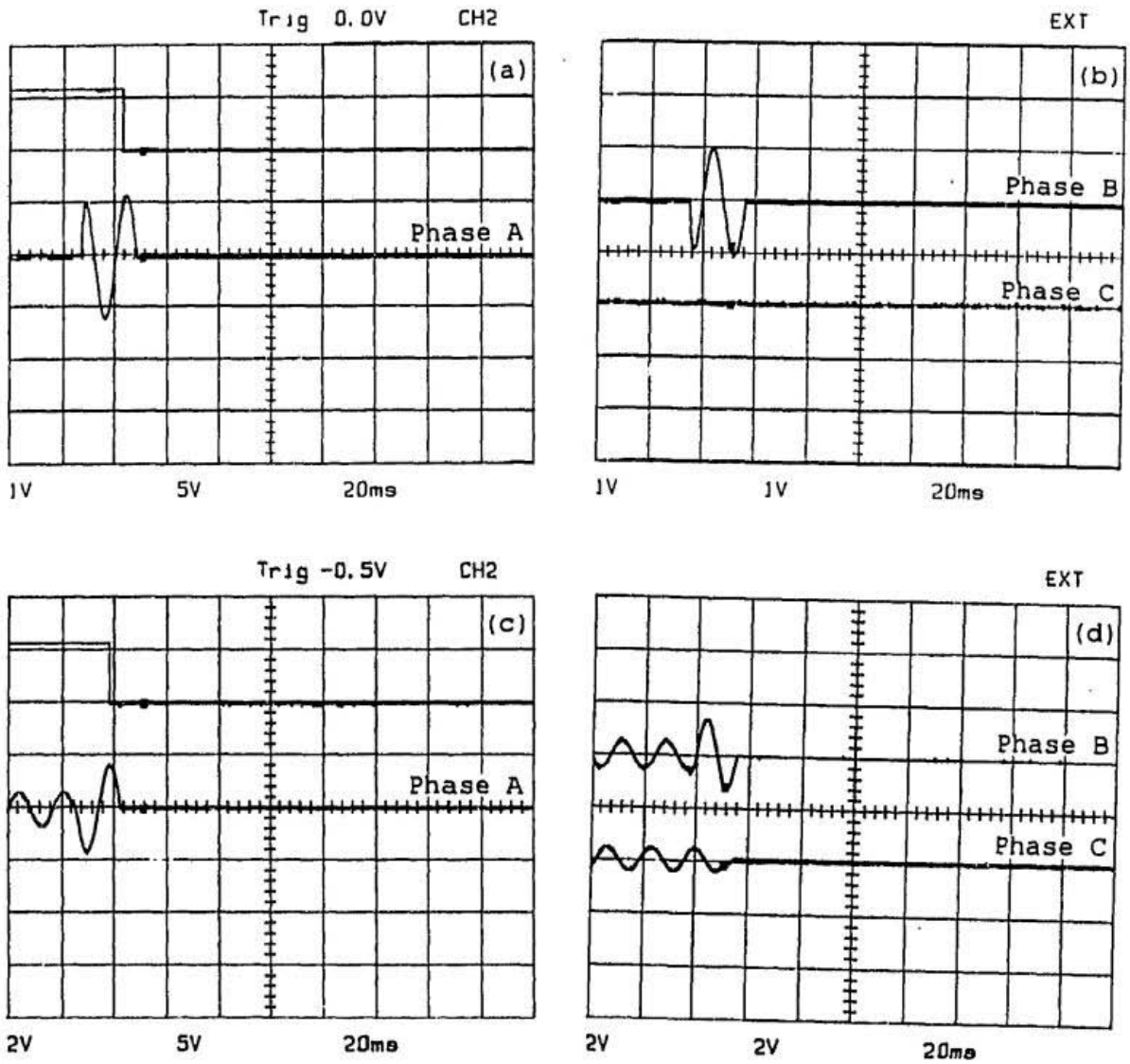

Figure C.13: Secondary side between tap fault in phase B, occurred before inrush – (a),(b) without load; (c),(d) with load; (1V = 12.5 A).

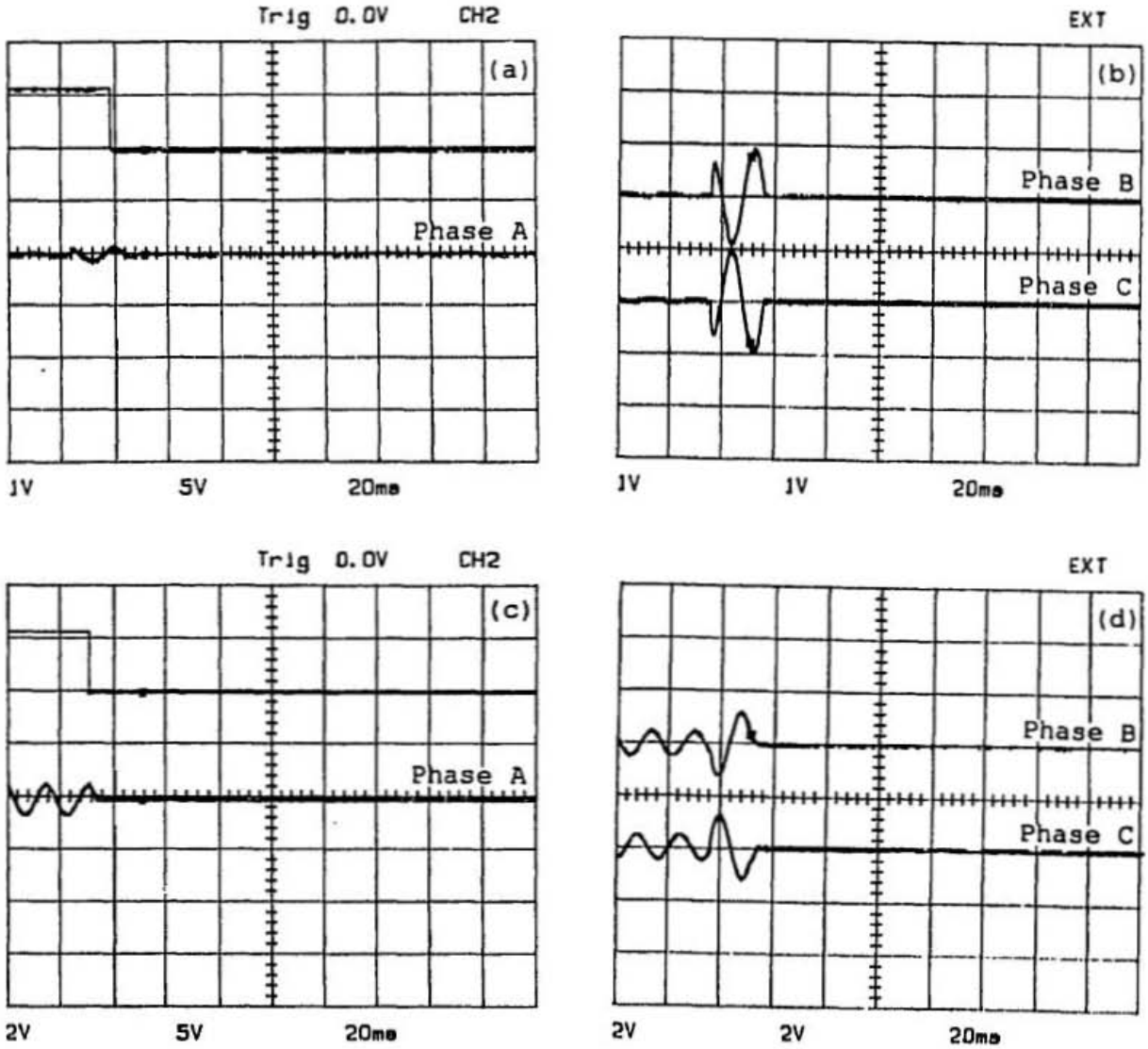

Figure C.14: Secondary side between tap fault in phase B, occurred after inrush - (a),(b) without load; (c),(d) with load; (1V = 12.5 A).

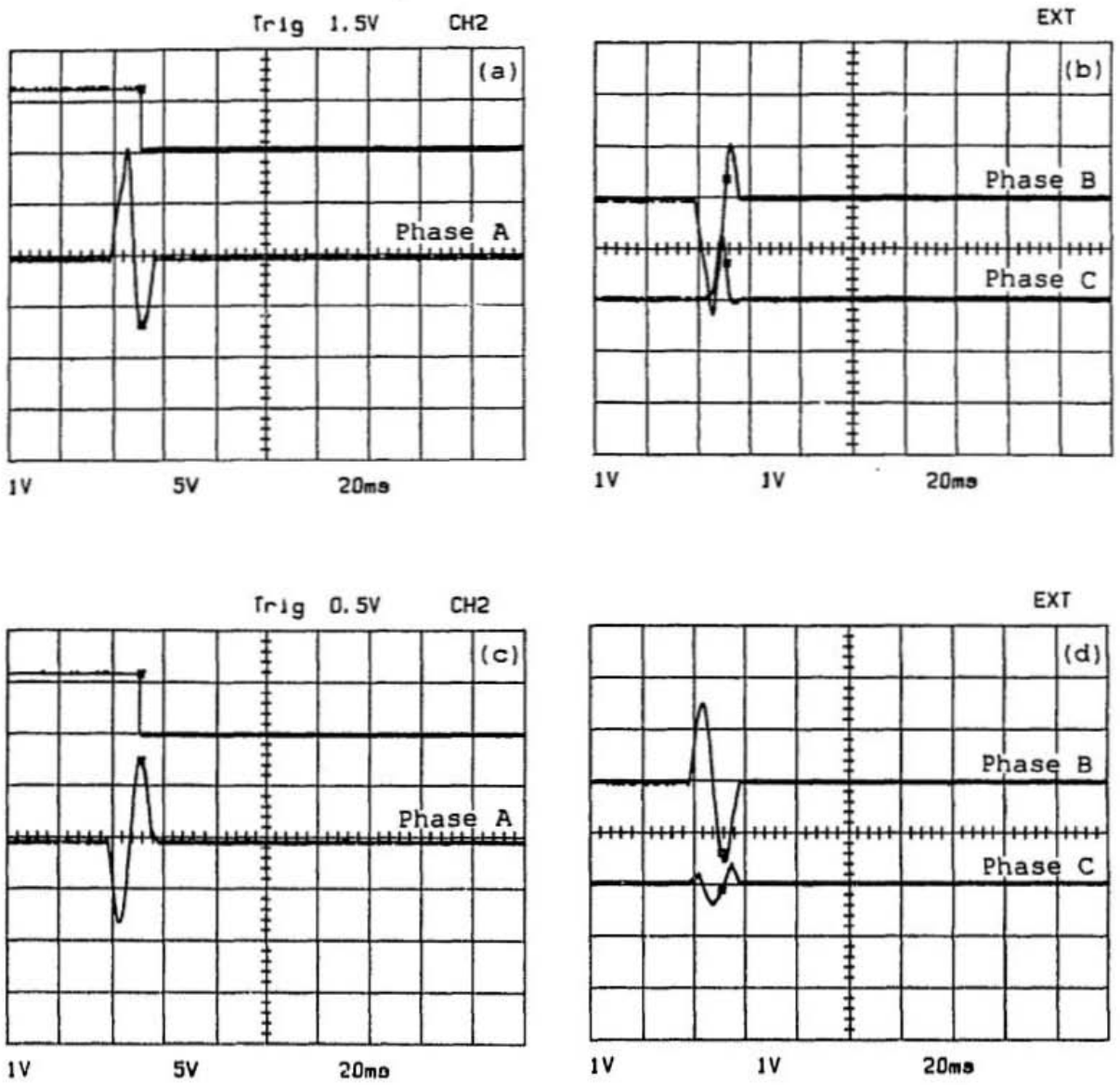

Figure C.15: Secondary side between tap fault in phase C, occurred before inrush – (a),(b) without load; (c),(d) with load; (1V = 12.5 A).

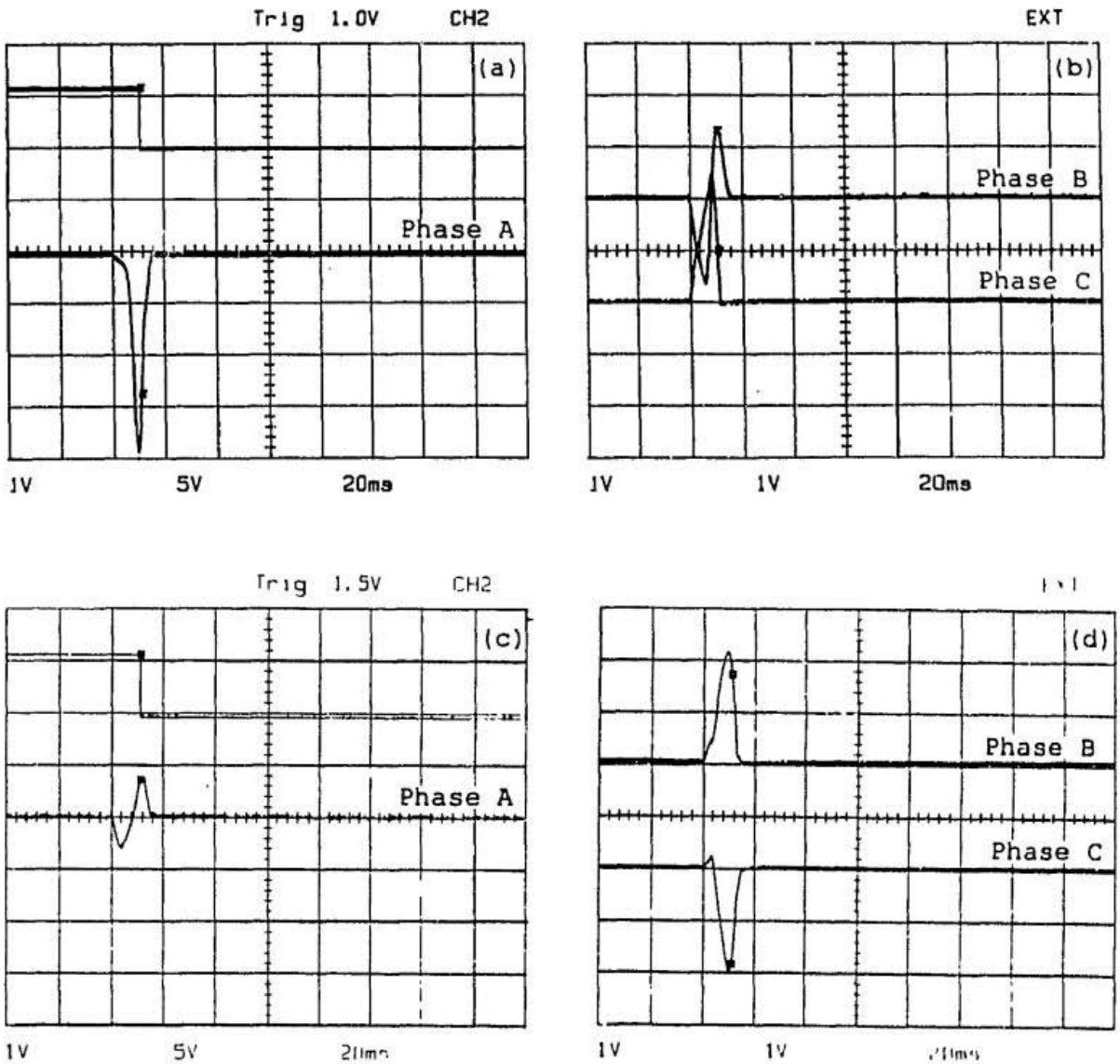

Figure C.16: Secondary side between tap fault in phase C, occurred after inrush - (a),(b) without load; (c),(d) with load; (1V = 12.5 A).